



1. Basics of MR Spectroscopy

M. Albert Thomas Ph.D.
Professor

Department of Radiological Sciences
University of California, Los Angeles

M219: Introduction to Magnetic Resonance Imaging/03/04/24

Overview



- Basics of MRI and MRS Physics
- Single-voxel localized MRS
- Selected Applications





1. Basics of MR Imaging (MRI) and MR Spectroscopy (MRS)



Historical Perspective

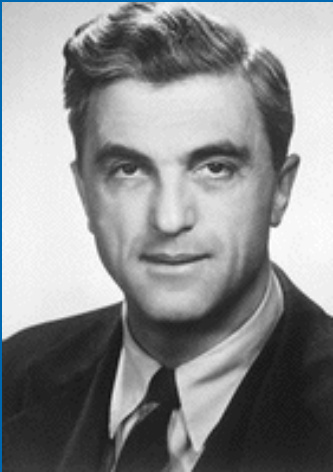


➤ 1940's

- Radio (RADAR) technology developed during WWII lead to a new approach to measuring the proton spin
 - Protons have an electric charge
 - Protons have spin
 - Therefore it could be possible to measure the spin by placing the protons in a magnetic field and then measuring radio frequency emissions or absorptions
- Edward Purcell (Harvard/MIT) and Felix Bloch (Stanford) were awarded the Nobel Prize in Physics in 1952 for independently detecting nuclear magnetic resonance signals for the first time using this methodology

Magnetic Resonance

Nobel Prize in Physics 1952



Felix Bloch Ph.D.



Edward Purcell Ph.D.





Historical Perspective

➤ 1950-1970's

- **NMR became a much used technique for study of molecular structure**
 - Chemistry
 - Molecular Biology
 - Materials Science
- **Prof. Richard Ernst developed a highly efficient technique based on the Fourier Transform for the detection and quantification of the NMR signal**
 - 1991 Nobel Prize in Chemistry
 - Fourier transform technique also proved to be the most efficient approach for MRI



Historical Perspective

➤ 1970's

- Prof. Raymond Damadian (SUNY-Downstate Medical Center) proposed that cancer tissue had abnormal relaxation time and built the first human MRI scanner
- Prof. Paul Lauterbur[†] (SUNY-Stony Brook) demonstrated how to make images from NMR signals using magnetic field gradients in conjunction with a 'back projection' technique used in CT imaging
 - Awarded the 2003 Nobel Prize in Medicine or Physiology with Mansfield
- Prof. Peter Mansfield (Nottingham) developed a more efficient 'echo planar imaging' technique and did fundamental studies involving MRI of solids
 - Awarded the 2003 Nobel Prize in Medicine or Physiology with Lauterbur

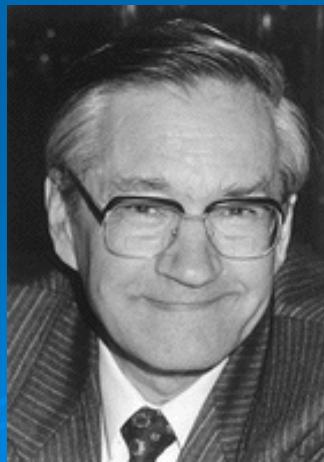
Nobel Laureates in *Magnetic Resonance*



Felix Bloch **Edward Mills Purcell**
Nobel Prize in Physics 1952



Paul C. Lauterbur **Sir Peter Mansfield**
Nobel Prize - Medicine 2003



Richard R. Ernst
Nobel Prize in Chemistry in 1991



Historical Perspective

➤ 1980's

- First commercial MRI scanners based on the Fourier imaging technique
- First commercial superconducting MRI magnets

➤ 1990's

- Development of medical and basic science applications

➤ 2000's

- Hardware and software engineering sophistication

Nuclear Magnetic Resonance

Nuclear spin moment

$$\mu = \gamma \hbar I$$

μ - magnetic moment

γ - gyromagnetic ratio

- I - spin quantum number

\hbar - Planck's constant

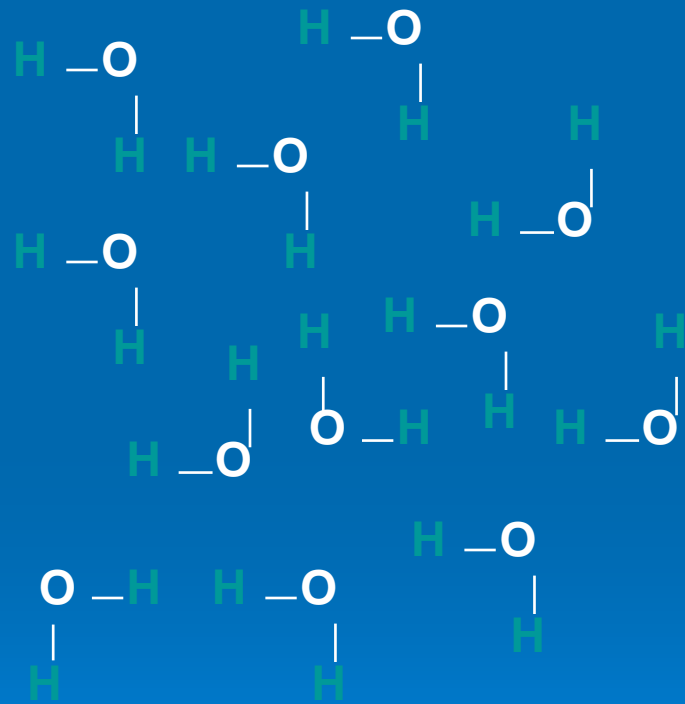


I is a property of the nucleus

Mass #	Atomic #	I
Odd	Even or odd	1/2, 3/2, 5/2, ...
Even	Even	0
Even	Odd	1, 2, 3

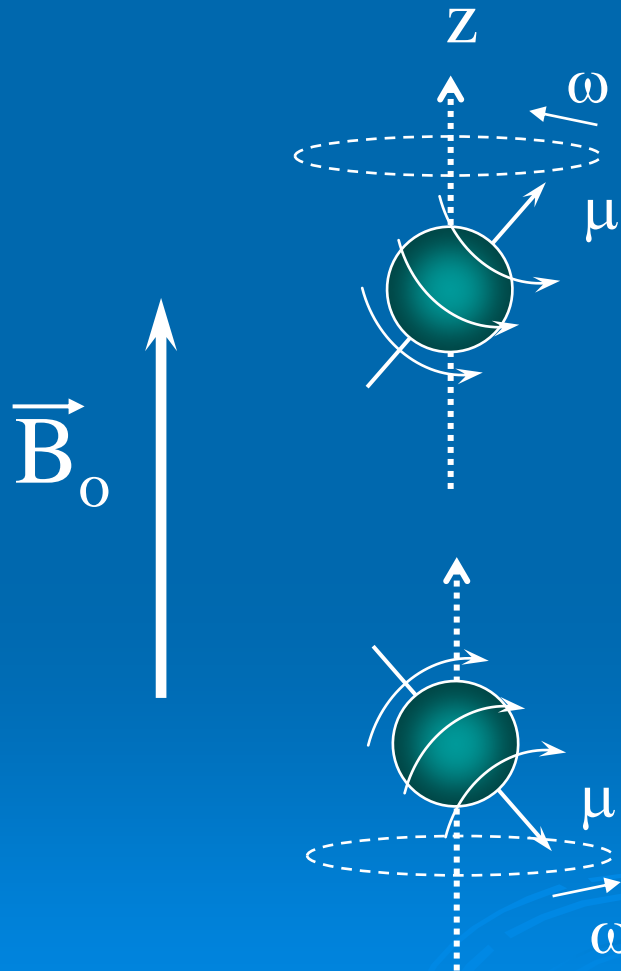


Water Molecule



Apply an external magnetic field

(i.e., put your sample in the magnet)



$$\omega = \gamma B_0 = \nu/2\pi$$

ω - resonance frequency
in radians per second,
also called Larmor frequency

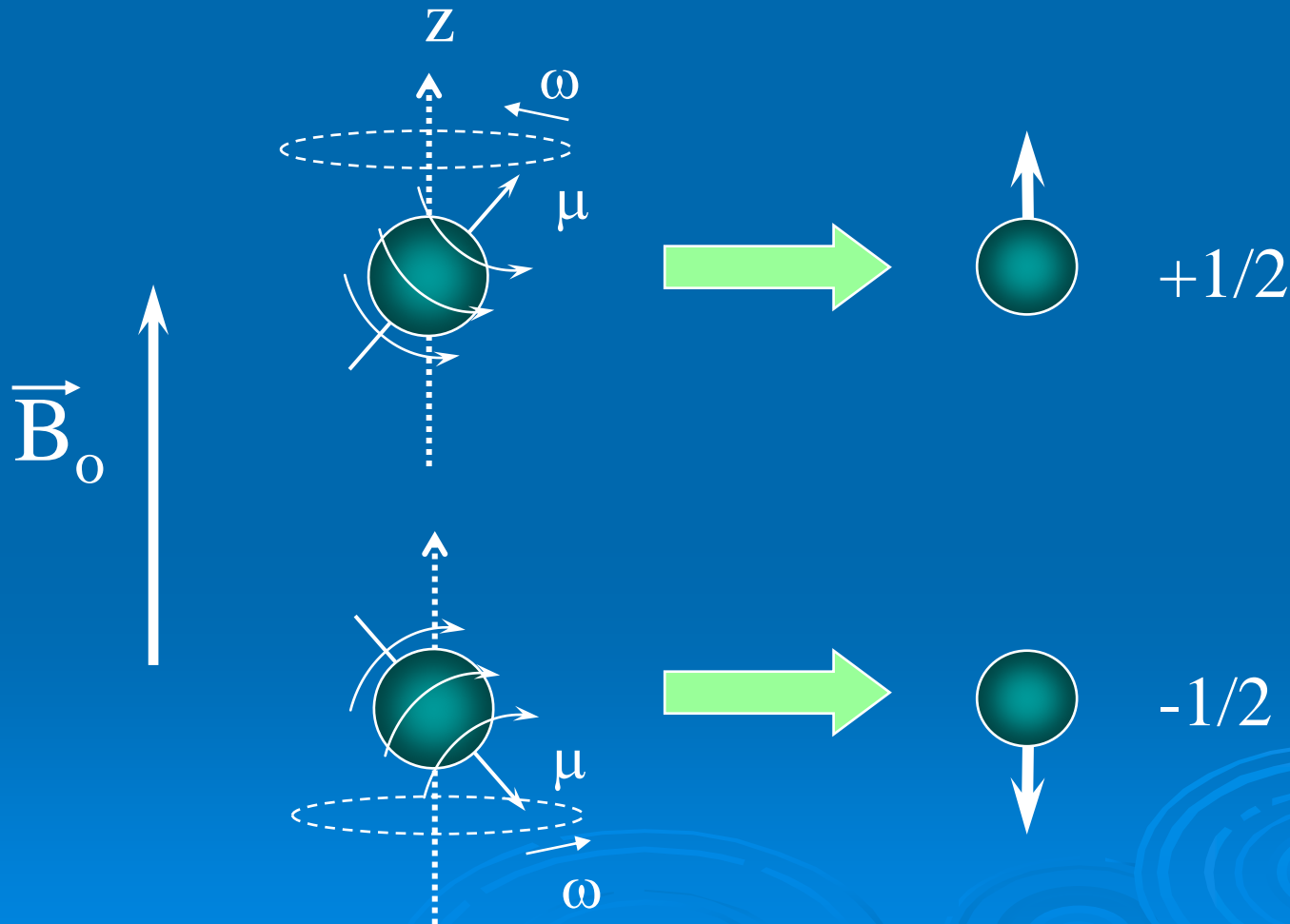
ν - resonance frequency
in cycles per second, Hz

γ - gyromagnetic ratio

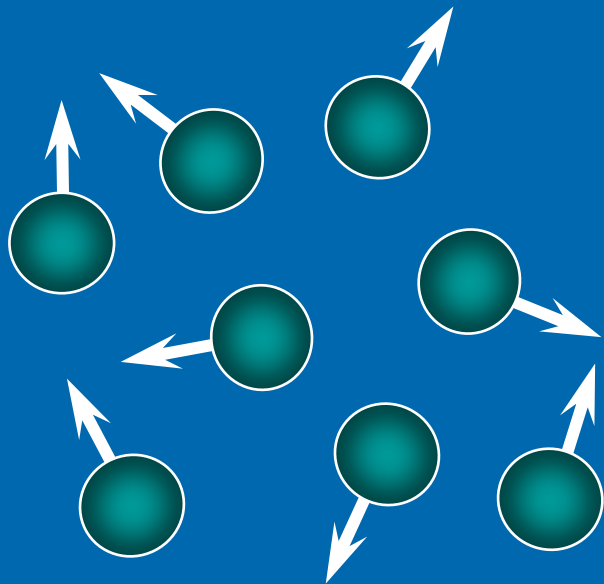
B_0 - external magnetic
field (the magnet)

Spin 1/2 nuclei will have two
orientations in a magnetic field
+1/2 and -1/2.

Net magnetic moment

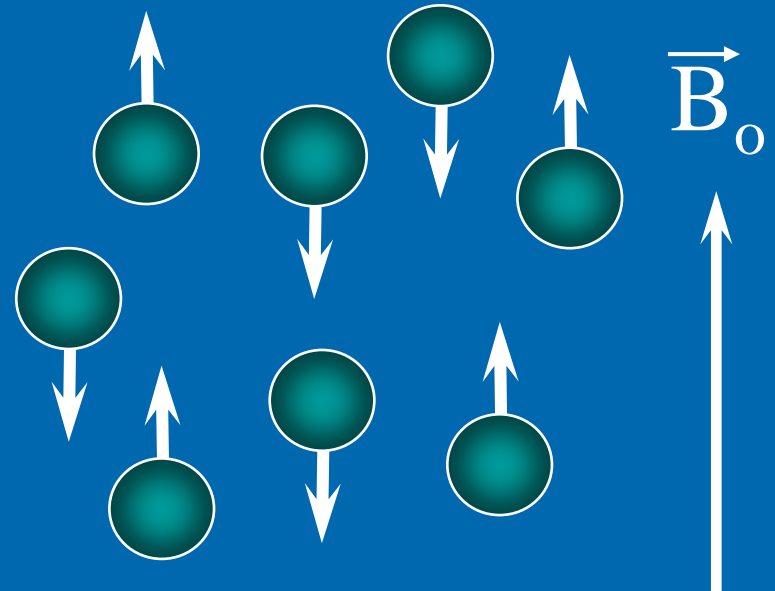


Ensemble of Nuclear Spins



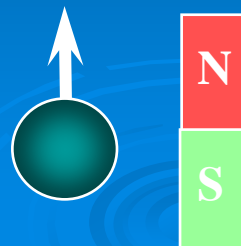
$$\vec{B}_0 = 0$$

Randomly oriented



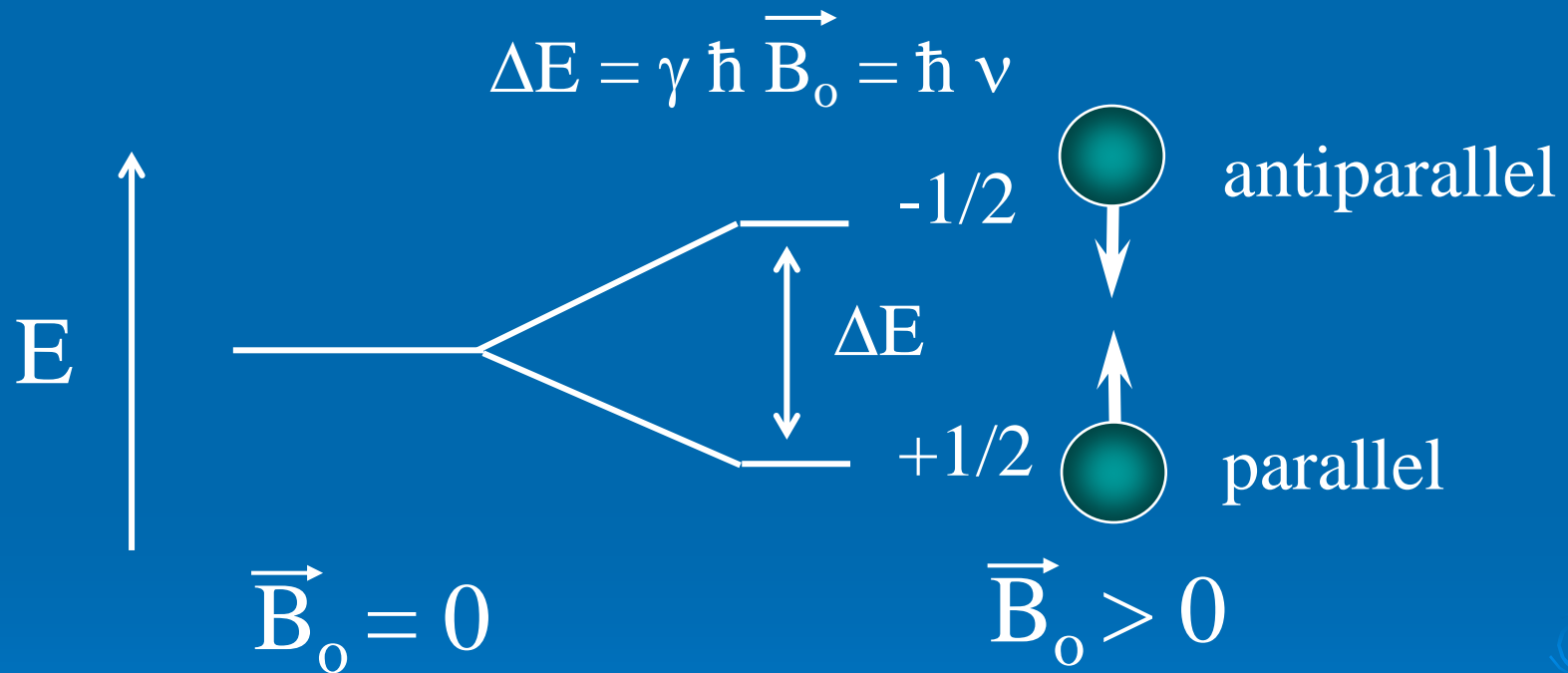
$$\vec{B}_0 > 0$$

Highly oriented



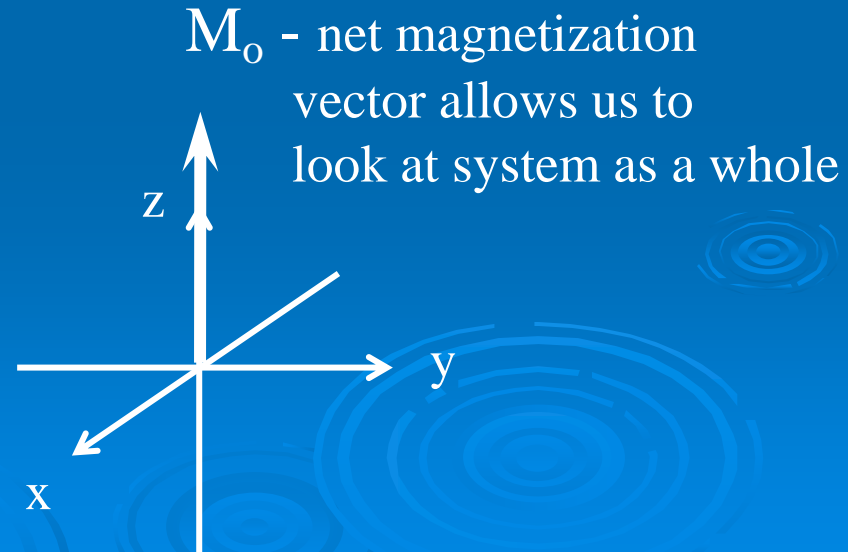
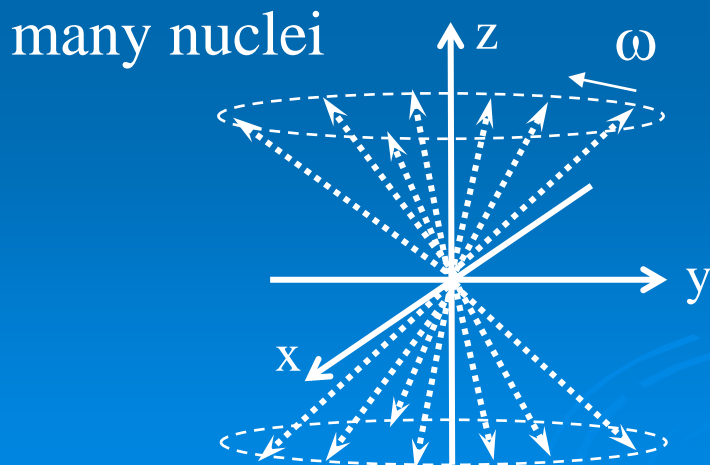
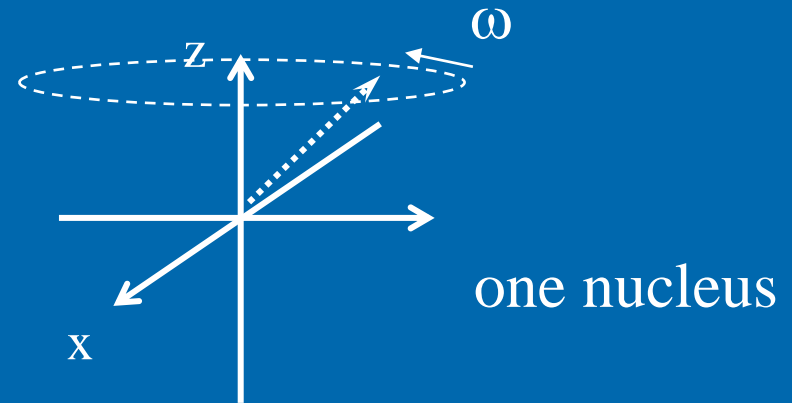
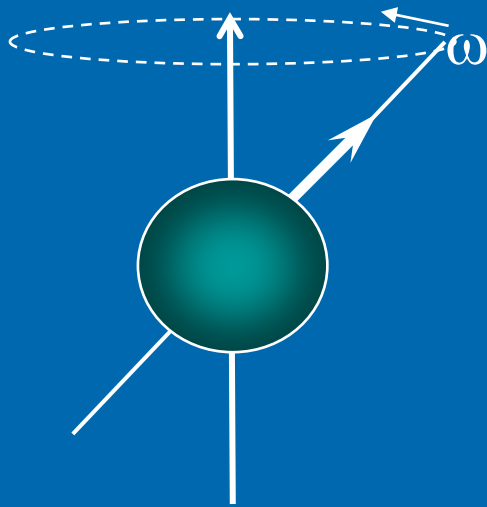
Each nucleus behaves like a bar magnet.

Allowed Energy States for a Spin 1/2 System



Therefore, the nuclei will absorb light with energy ΔE resulting in a change of the spin states.

The net magnetization vector





MR Imaging

Larmor Equation:

$$\omega = \gamma B_0$$

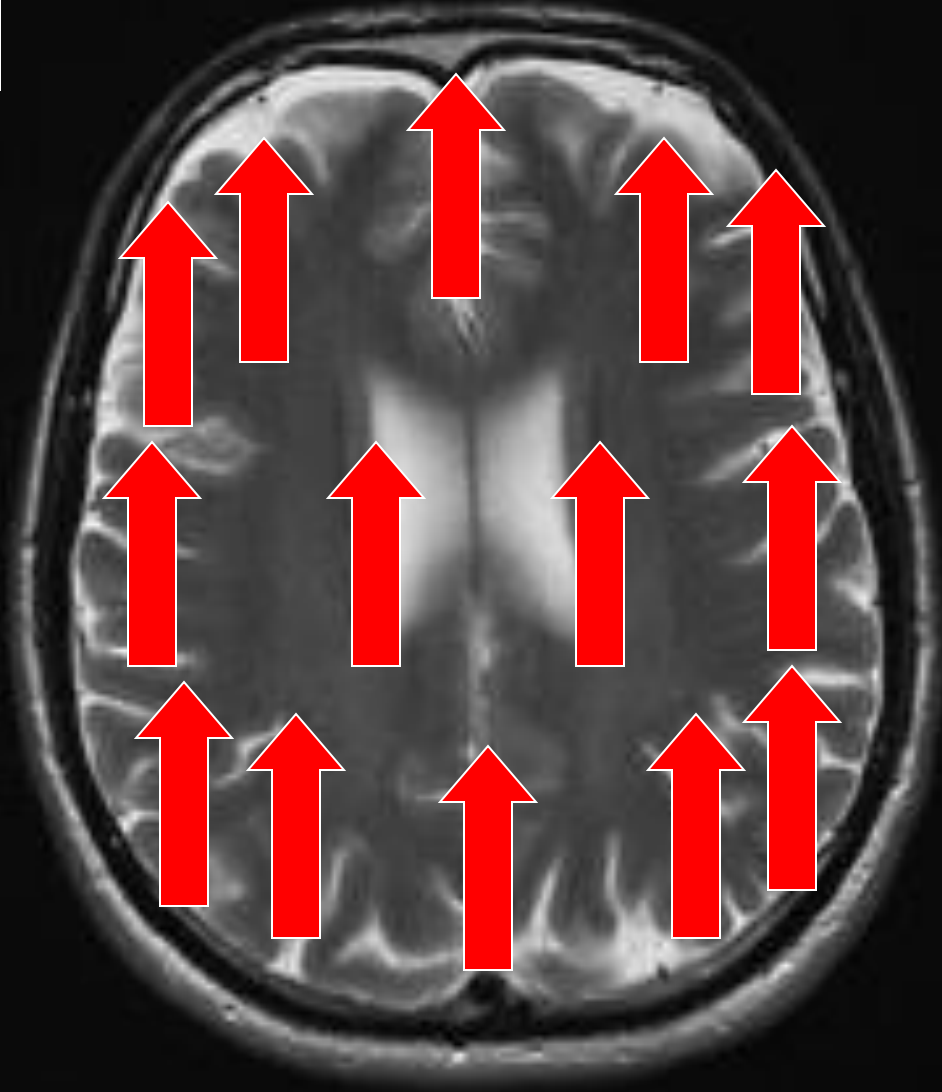
Larmor
Frequency

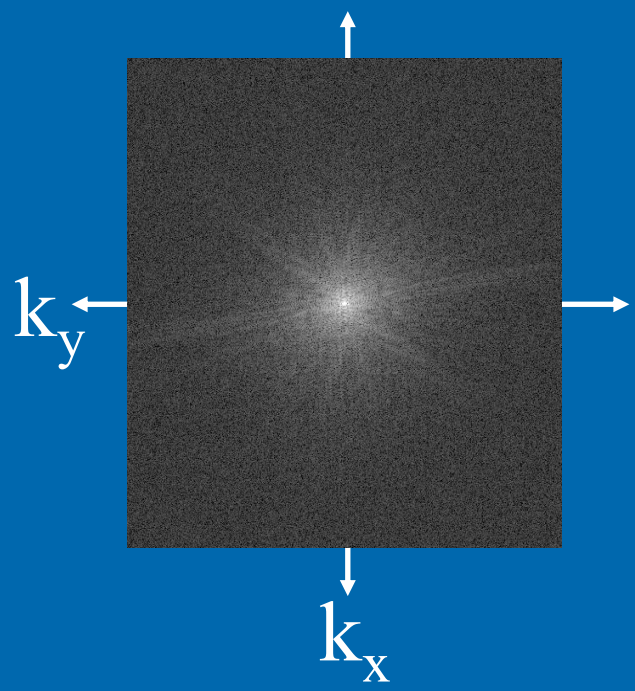
gyromagnetic
constant

Apply spatially
varying
frequency and phase
encoding magnetic
field gradients

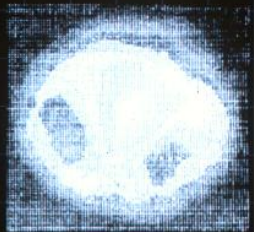


Water

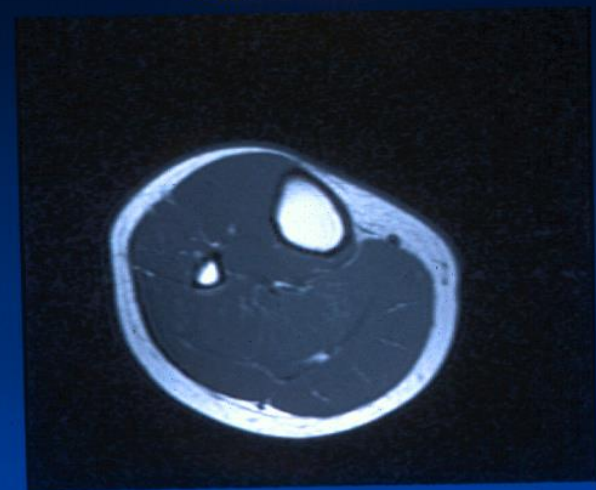




MRI: Day one



Recent MRI of Calf muscle



Magnetic Resonance Imaging (MRI)

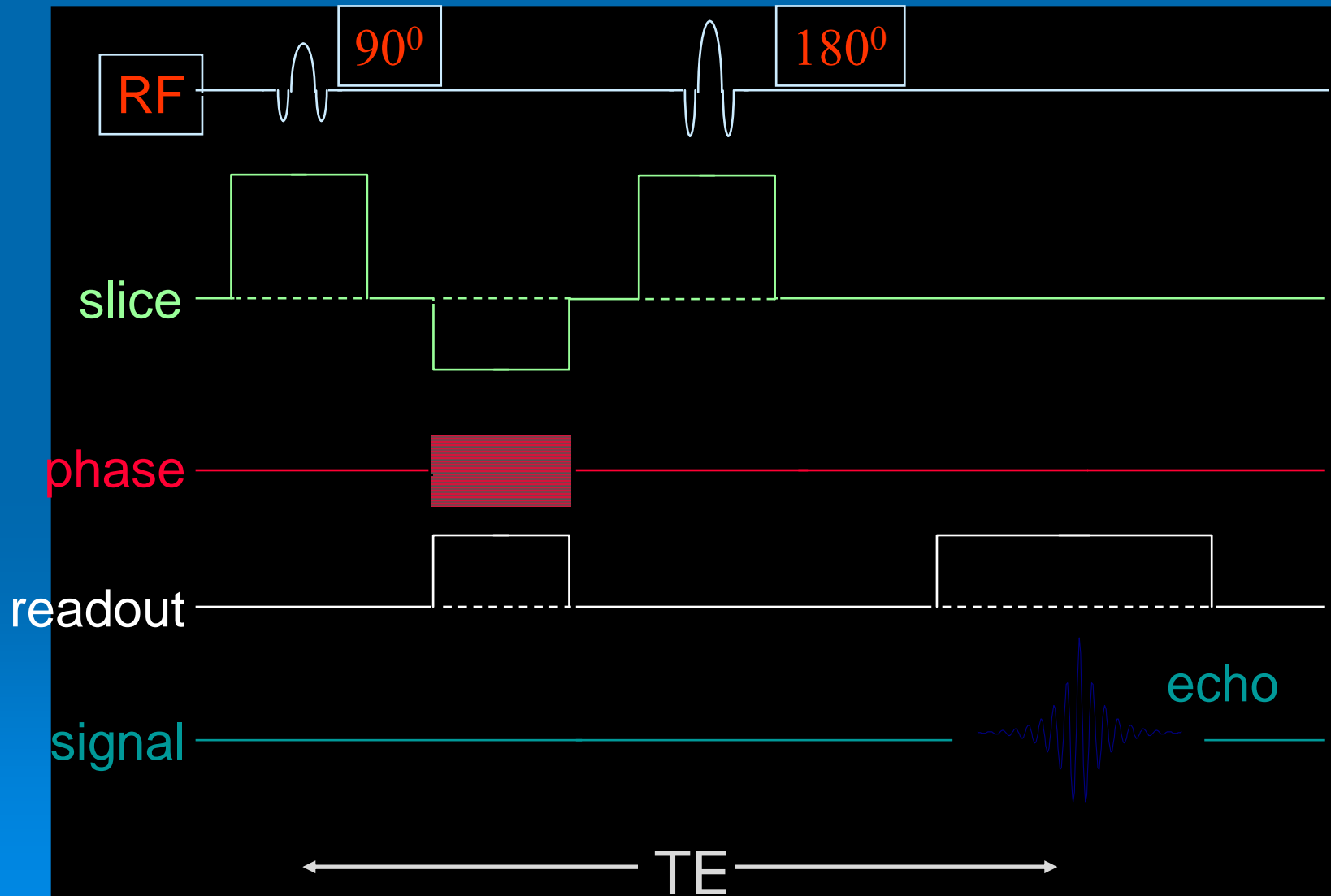
- MRI exploits Nuclear Magnetic Resonance (NMR) to produce water-based images
 - Signal from ^1H in water
 - Gray scale caused by T1/T2 relaxation and ^1H density within a voxel
- MRI resolution
 - 512x512 voxels in a slice
 - Sub-millimeter voxel volume
- Structural differences cause T1/T2 relaxation variation among voxels
 - No biochemical information

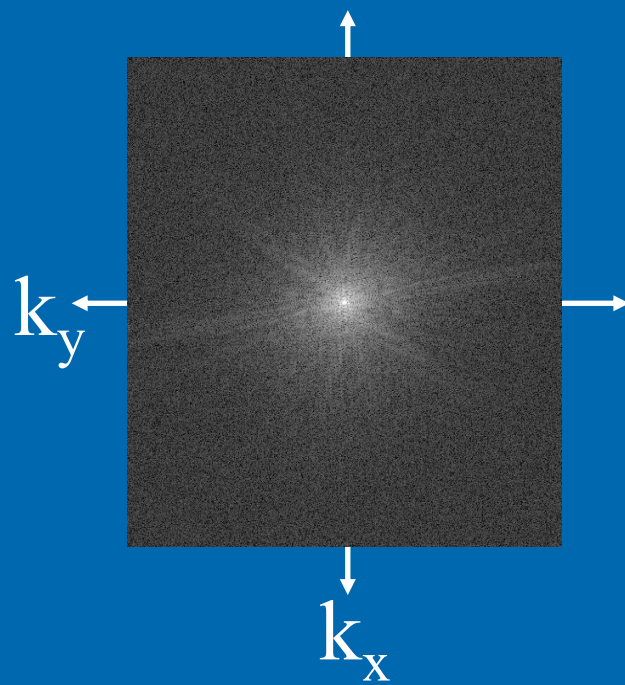


Magnetic Resonance Imaging

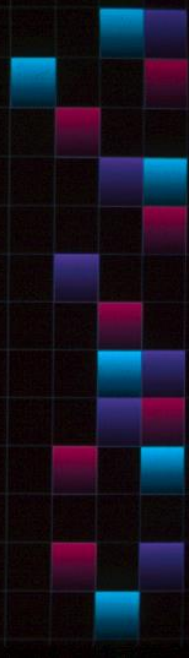
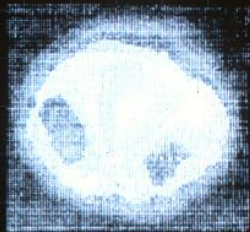
- provides anatomical images
- T1 and T2 Weighted MRI
- Contrast enhanced MRI
- MR Angiography (MRA)
- Interventional MRI (iMR)
- functional MRI (fMRI)
- Perfusion MRI
- Magnetization transfer (MT) MRI and Spin-locking
- Diffusion-weighted MRI (DWI) and DTI

Spin Echo MRI *pulse timing*

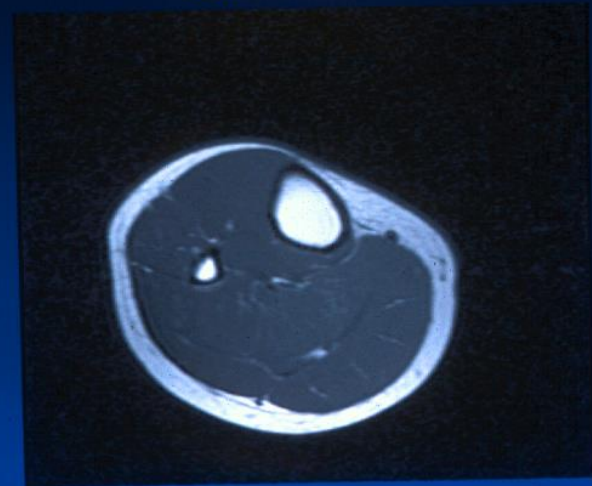




MRI: Day one



**Recent MRI of
Calf muscle**



Problems with Anatomical Imaging

- Despite its superb soft tissue contrast and multiplanar capability, anatomical MRI is largely limited to depicting morphological abnormality.
- Anatomical MRI suffers from nonspecificity. Different disease processes can appear similar upon anatomic imaging, and in turn a single disease entity may have varied imaging findings.
- The underlying metabolic or functional integrity of brain cannot be adequately evaluated based on anatomical MRI alone. To that end, several physiology-based MRI methods have been developed to improve tumor characterization.

Functional Imaging

- Four physiology-based MRI methods have been developed to improve tissue characterization:
- Diffusion Weighted (DW) MRI: In addition to early diagnosis of cerebral ischemia, DW MRI is extremely sensitive in detecting other intracranial disease processes, including cerebral abscess, traumatic shearing injury, etc.
- Perfusion Imaging: Dynamic susceptibility-weighted contrast-enhanced (DSC) perfusion MRI of the brain provides hemodynamic information.
- CEST/Para-CEST/APT: Recently developed new class of MR contrast agents
- MR Spectroscopy

In Vivo NMR Spectroscopy

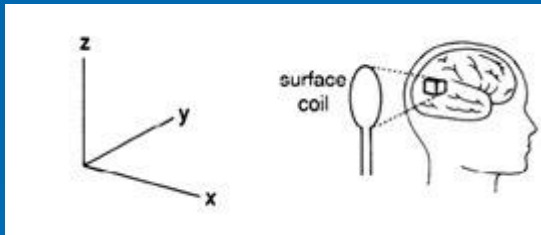
1987, *The British Journal of Radiology*, 60, 367-373

APRIL 1987

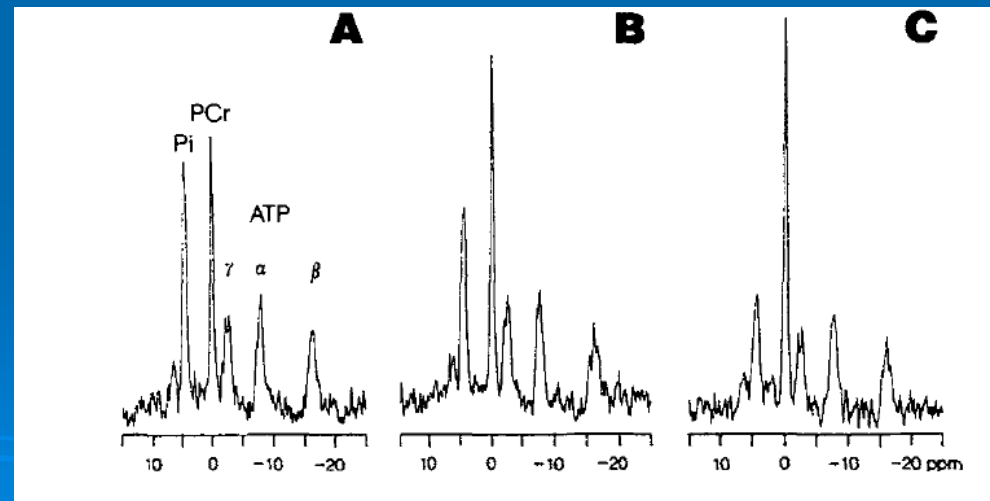
The study of human organs by phosphorus-31 topical magnetic resonance spectroscopy

By Rolf D. Oberhaensli, M.D., Graham J. Galloway, Ph.D., David Hilton-Jones, M.R.C.P., Peter J. Bore, F.R.C.S., Peter Styles, D.Phil., Bheeshma Rajagopalan, M.R.C.P., D.Phil., Doris J. Taylor, D.Phil. and George K. Radda, D.Phil., F.R.S.

MRC Clinical Magnetic Resonance Facility, John Radcliffe Hospital, Headington, Oxford OX3 9DU

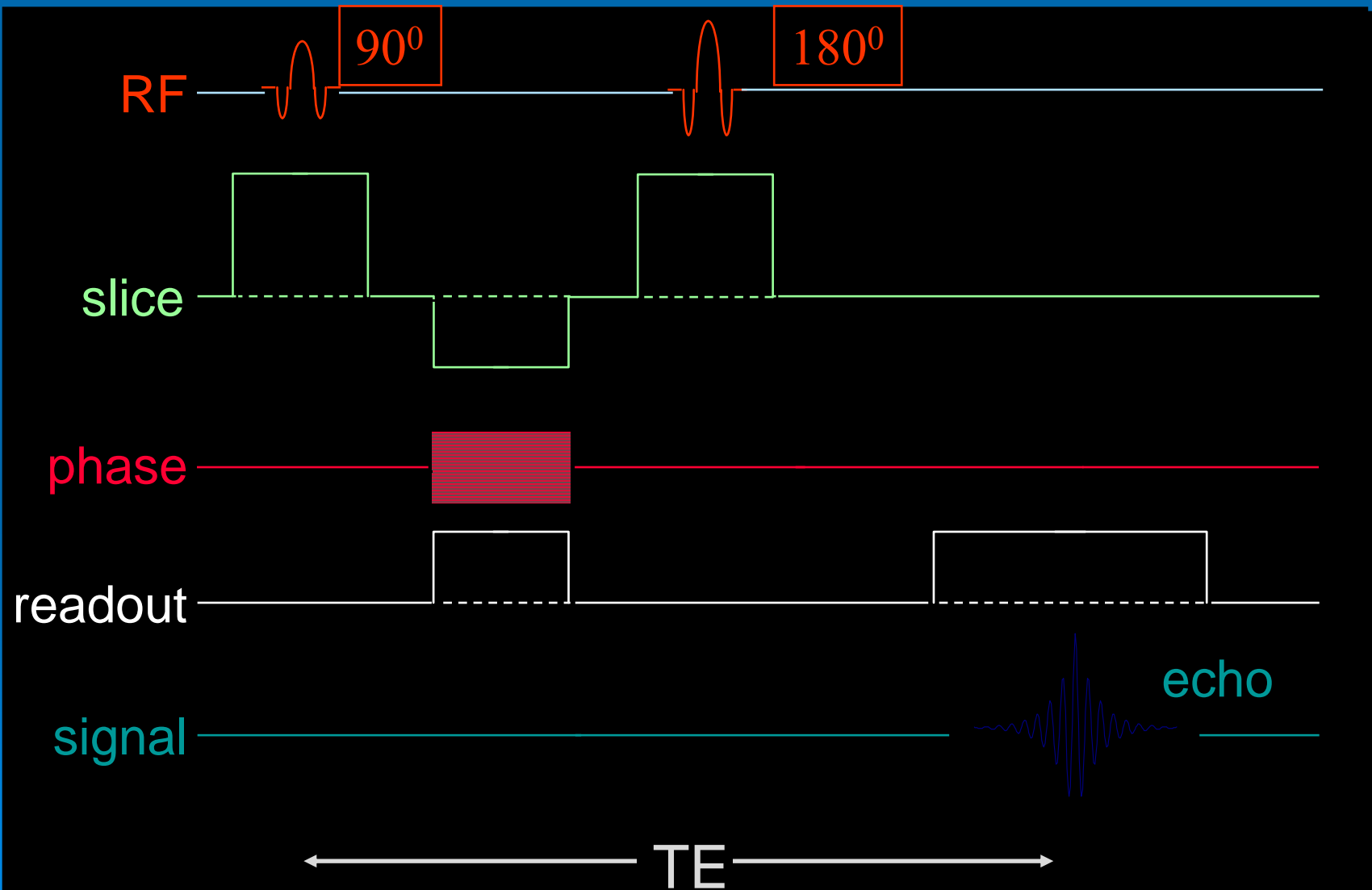


Typical 10-second spectra (2 FIDs) obtained from a single subject at the end of exercise (A) and at 15 (B) and 35 seconds (C) into the recovery period (different levels of work :2-18; 10 + 3.6) and reached different end-exercise force levels (64-599 J/min; 274 +- 125).



Lodi et al MAGMA 1997

Spin Echo MR Spectroscopy *pulse timing*



MR Spectroscopy

Larmor Equation:

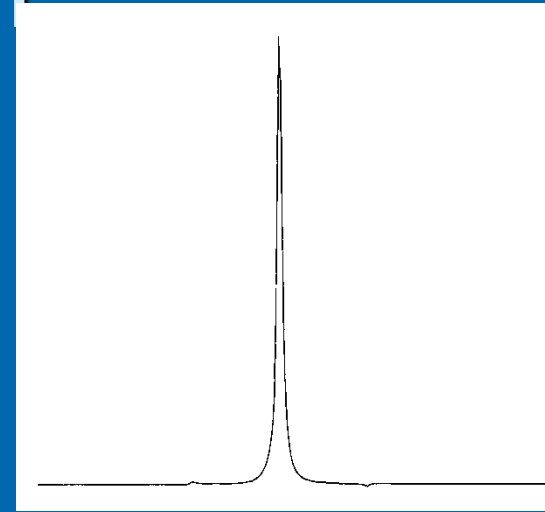
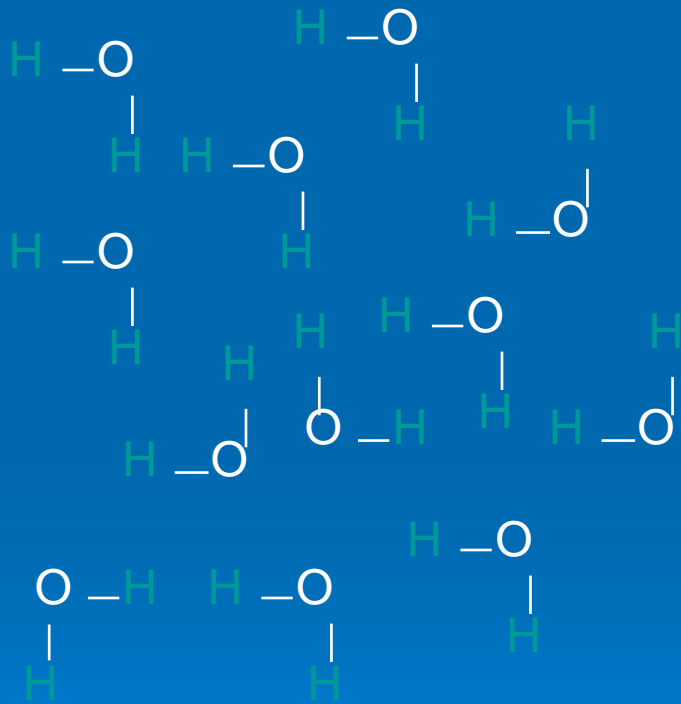
$$\omega = \gamma B_0$$

Larmor
Frequency

gyromagnetic
constant

Constant applied
external magnetic field

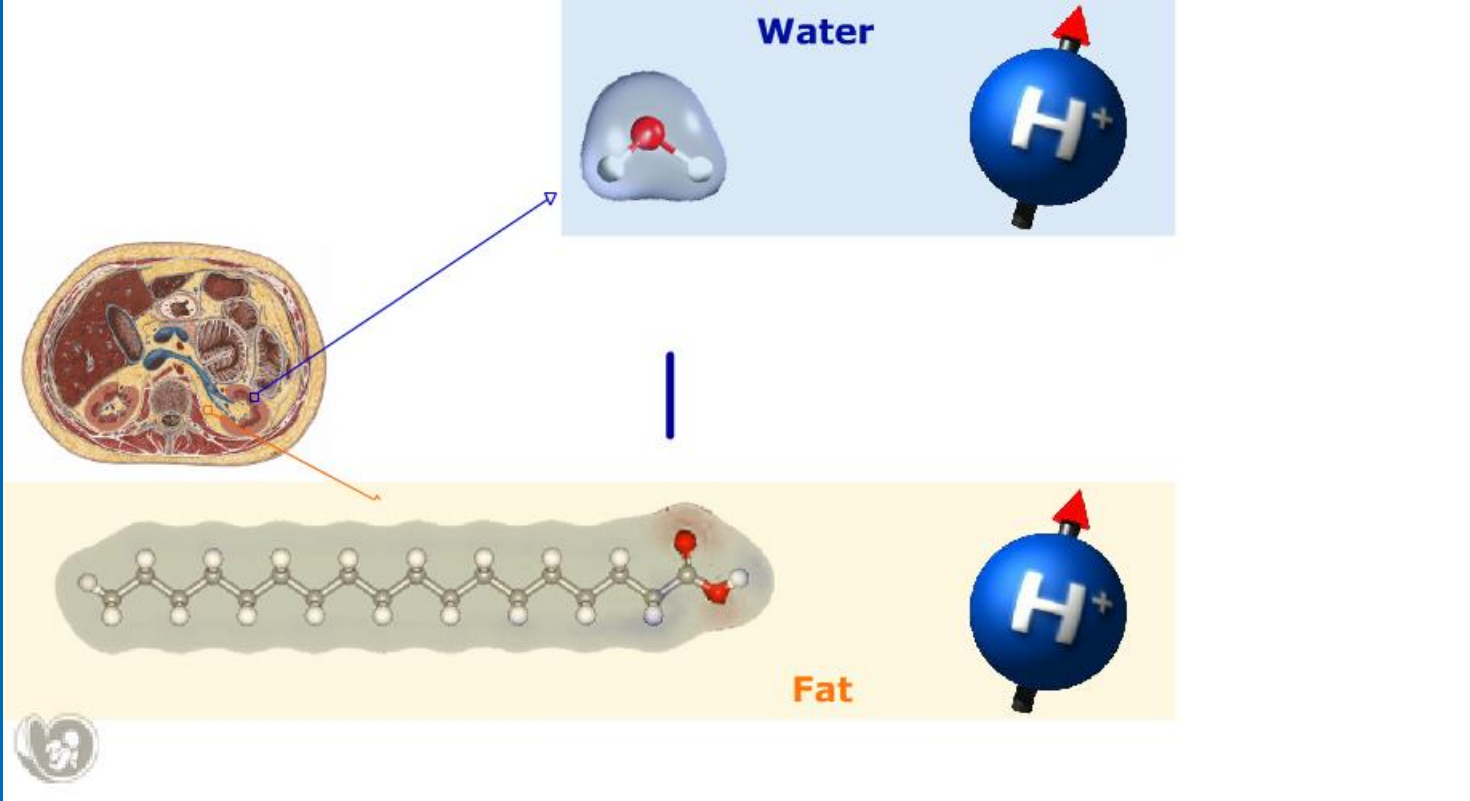
MR Spectrum

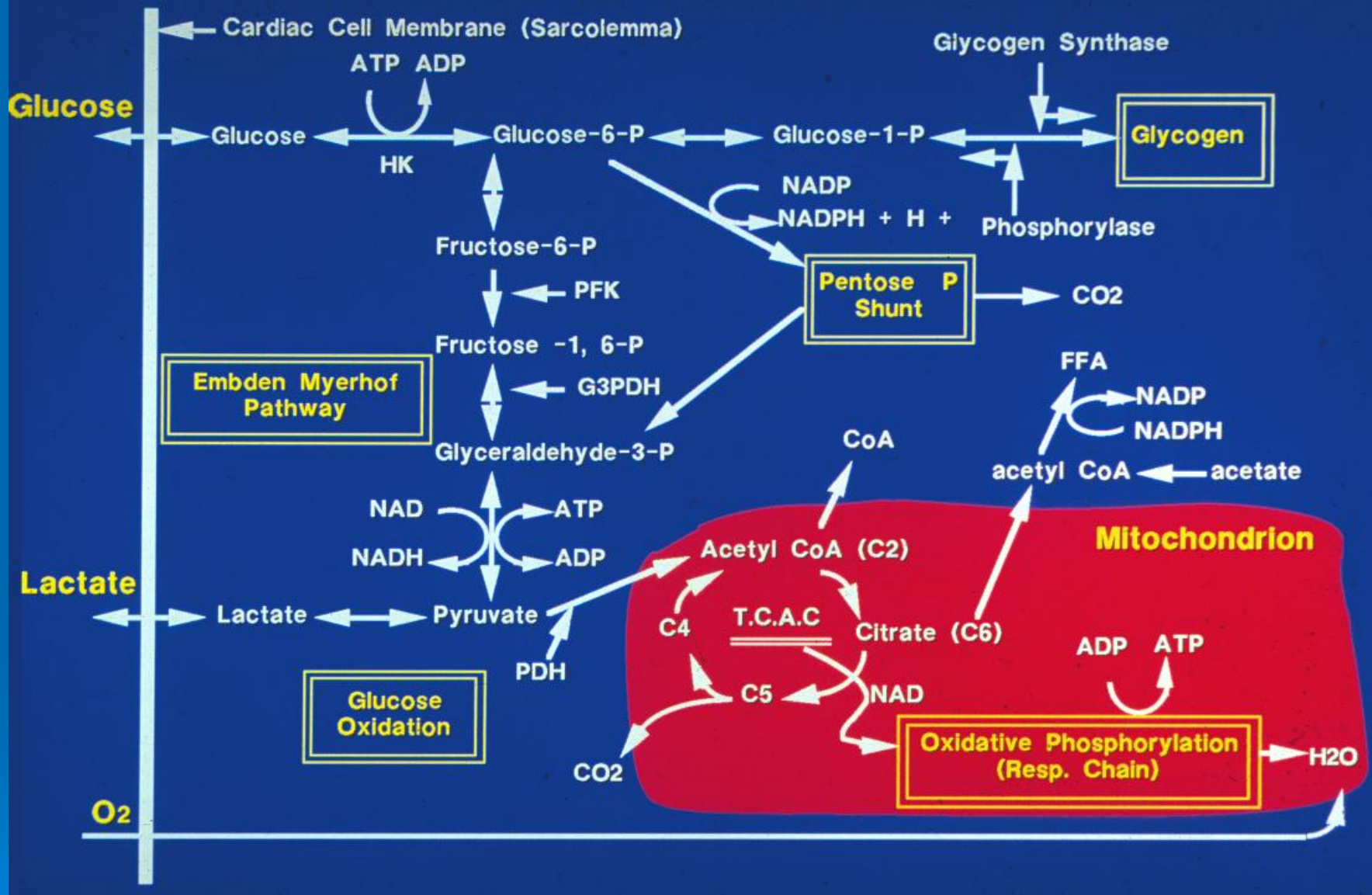


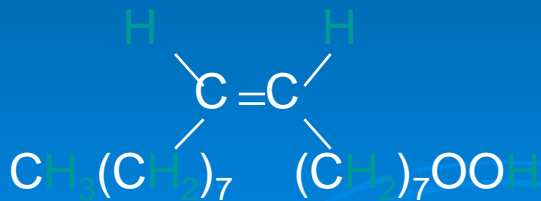
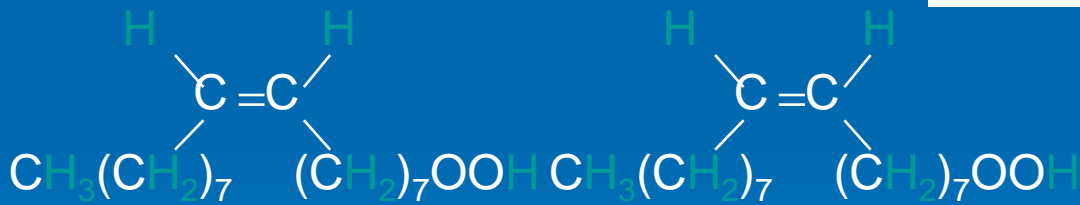
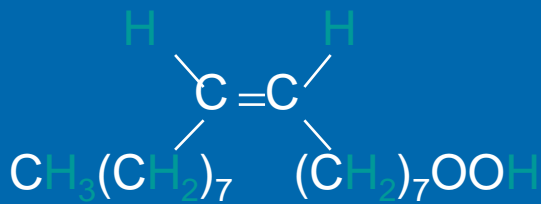
Area \propto # of spins

FWHM $\propto 1/T_2^*$

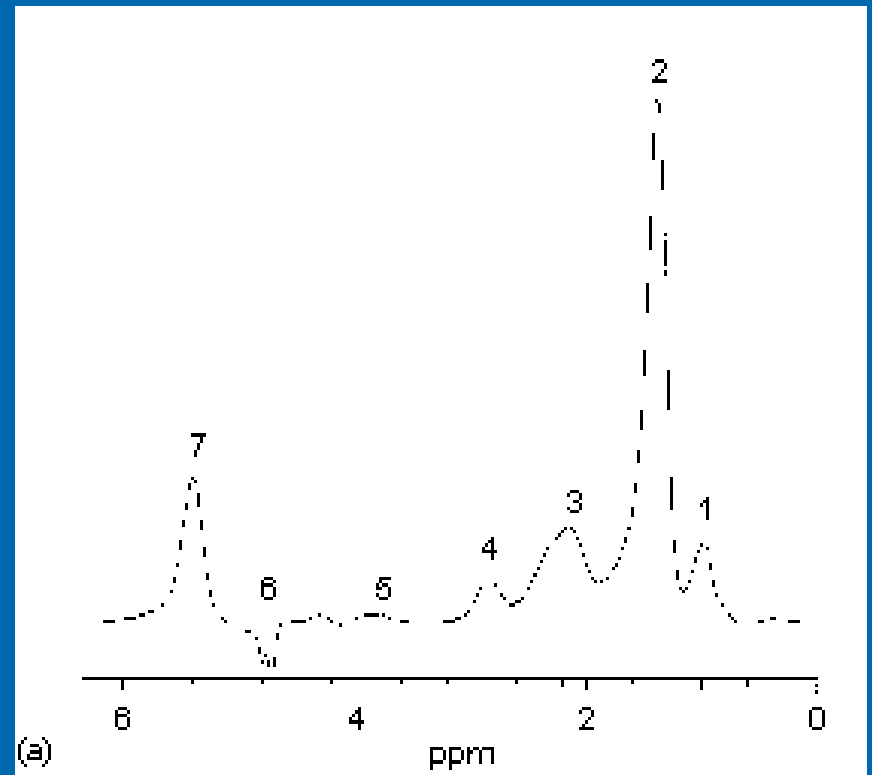
$$\omega = \gamma B_0 = \text{constant}$$







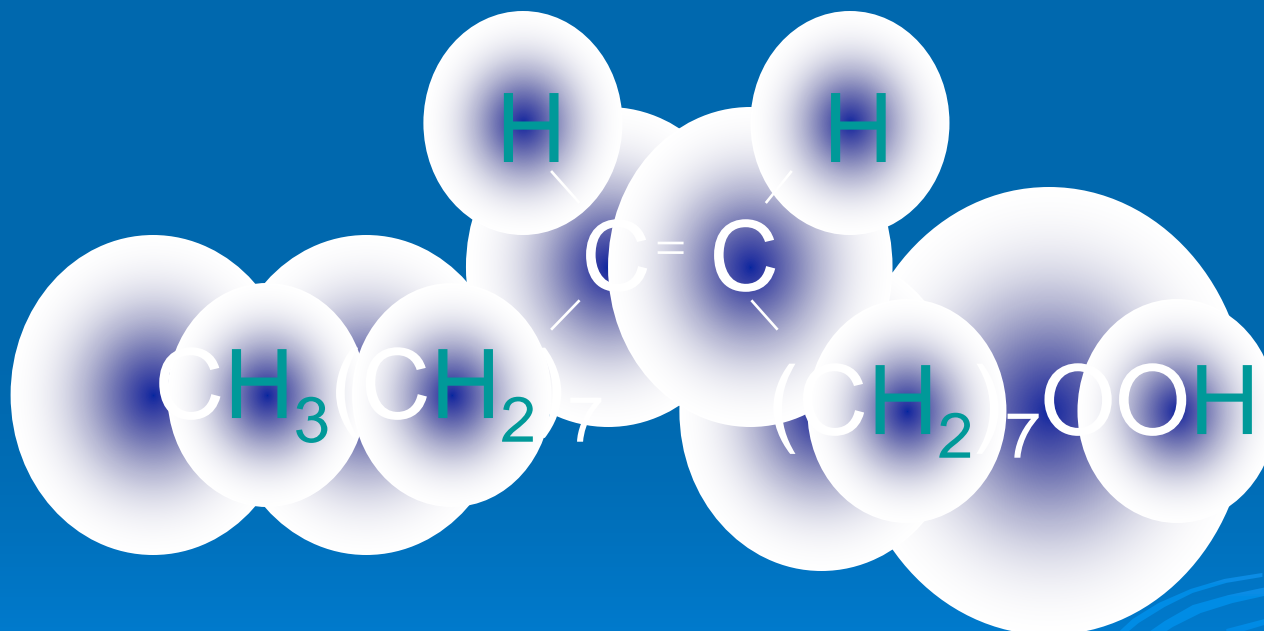
Oleic Acid (Corn Oil)



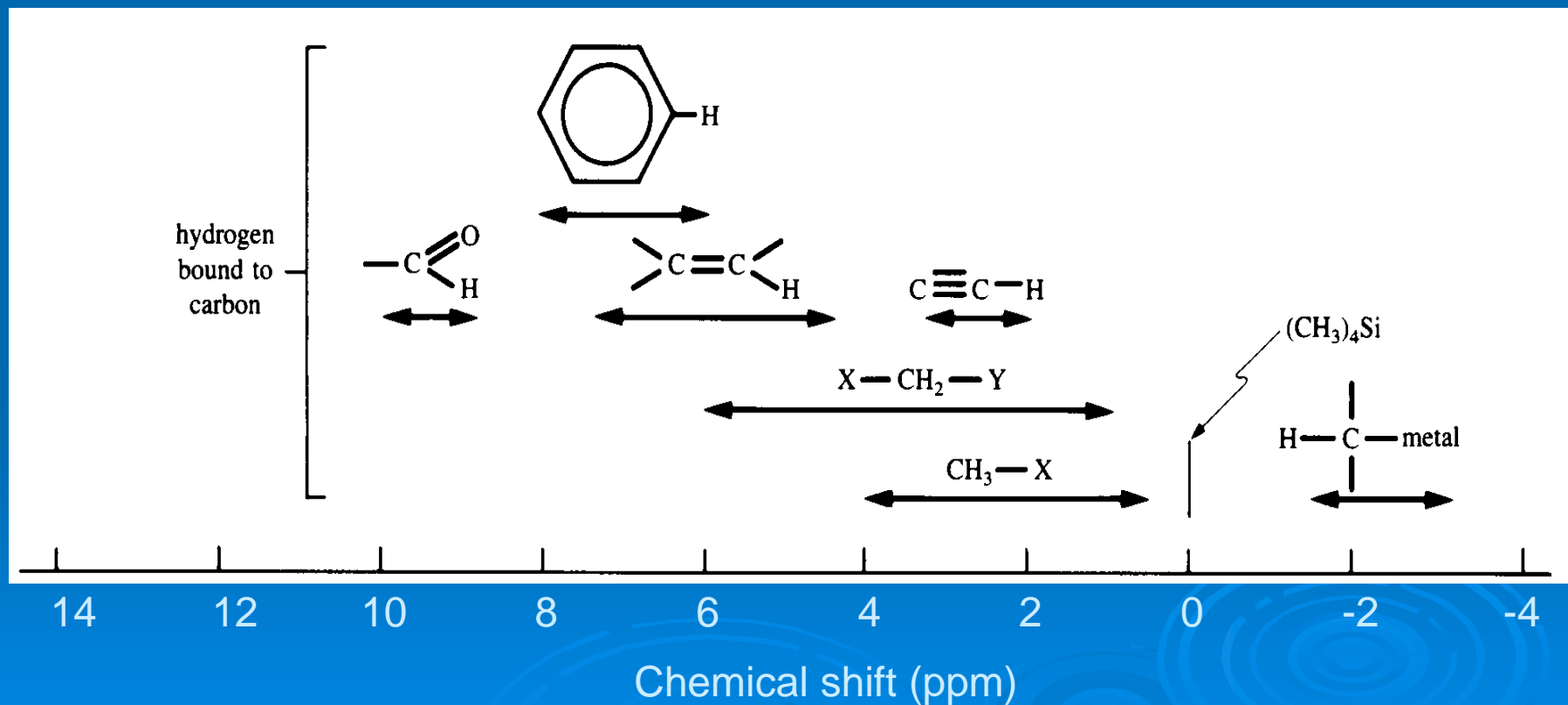
$$\omega = \gamma B_0 \neq \text{constant}$$

$$\omega = \gamma B_0(1 - \sigma)$$

shielding
constant



Chemical shifts of H bound to C



Chemical Shift

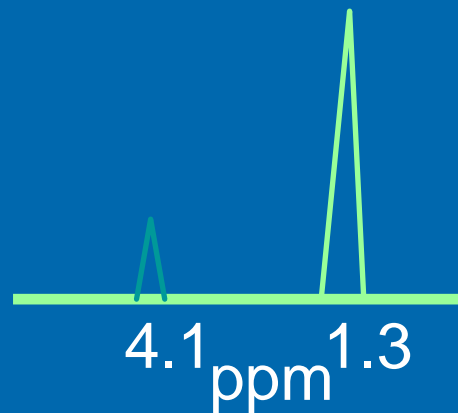
- The frequency shift increases with field strength. For example, shift difference between water and fat

$(\omega_{\text{water}} - \omega_{\text{fat}})$ at 1.5 T is 255 Hz at 3.0 T is 510 Hz

$$\delta = (\omega_{\text{water}} - \omega_{\text{fat}}) 10^6 / \gamma B_0, \text{ in ppm units}$$

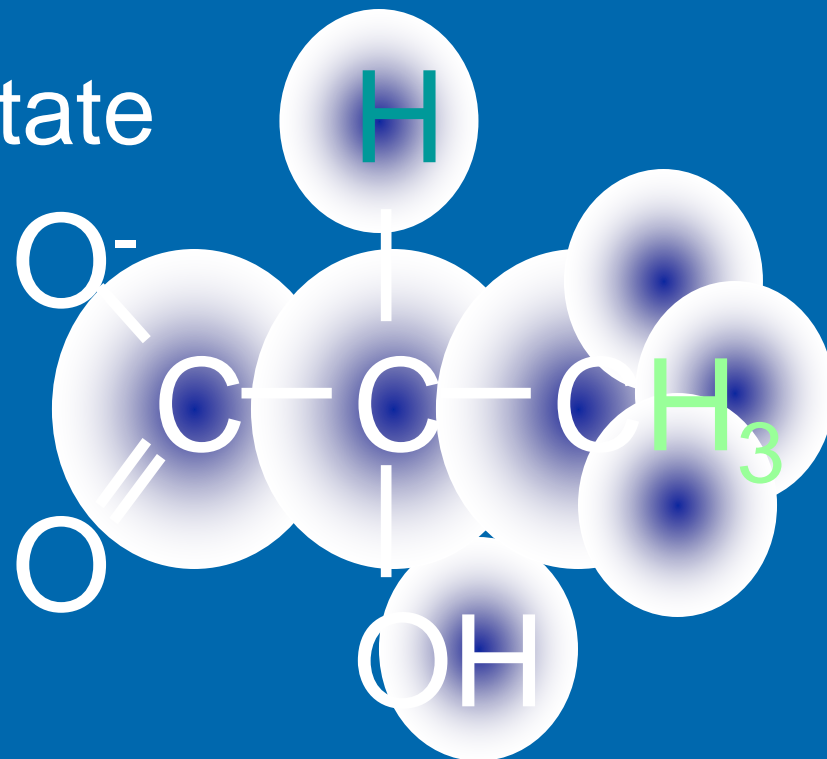
$\delta_{\text{water-fat}}$ is 3.5 ppm independent of field strength

- By convention
 - Signals of weakly shielded nuclei with higher frequency are on the left
 - Signals of more heavily shielded nuclei with lower frequency are on the right
- Chemical shift of water is set to 4.7 ppm at body temperature



Spectrum with shielding

Lactate



$$\omega = \gamma B_0$$



$$\omega = \gamma B_0 (1 - \sigma)$$

Indirect Spin-Spin Coupling (J-coupling)

$$\omega = \gamma B_0$$

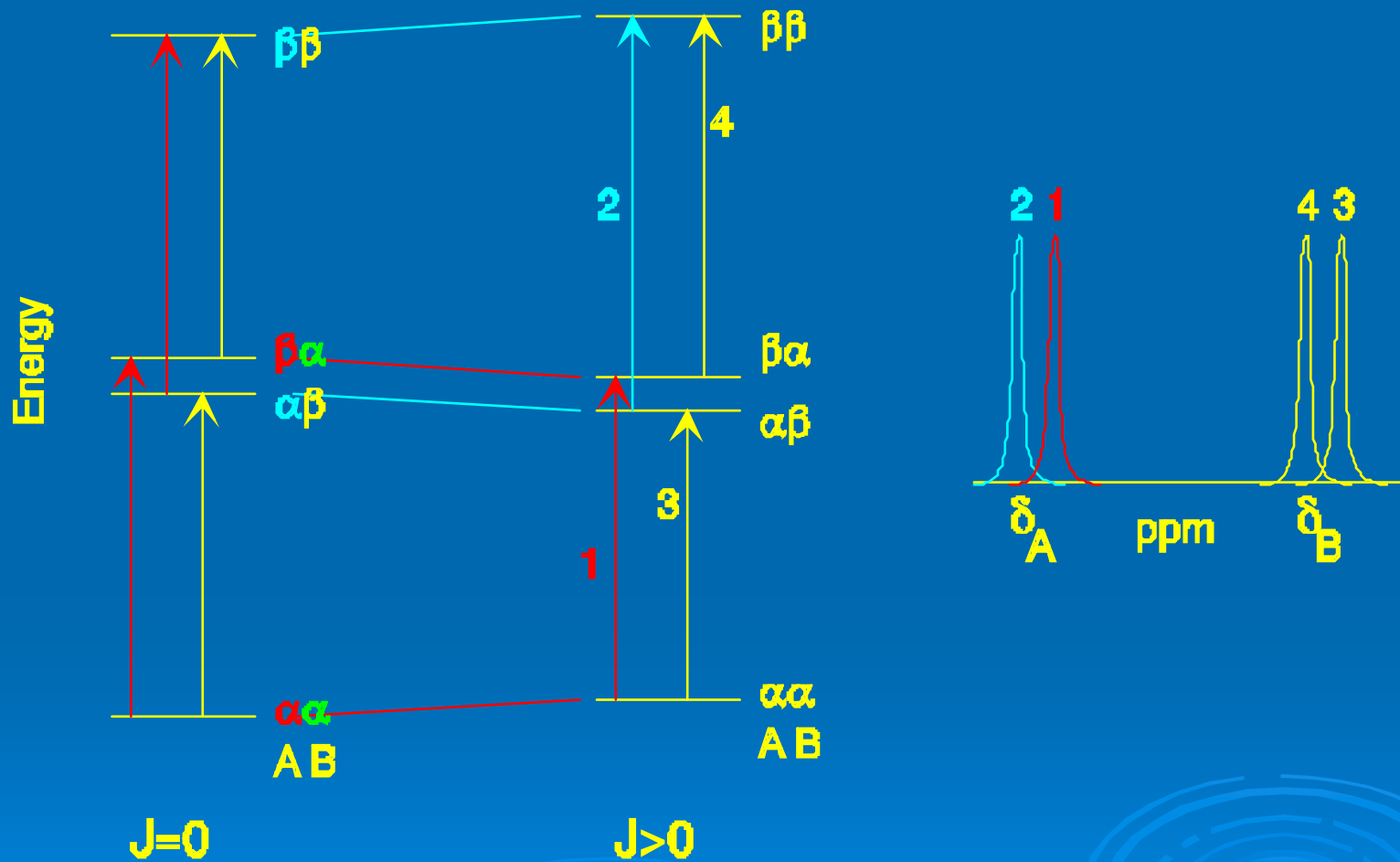


$$\omega = \gamma B_0(1 - \sigma)$$



$$\omega = \gamma B_0(1 - \sigma) + f(J)$$

Stationary Energy States

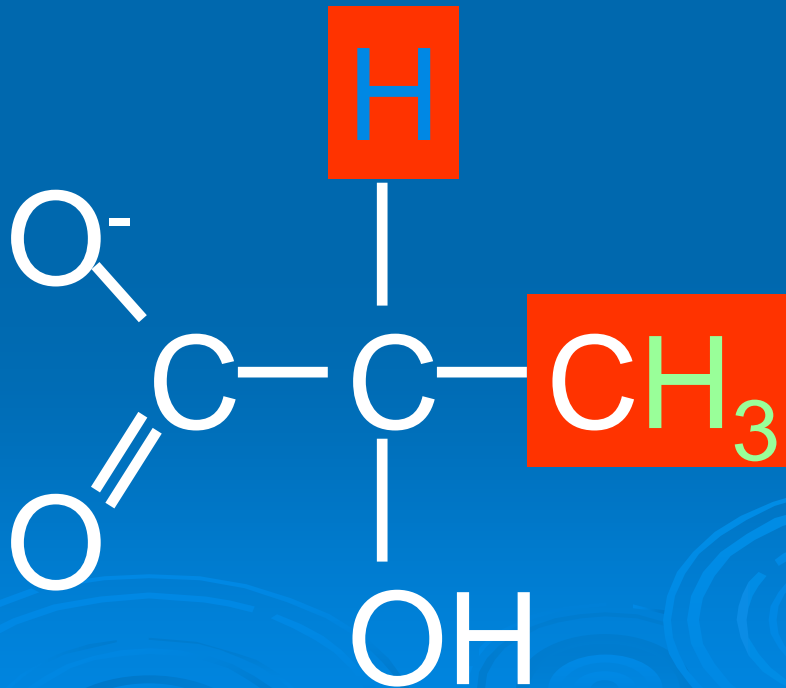


$$\omega = \gamma B_0$$



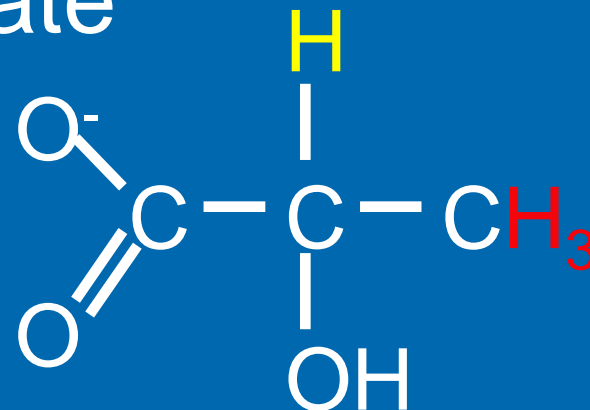
$$\omega = \gamma B_0 (1 - \sigma)$$

Lactate



Spin-spin coupling: acetate

The n+1 rule

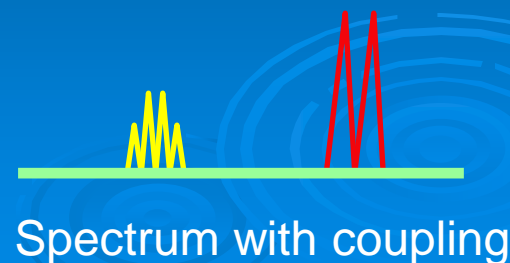
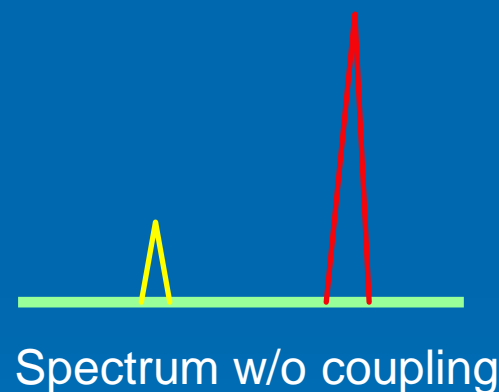


H_3 has $n=1$ neighbor H
which is in $n+1=2$ states :

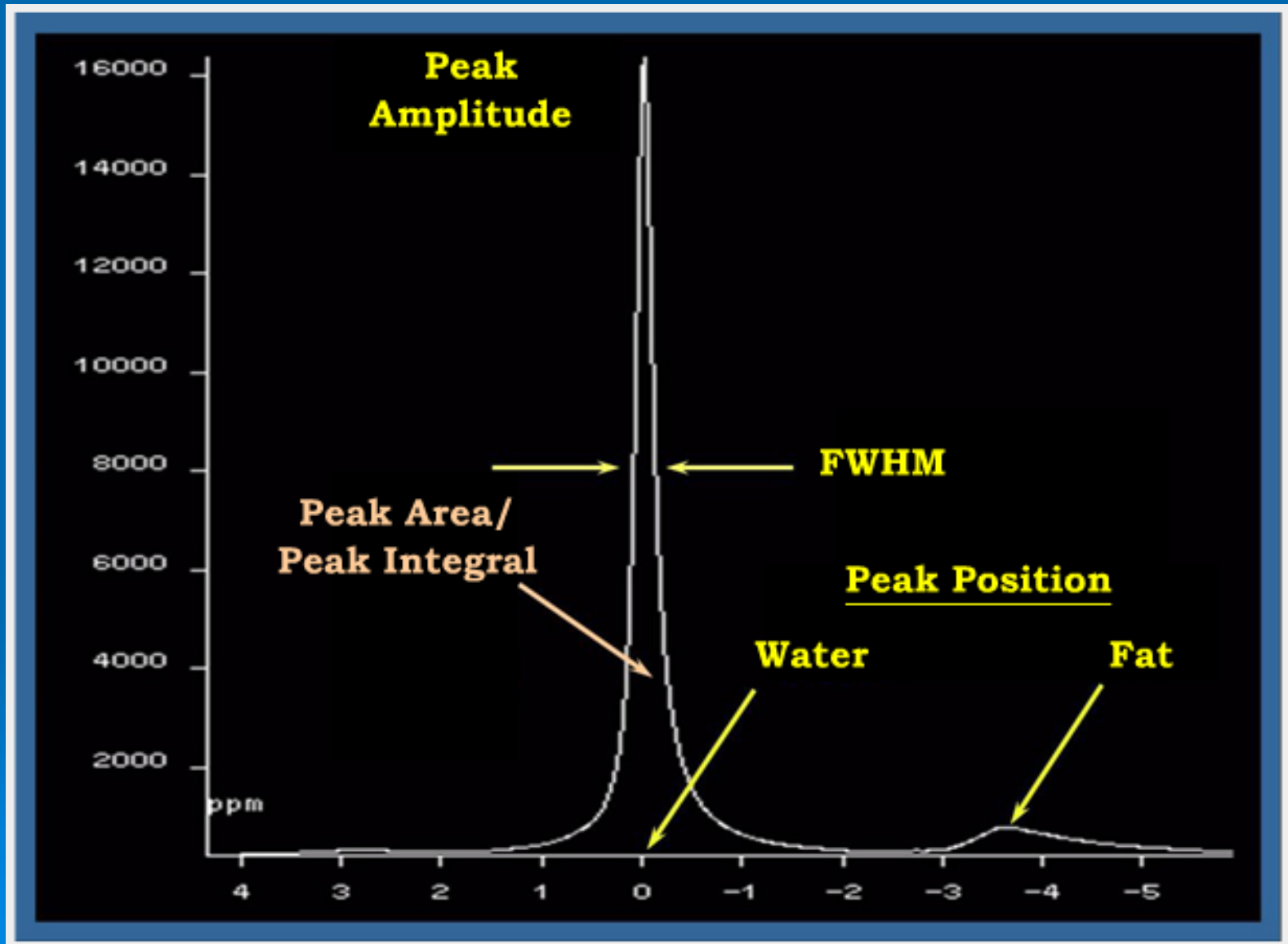
α ,	1
β	1

H has $n=3$ neighbors H_3
which are in $n+1=4$ states :

$\alpha\alpha\alpha$,	1
$\alpha\alpha\beta$, $\alpha\beta\alpha$, $\beta\alpha\alpha$,	3
$\alpha\beta\beta$, $\beta\beta\alpha$, $\beta\alpha\beta$,	3
$\beta\beta\beta$	1

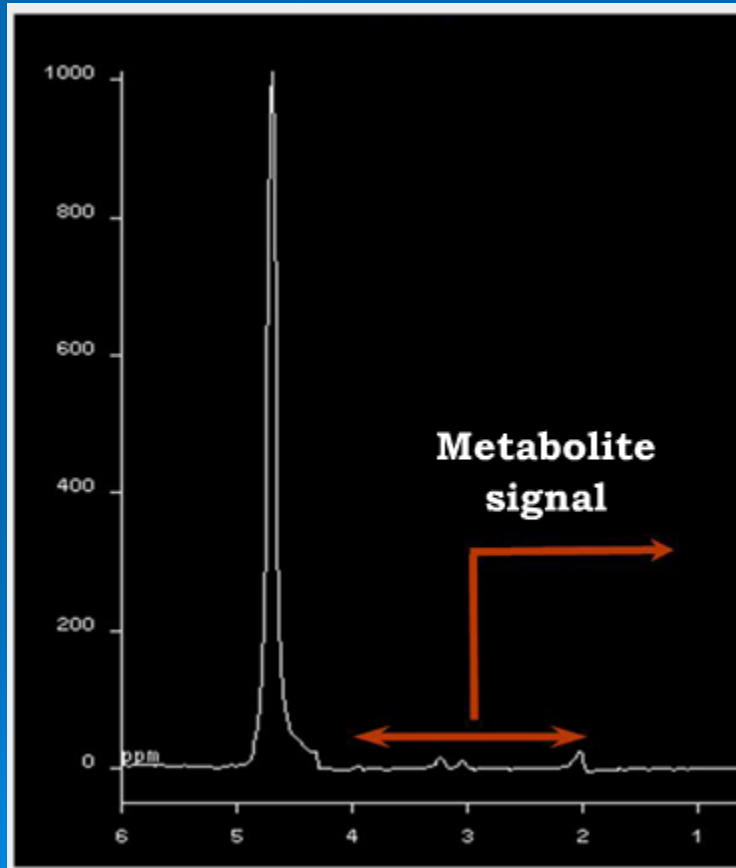


MR Spectrum: Peak Characteristics

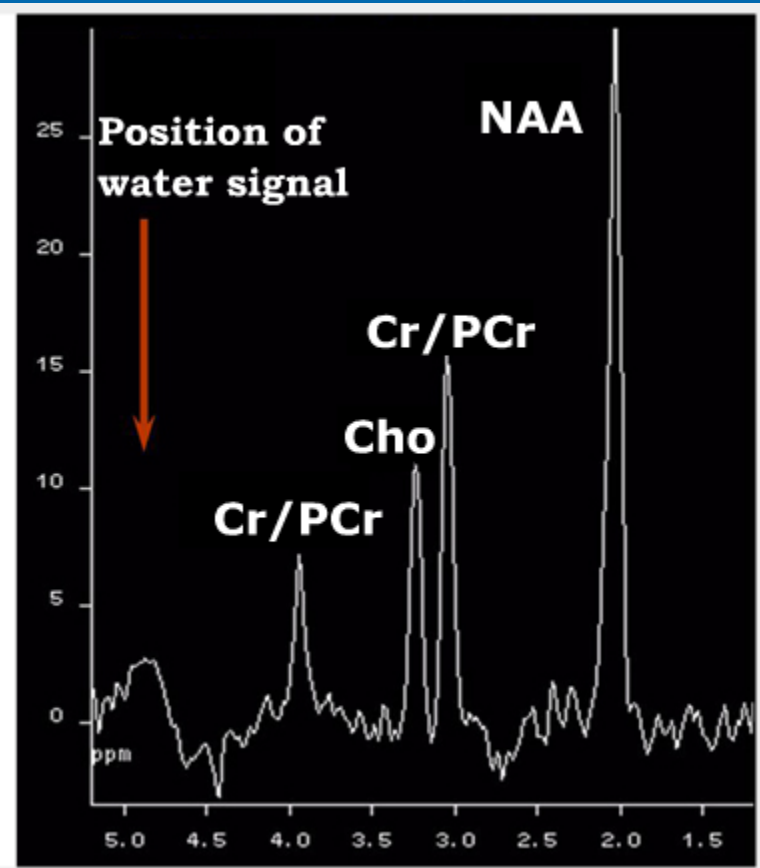


^1H MR Spectrum from Brain

Water Signal



Metabolite Signals



Cerebral metabolites

N-acetyl aspartate

Neuronal marker

Glutamate

Excitatory neurotransmitter

Creatine/Phosphocreatine

Supplier of phosphate to convert
ADP to ATP

Glutamine

Product of reaction of Glu with ammonia.

Choline

Total cerebral choline including neuro-
transmitter acetylcholine, phospho-
choline, and phosphotidylcholine

Glucose

Energy source.

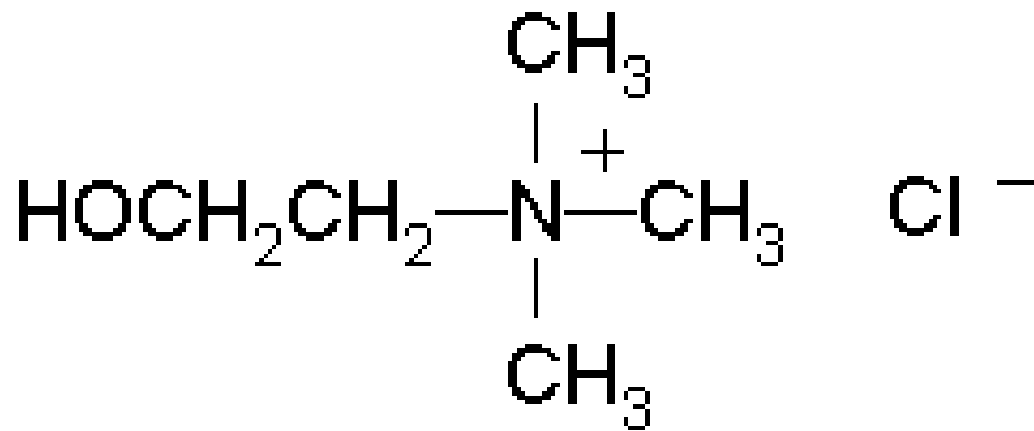
Myo-inositol

Storage form of hormonal messenger
inositol diphosphate

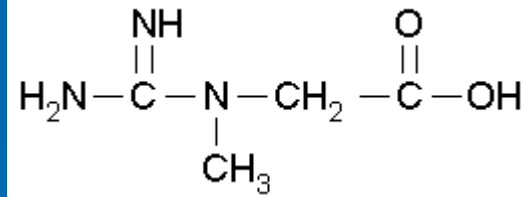
Lactate

End product of anaerobic glycolysis

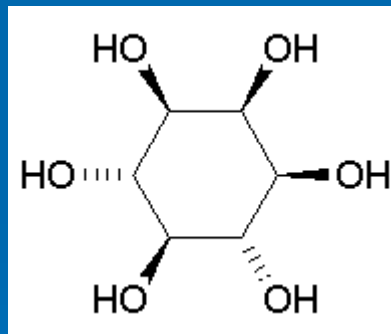
Choline



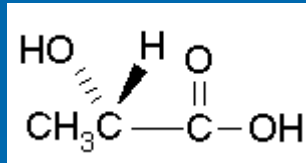
Creatine



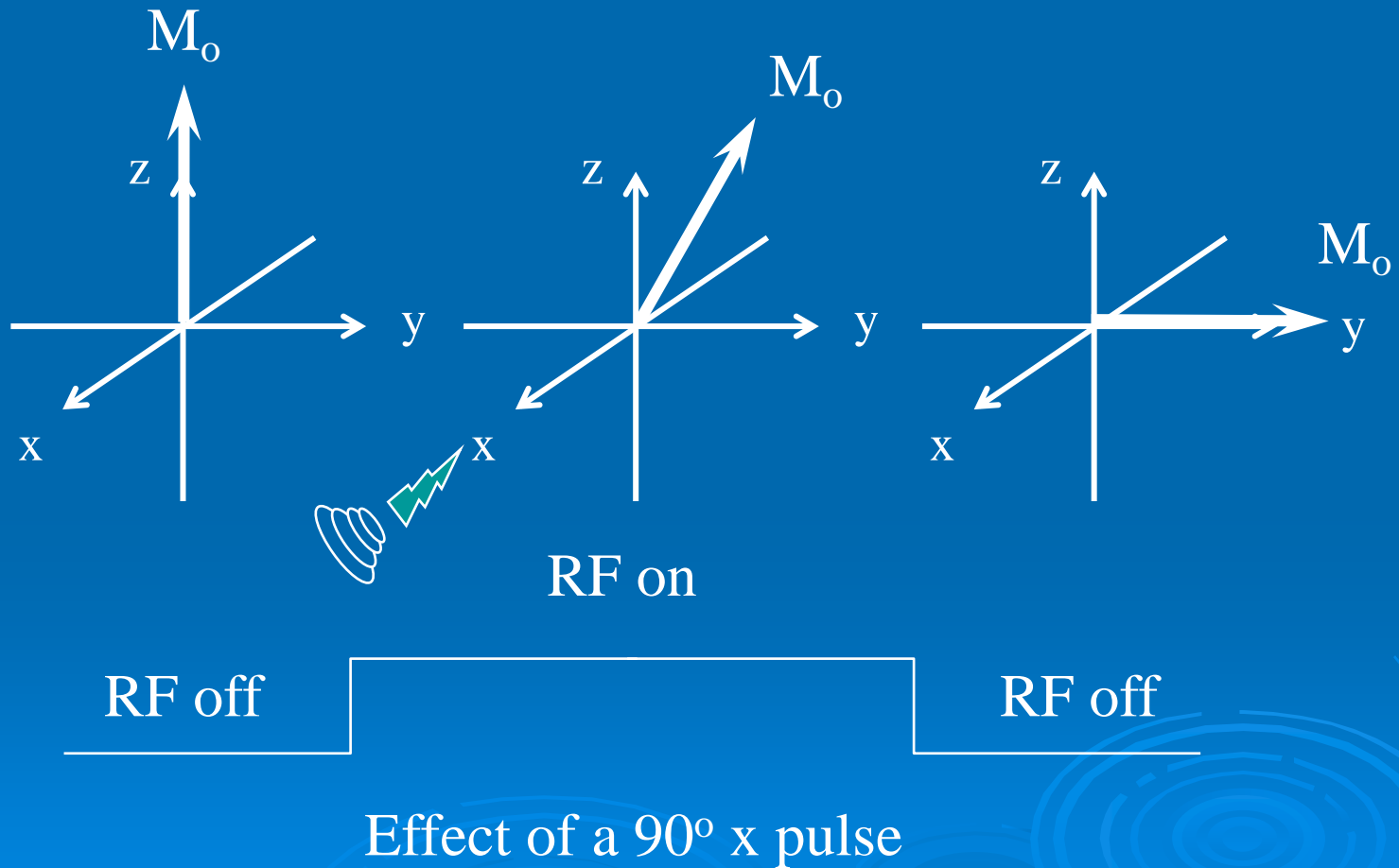
Myo-Inositol



Lactate



Nuclear Spin Dynamics



Excitation

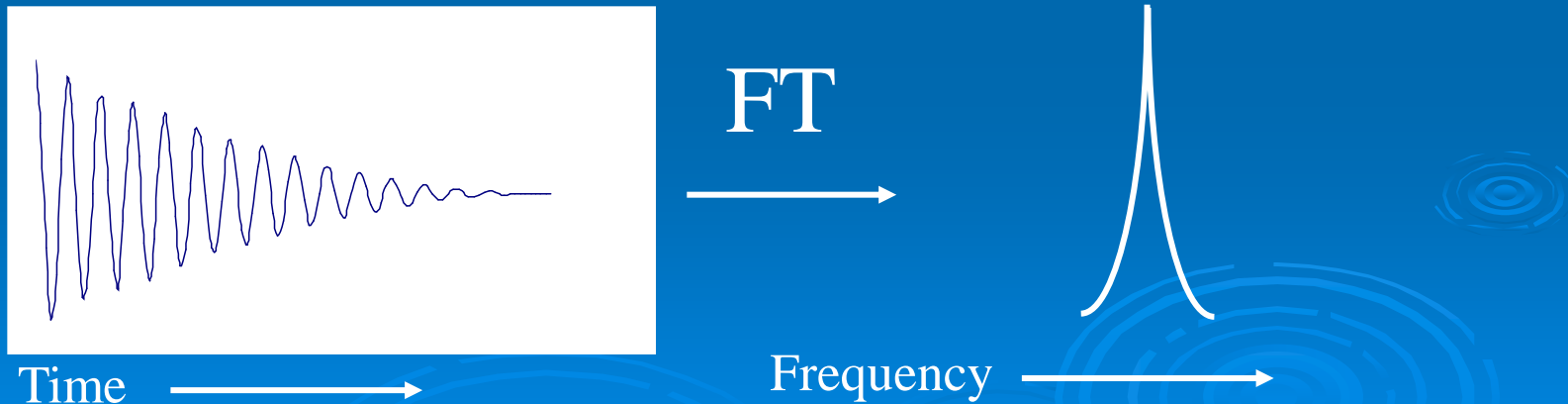
- When a nucleus is in B_0 the initial population of energy levels are determined by thermodynamics as described by the Boltzmann distribution
 - Lower energy levels will contain slightly more nuclei than the higher level
- Nuclear magnetization can only be observed by rotating the net longitudinal magnetization towards or onto the transverse plane
 - This can be accomplished by applying a second magnetic field in the transverse plane oscillating at the Larmor frequency

Free Induction Decay

The signals decay away due to interactions with the surroundings.

A free induction decay, FID, is the result.

Fourier transformation, FT, of this time domain signal produces a frequency domain signal.



Signal detection

- In principle, Signal intensity generated by a class of nuclei is linearly proportional to the number of nuclei in the sample
- In NMR peaks may be broadened by T_2^* losses, which is caused by spin-spin coupling and B_0 inhomogeneities

Signal detection

➤ Spectral Resolution

$$\text{Spectral Resolution} = \frac{1}{(\# \text{ complex points}) * \Delta t}$$

➤ MRI

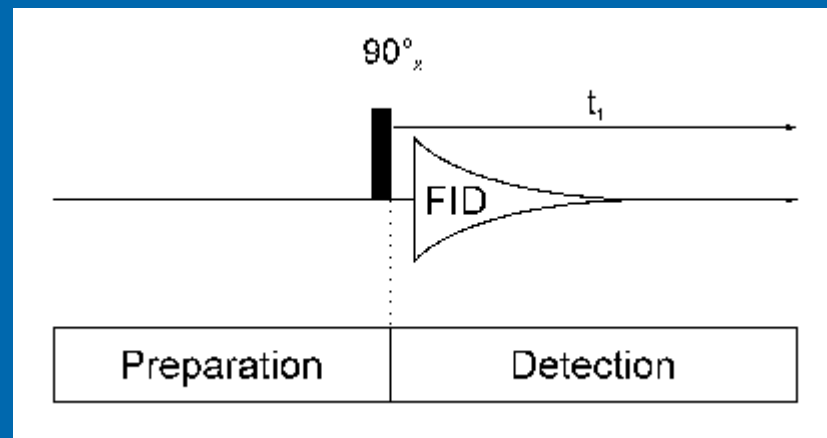
- 64, 128 or 256 complex points, short acquisition time
- Low spectral resolution (~350 Hz)
 - Limited to water and lipid concentration

➤ MRS

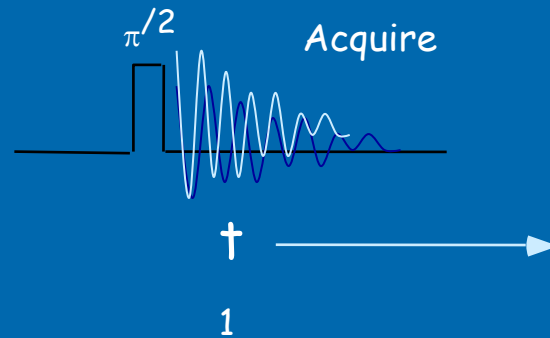
- 256-2048 complex points
- Much high spectral resolution (8-25 Hz)

1D NMR

Pulse Sequence



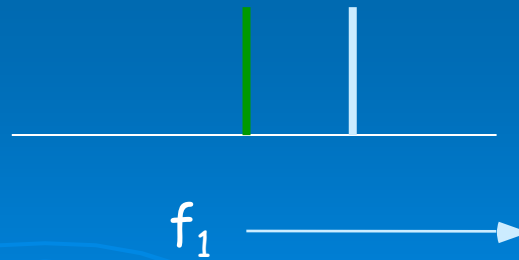
General One Dimensional Experiment



Fourier Transformation
resolves multiple frequencies
that overlap in the time domain



Fourier Transform
 $t_1 \rightarrow f_1$

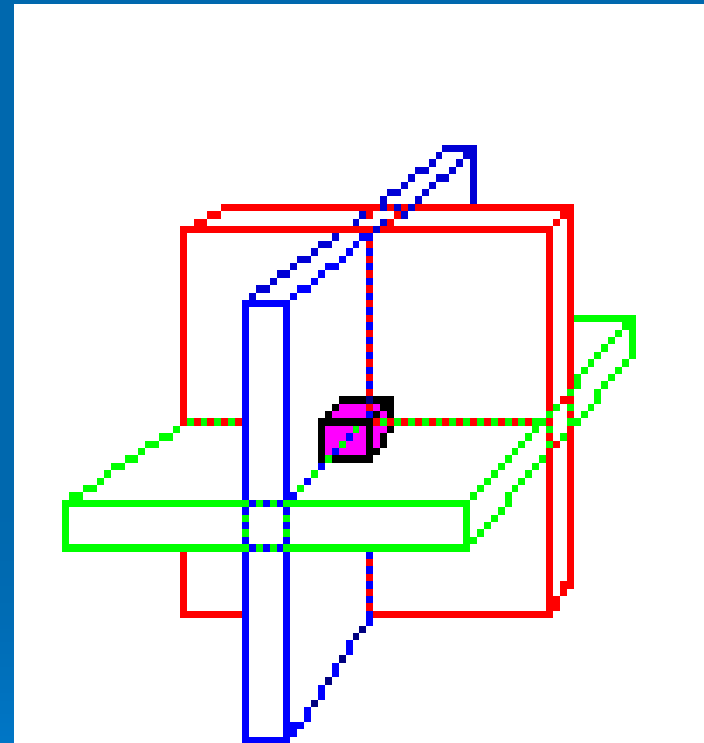
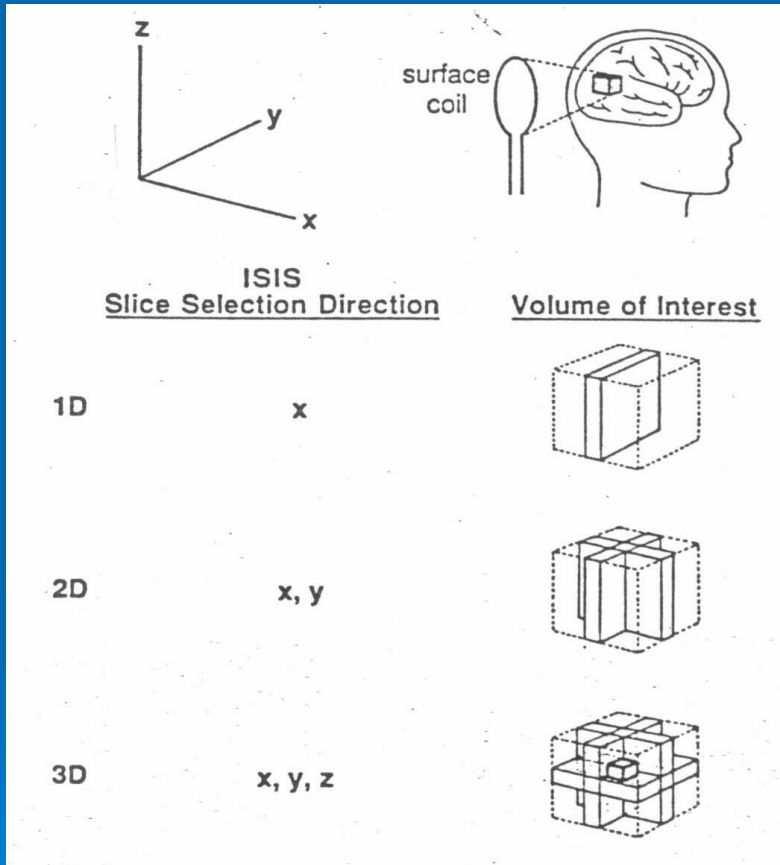


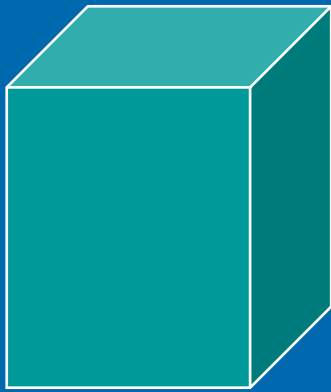


2. Single-Voxel MR Spectroscopy (MRS)

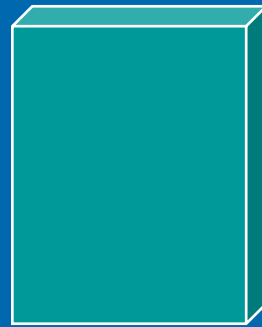


Localization

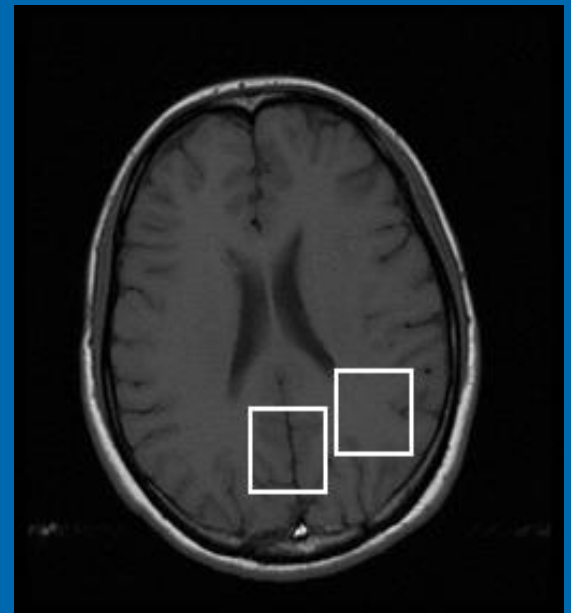




Volume



Slice



Column



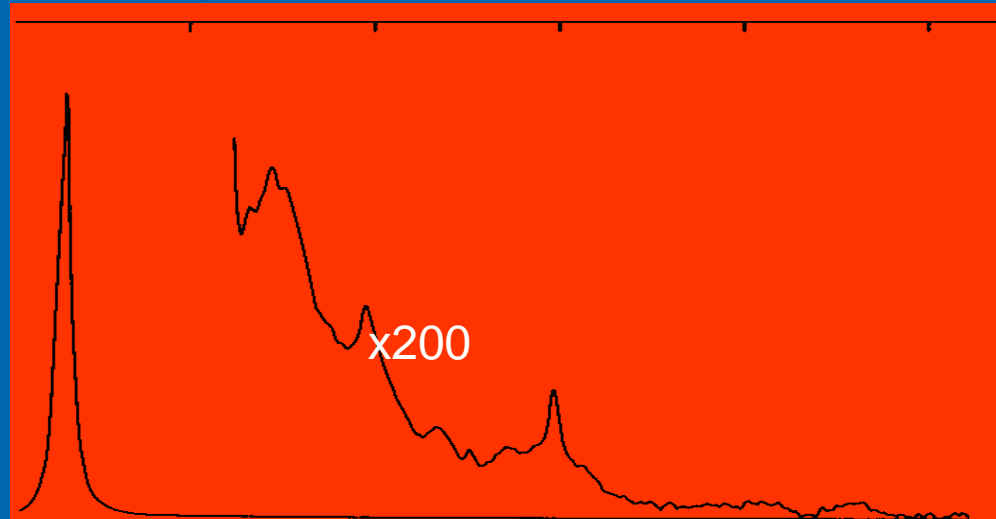
Voxel



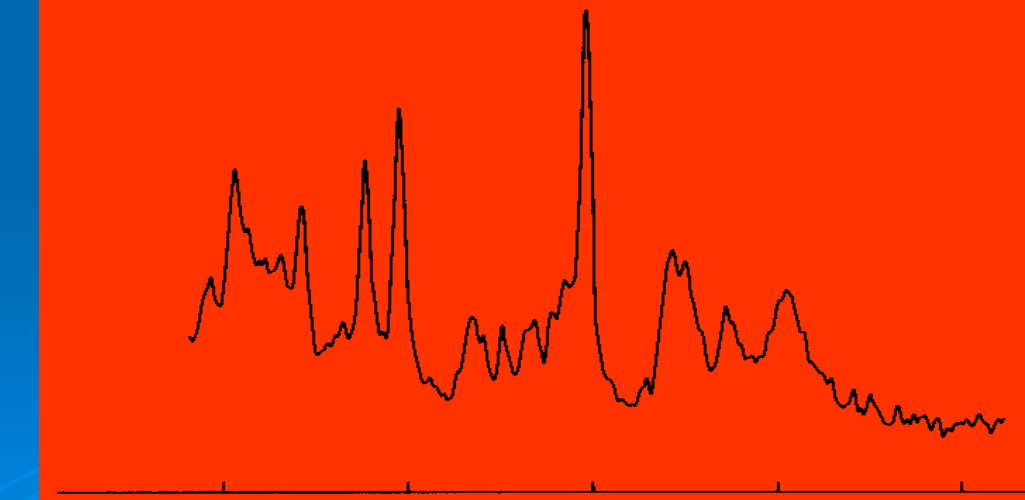
Selection
of voxel

Water: + for MRI, - for MRS

Before
suppression



After
suppression



ppm 4 3 2 1 0

*CHES*S

(global)



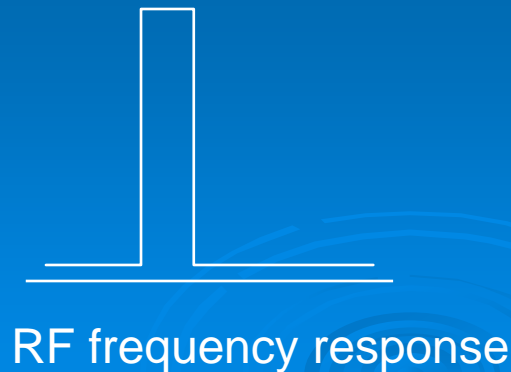
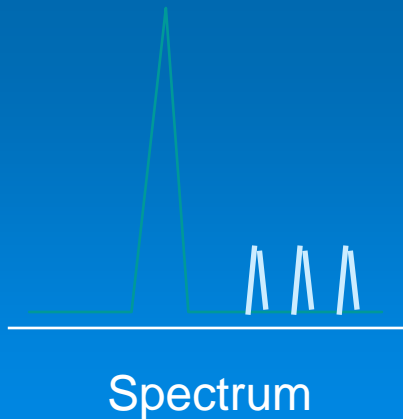
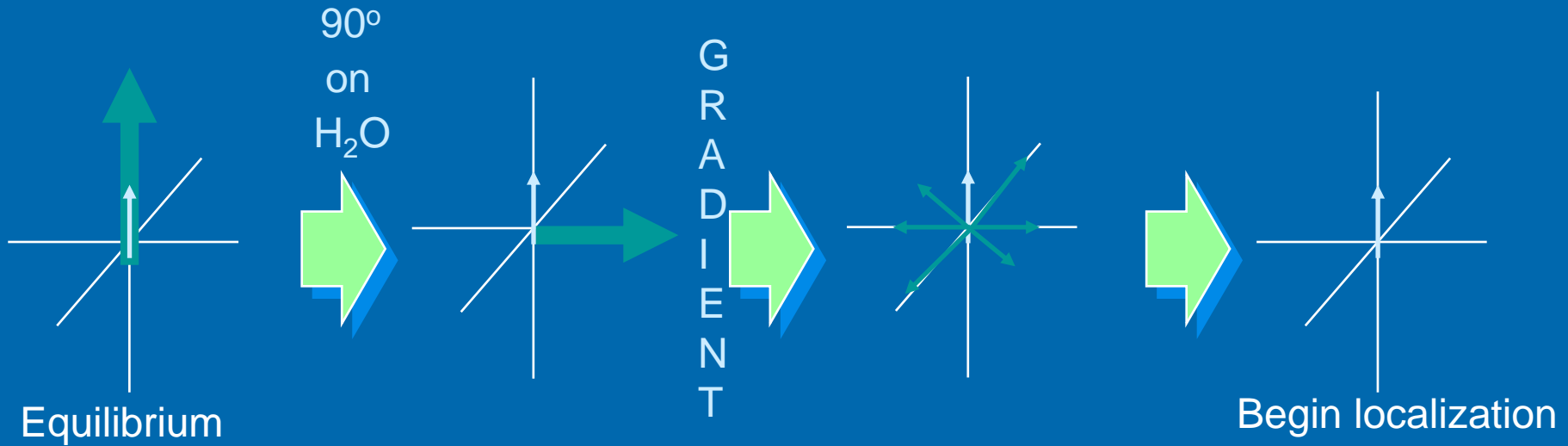
Water suppression



= water

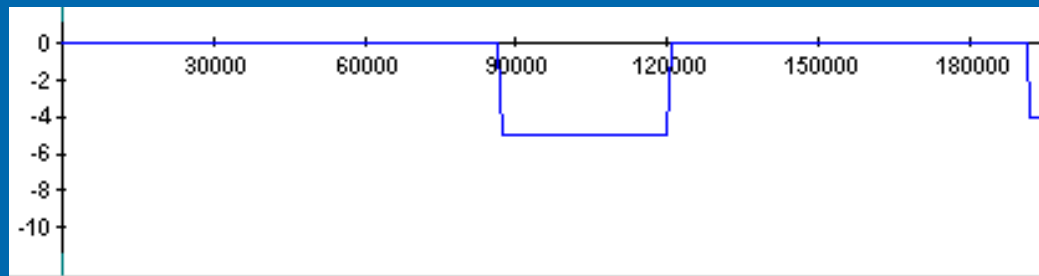


= metabolites

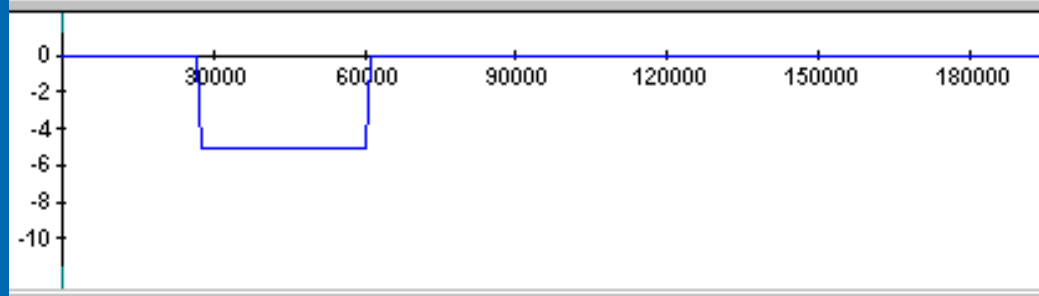


CHES (global)

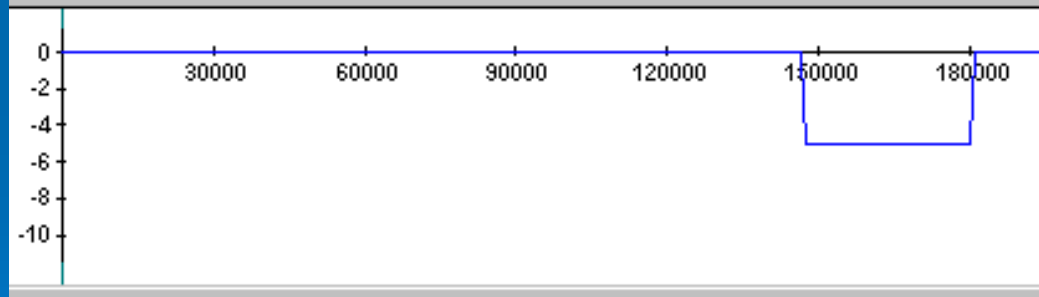
Gx



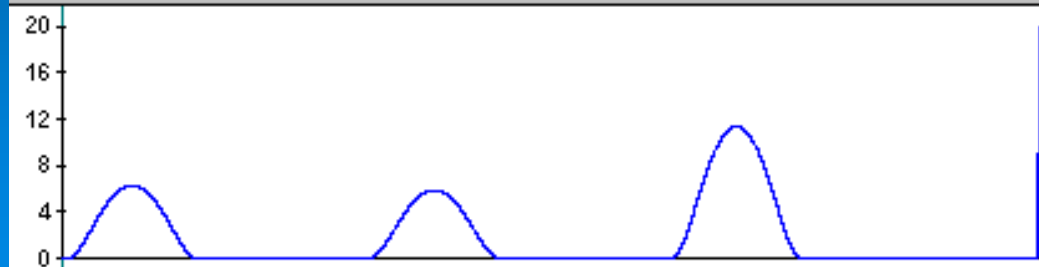
Gy



Gz

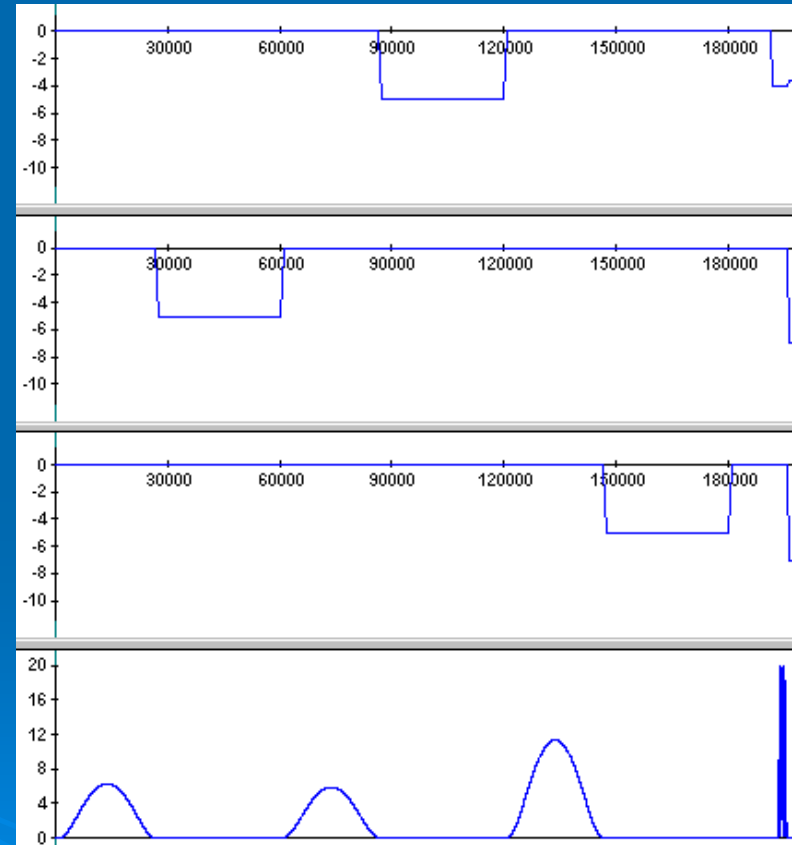


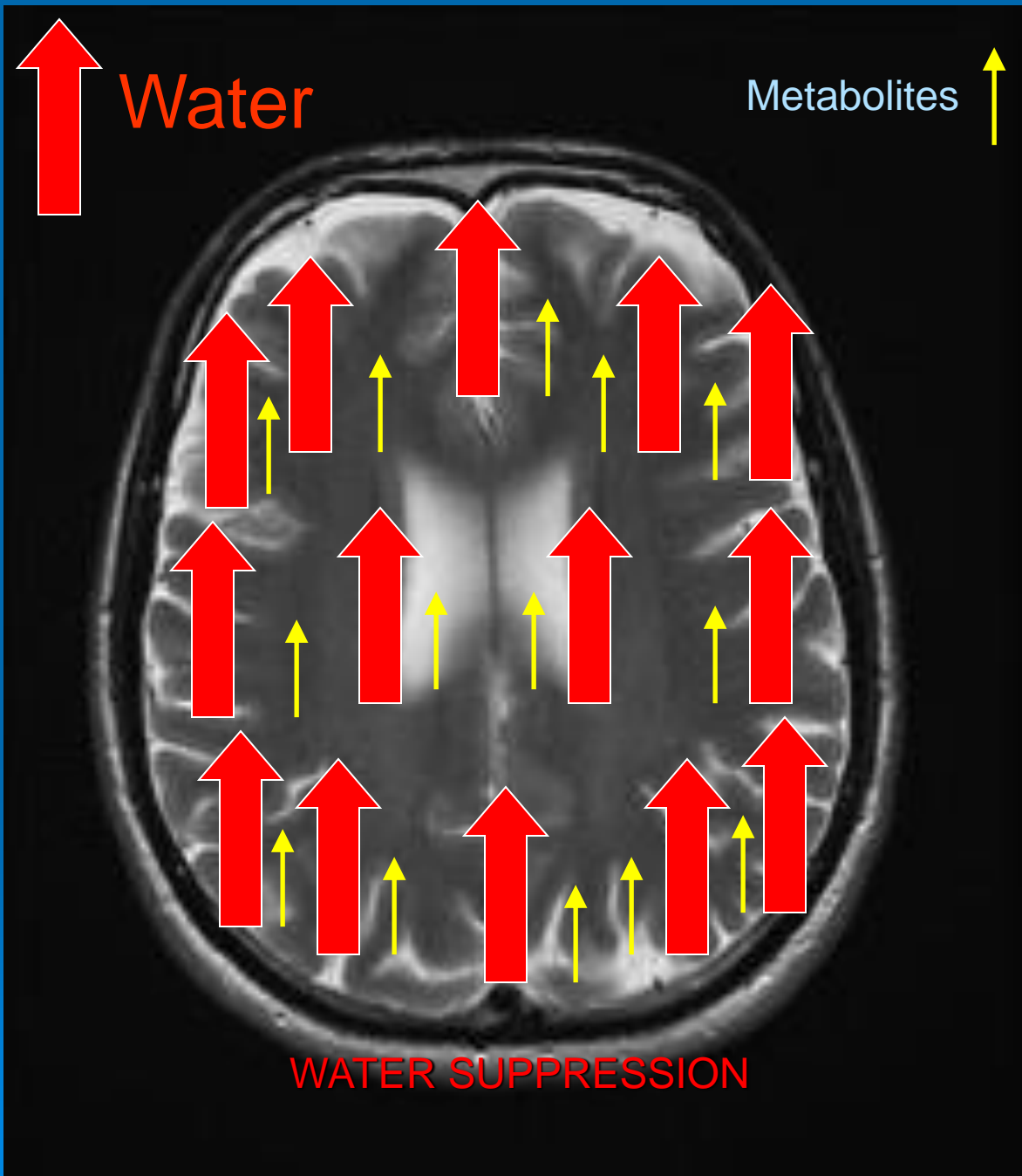
RF



Water Suppression

- Nomal water signal is ~ 5000 times stronger than metabolites
- Need to reduce it at least by 1000 times to get the right dynamic range.
- Common way is by frequency selective pulses followed by dephasing gradient.





Water

Metabolites

WATER SUPPRESSION

CHES
(global)

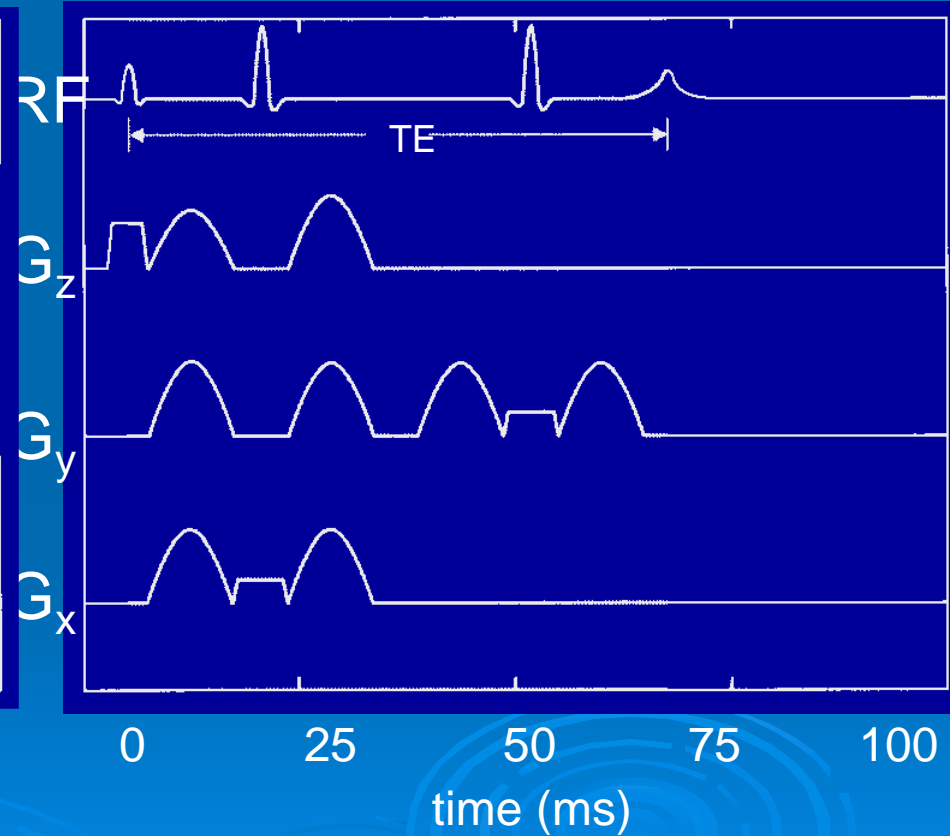
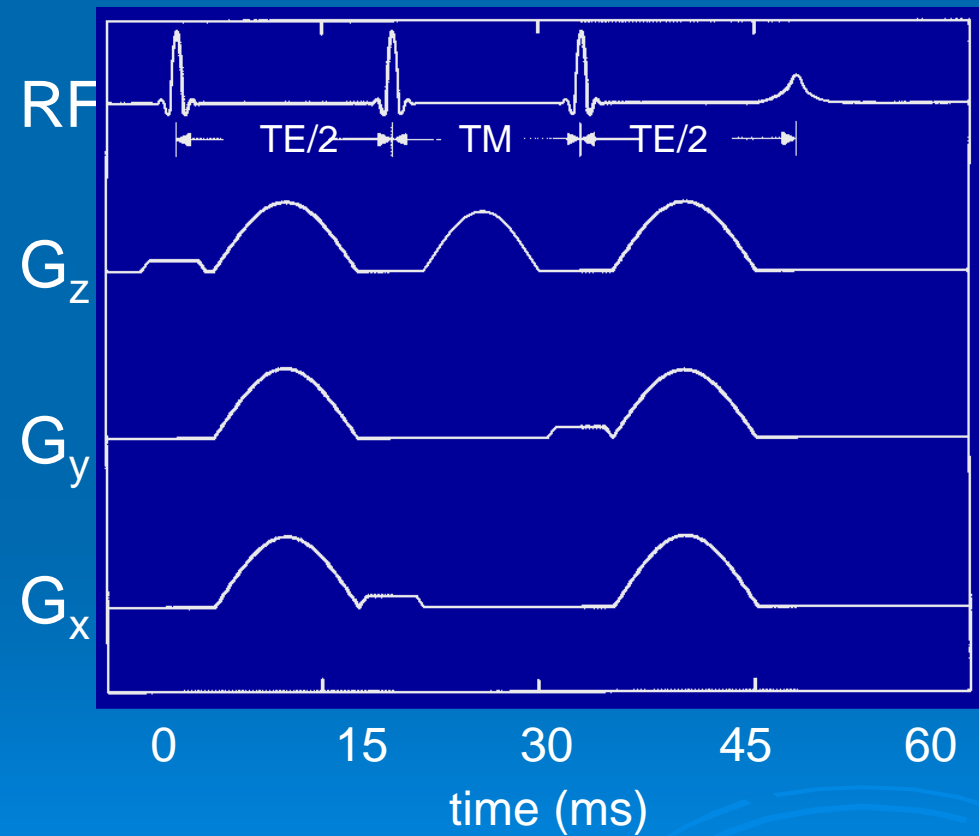
1D
STEAMSV
PRESSSV



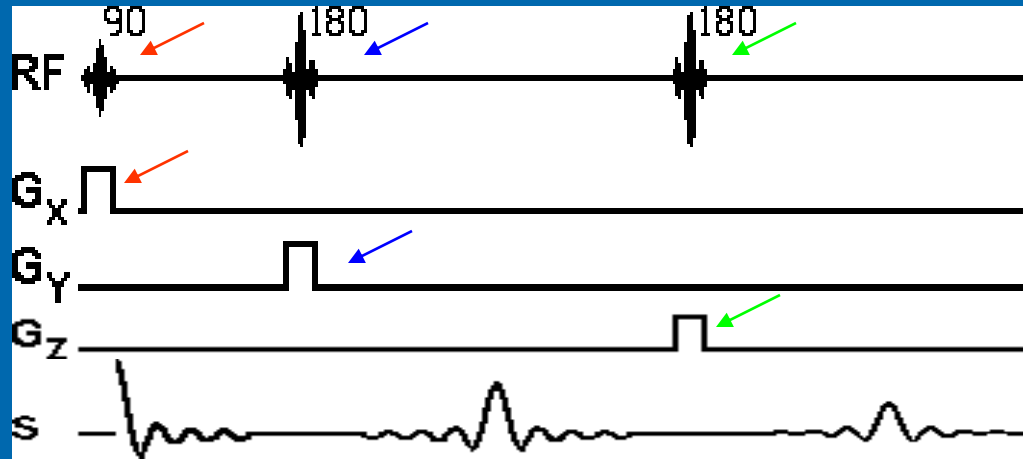
Localization

STEAM

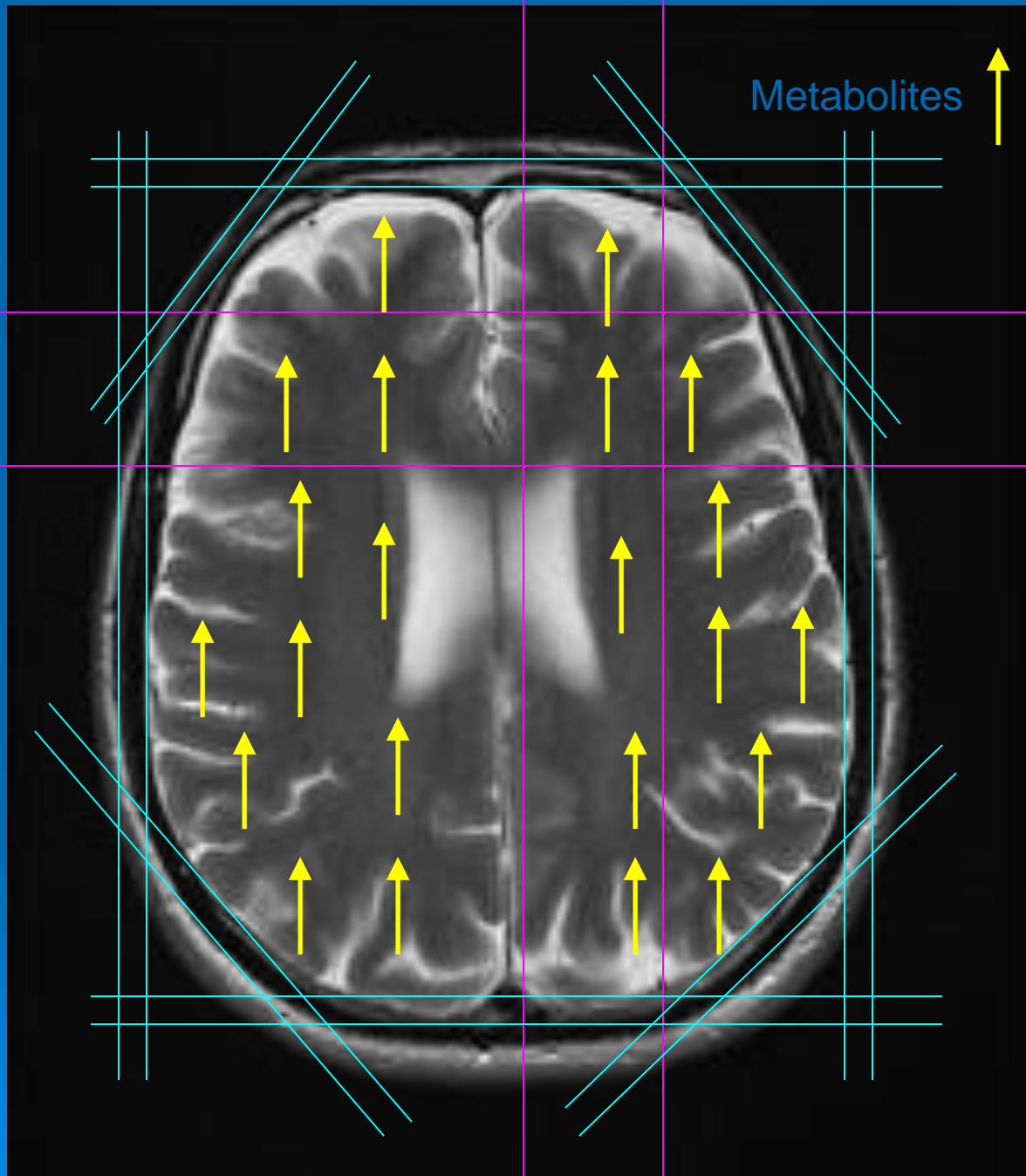
PRESS



PRESS-SV Sequence



*A second echo is recorded as the signal.
FT the echo to produces an NMR spectrum.*



Metabolites ↑

2 x 2 x 2 cm³
Voxel
Measured

2x2x2 cm³ Voxel, 5 Slices

Inferior

Superior

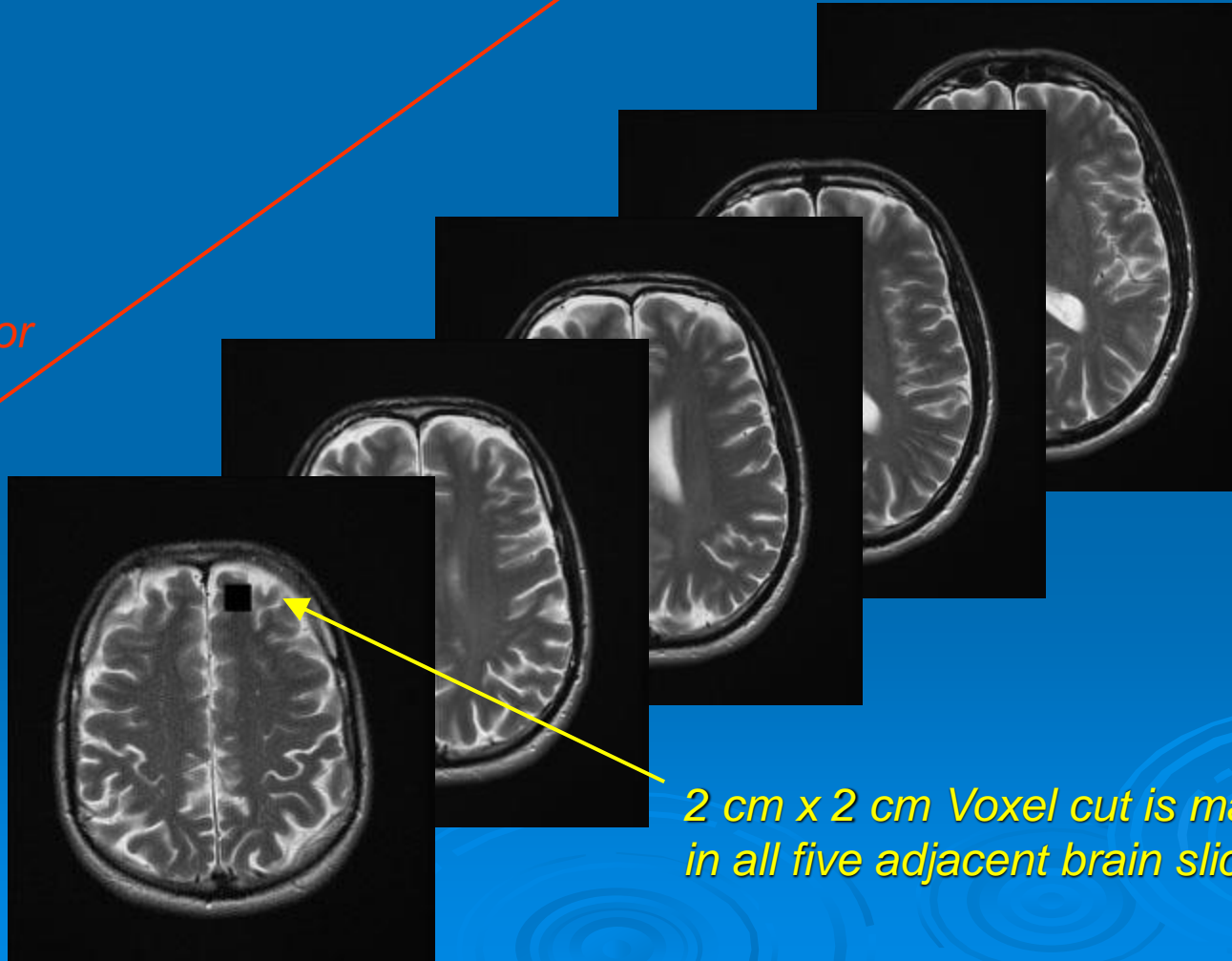


Shown are 5 vertically adjacent brain slices, each 4 mm thick (20 mm or 2cm total)

2x2x2 cm³ Voxel, 5 Slices

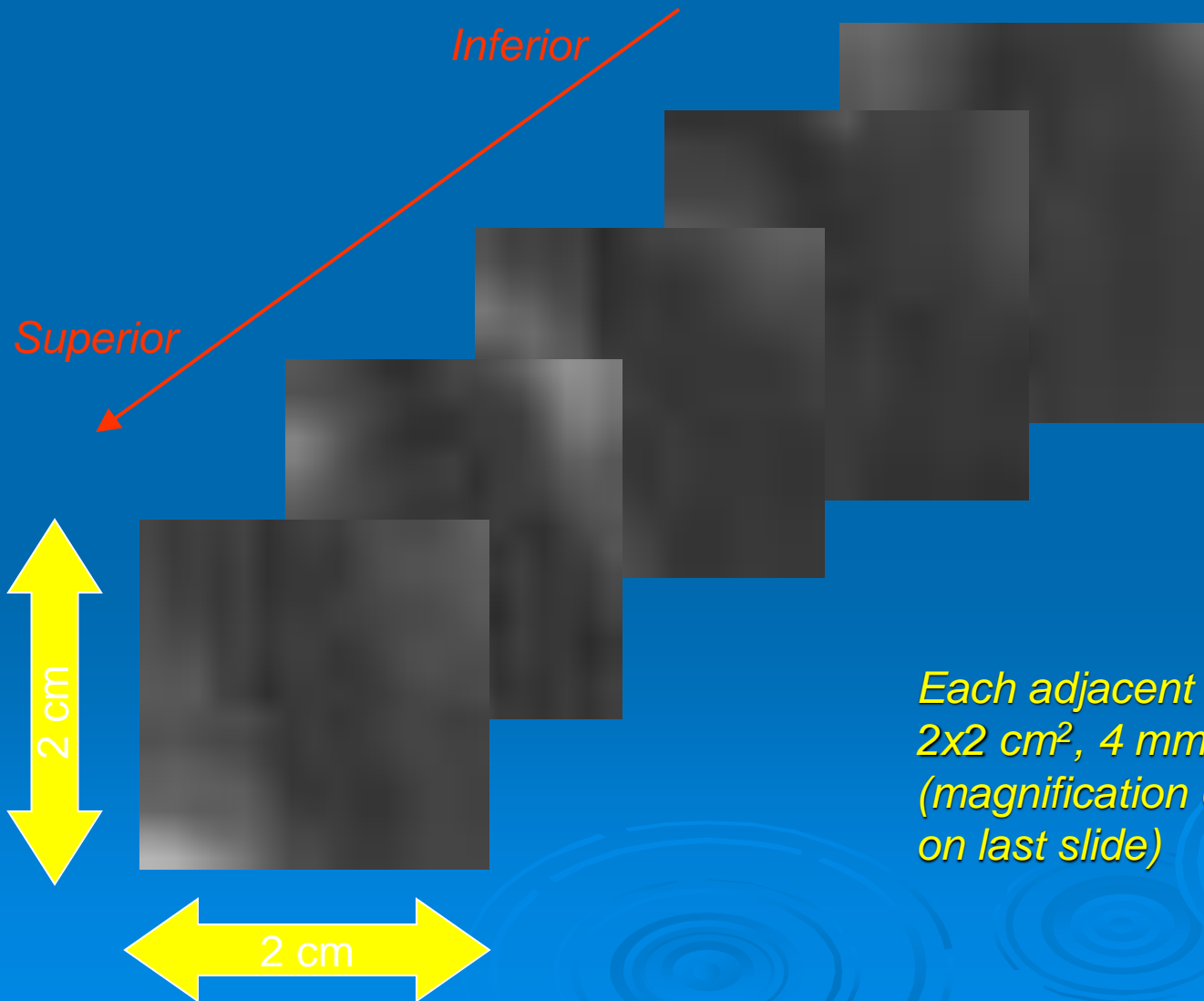
Inferior

Superior



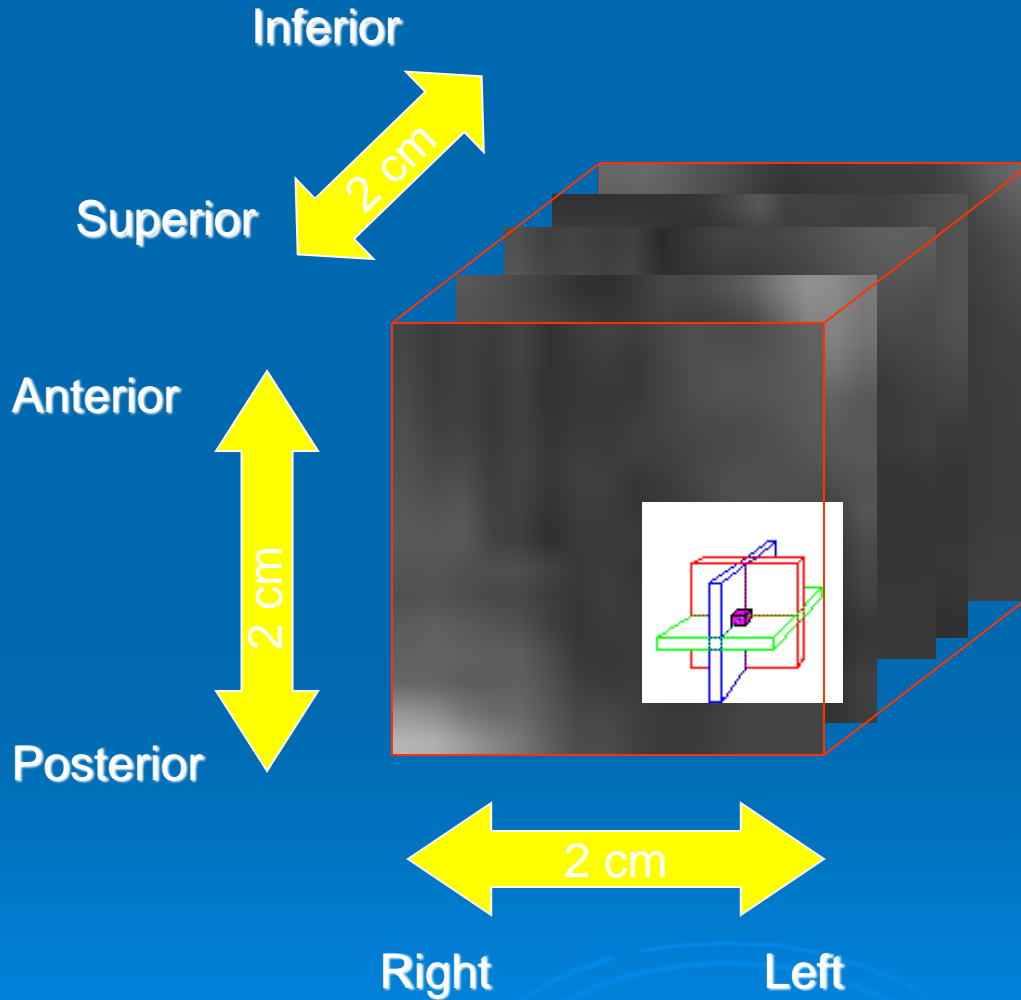
*2 cm x 2 cm Voxel cut is made
in all five adjacent brain slices*

5 Adjacent Voxel Slices

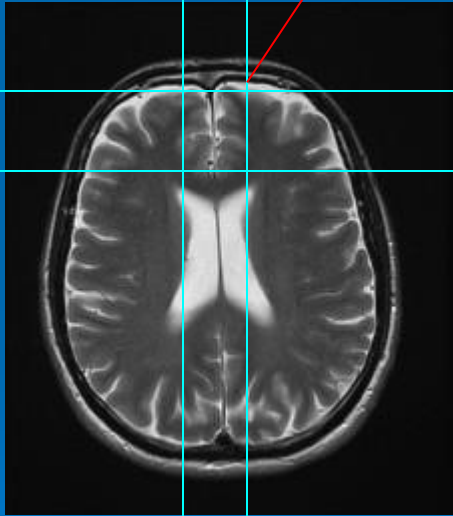


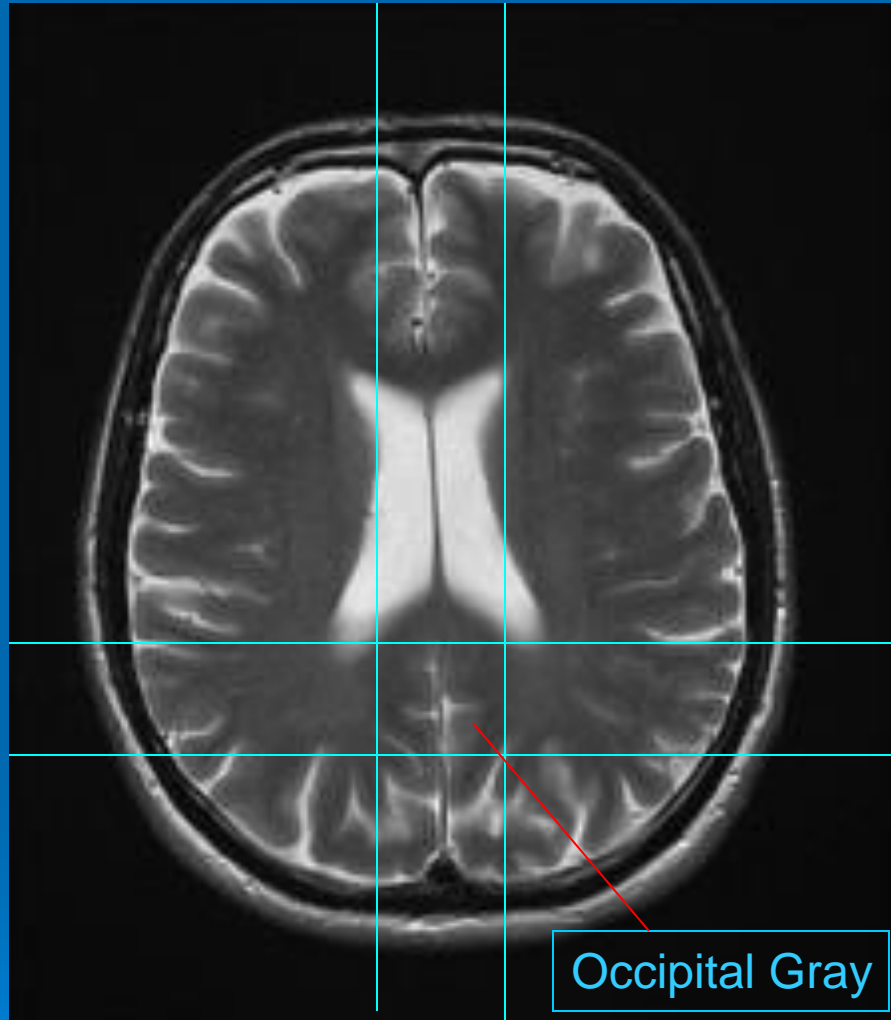
*Each adjacent slice is
2x2 cm², 4 mm thick
(magnification of cut
on last slide)*

2 x 2 x 2 cm³ Voxel



Frontal Gray



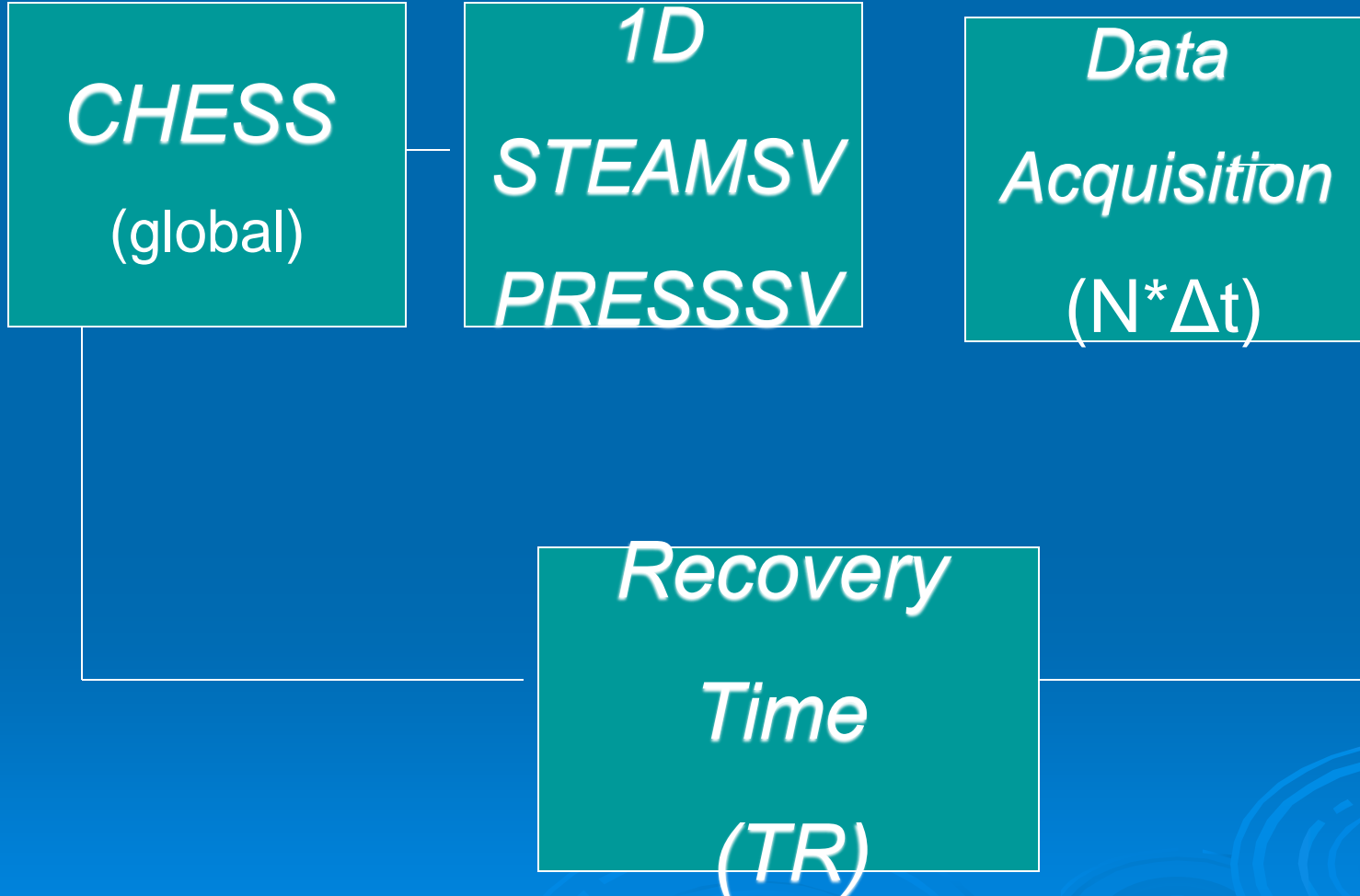


CHES
(global)

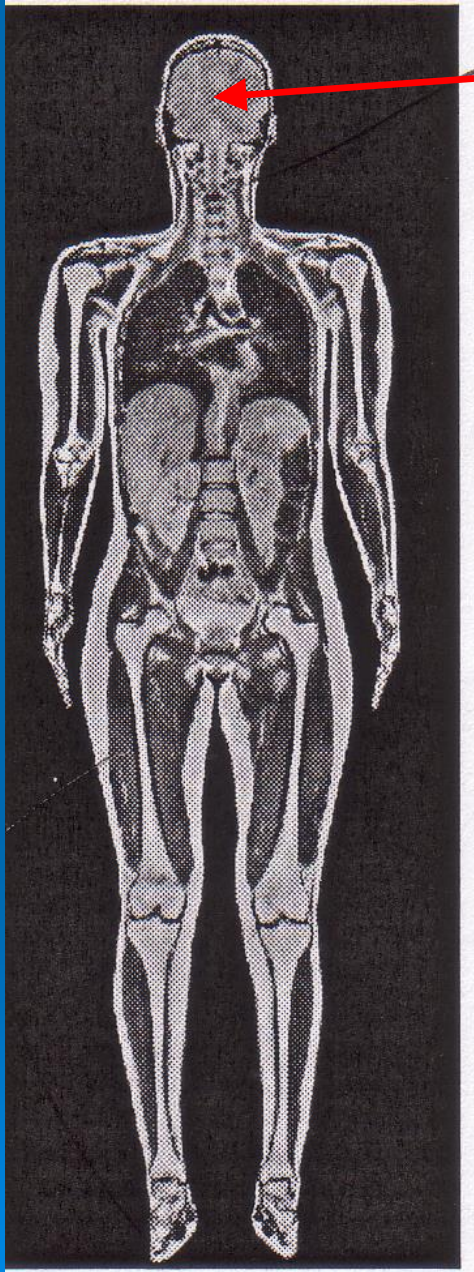
1D
STEAMSV
PRESSSV

Data
Acquisition
($N \cdot \Delta t$)

Recovery
Time
(*TR*)

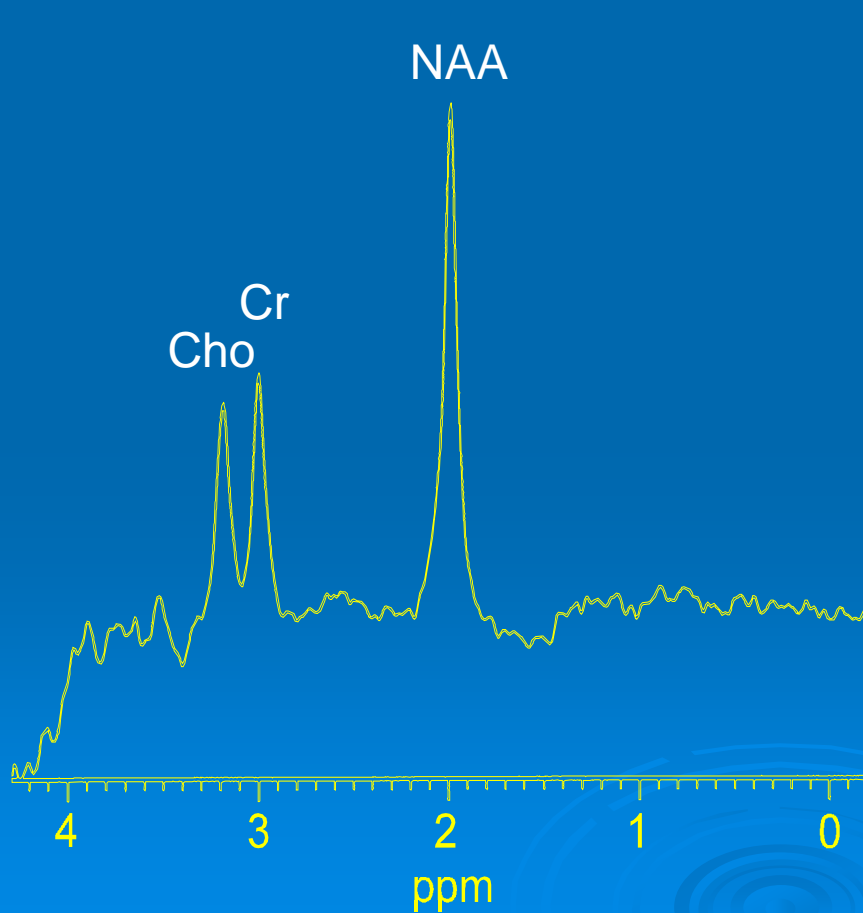


Brain MRI and MRS



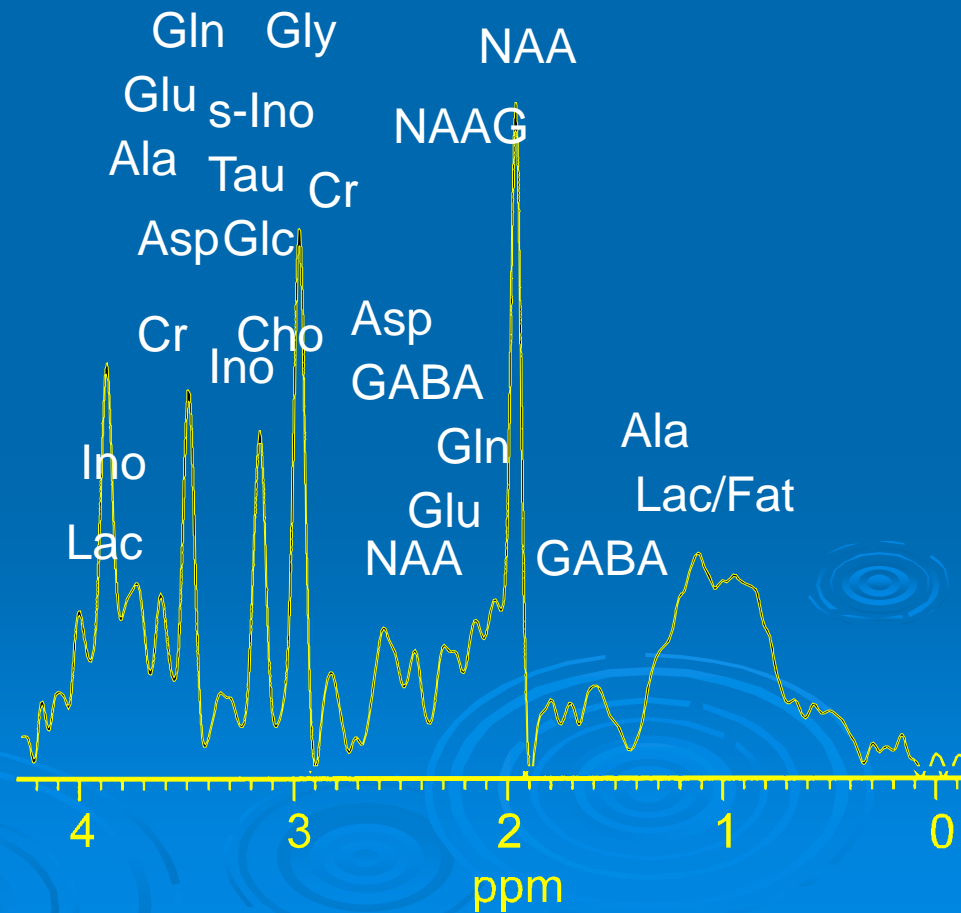
That was then ...

STEAM, TE=270ms, TR=1500ms



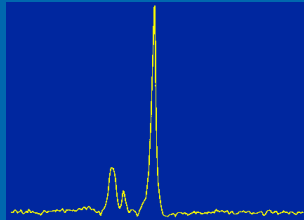
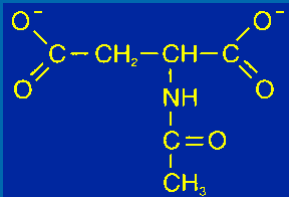
This is now.

STEAM, TE=20ms, TR=1500ms

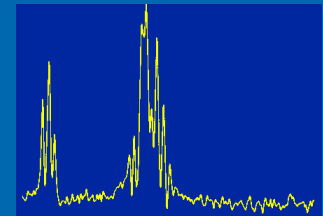
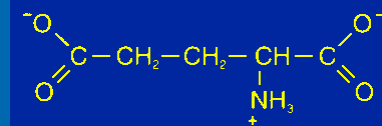


Cerebral metabolites

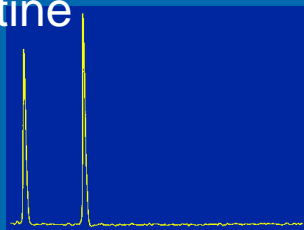
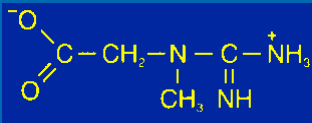
N-acetyl aspartate



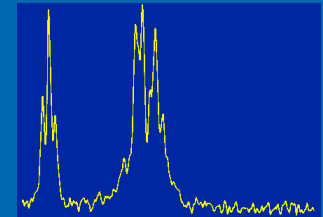
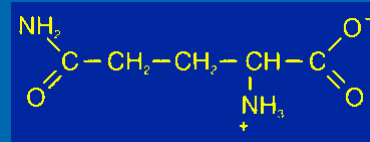
Glutamate



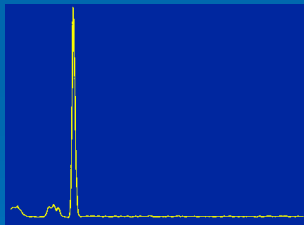
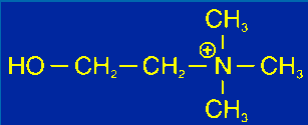
Creatine/Phosphocreatine



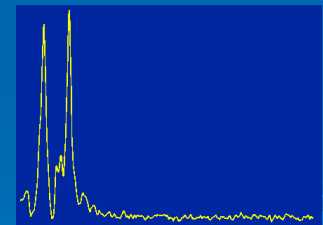
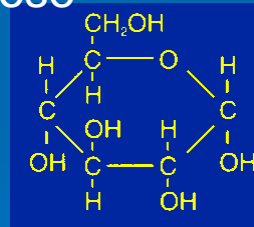
Glutamine



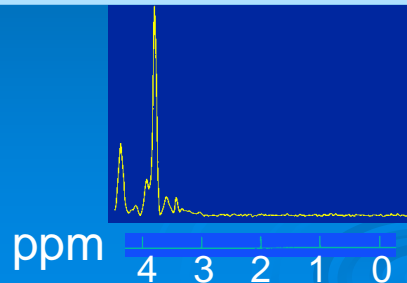
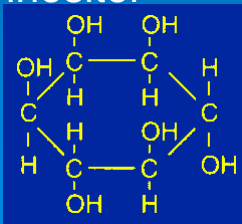
Choline



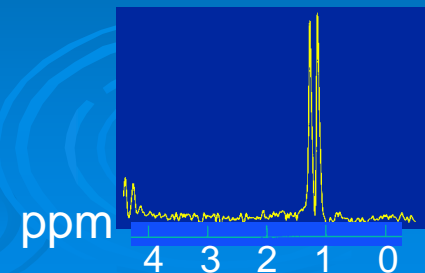
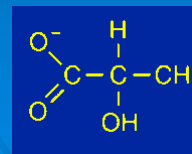
Glucose



Myo-inositol



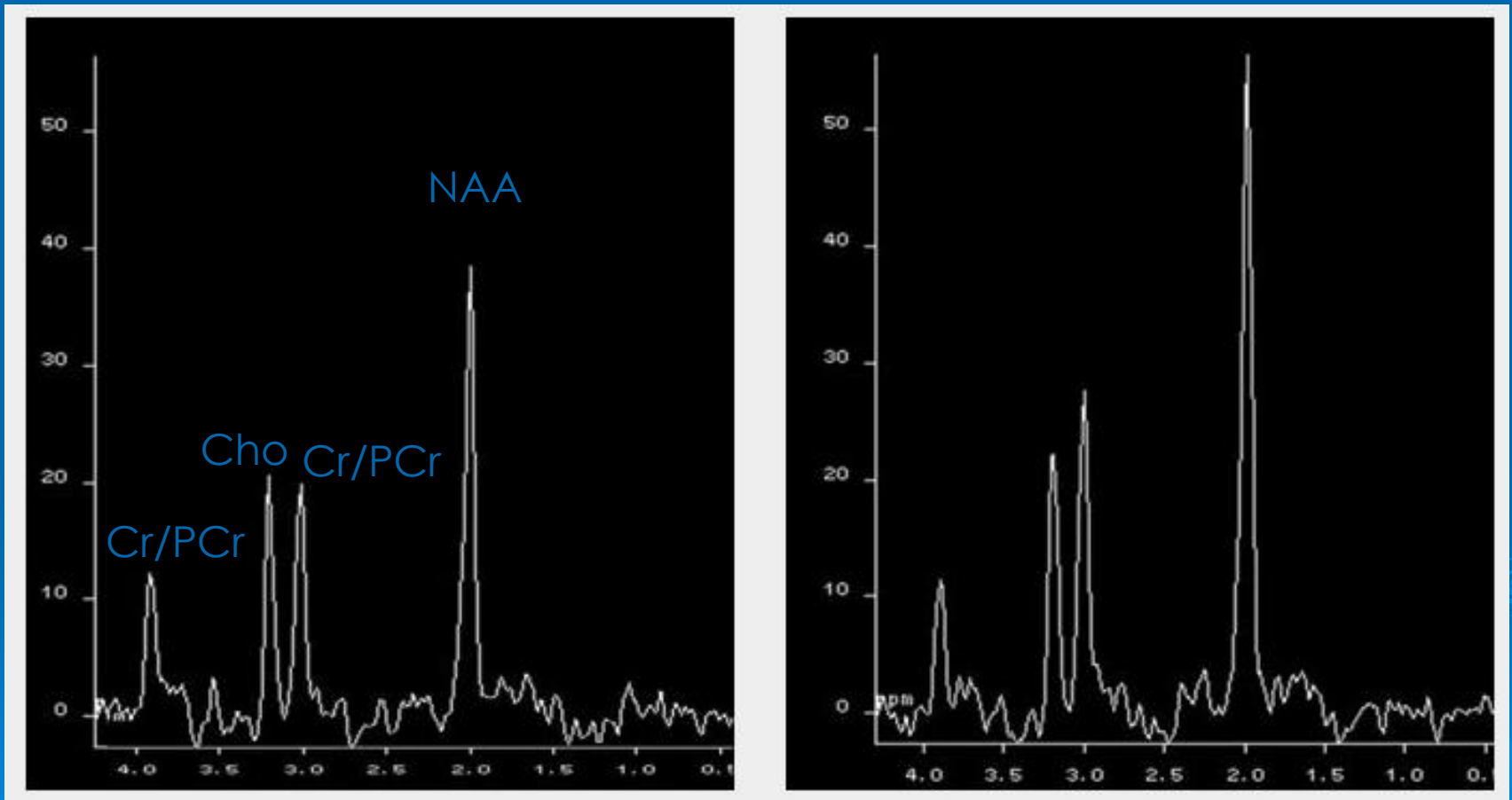
Lactate



Effect of Repetition Time (TR)

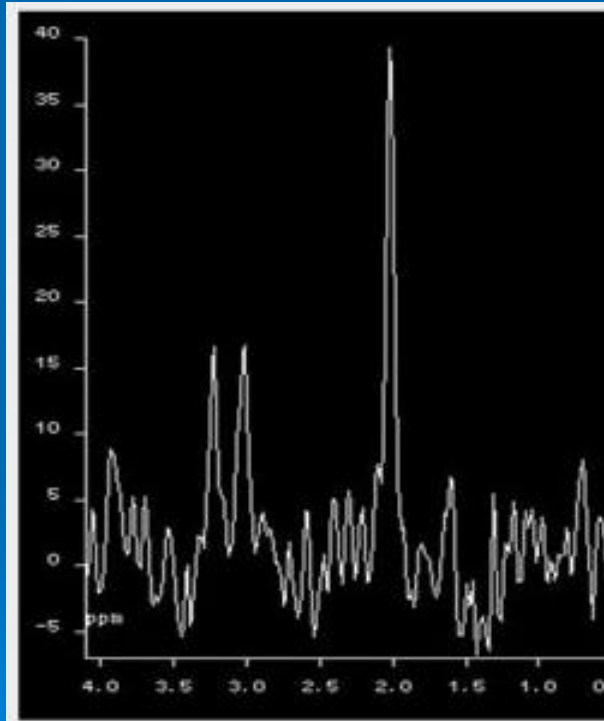
TR = 1500 ms

TR = 5000 ms

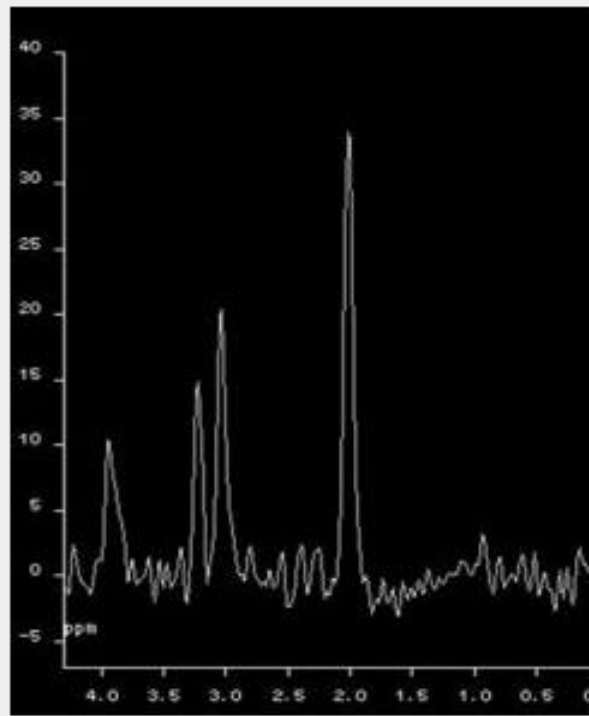


Effect of Signal Averaging

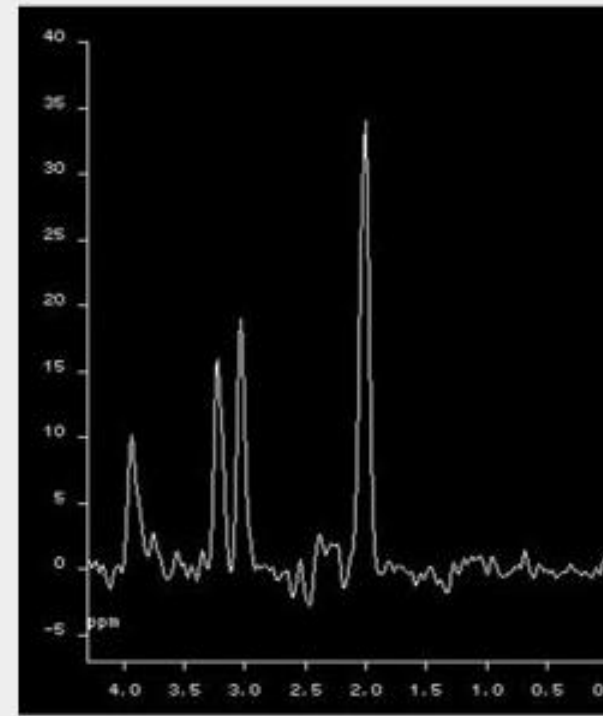
8 Averages



64 Averages

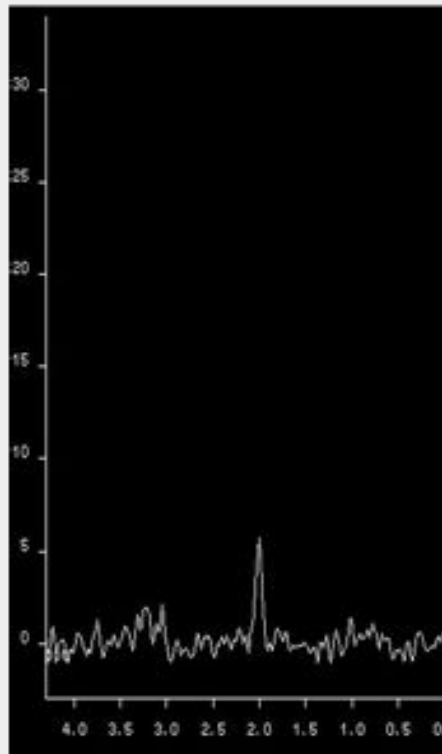


256 Averages

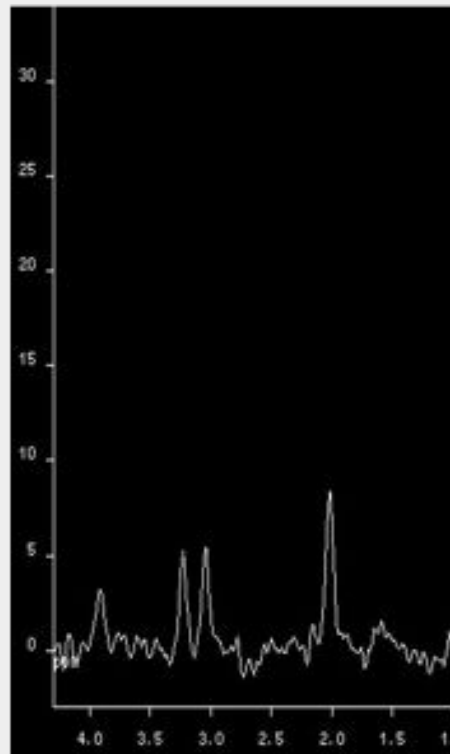


Effect of Voxel Size

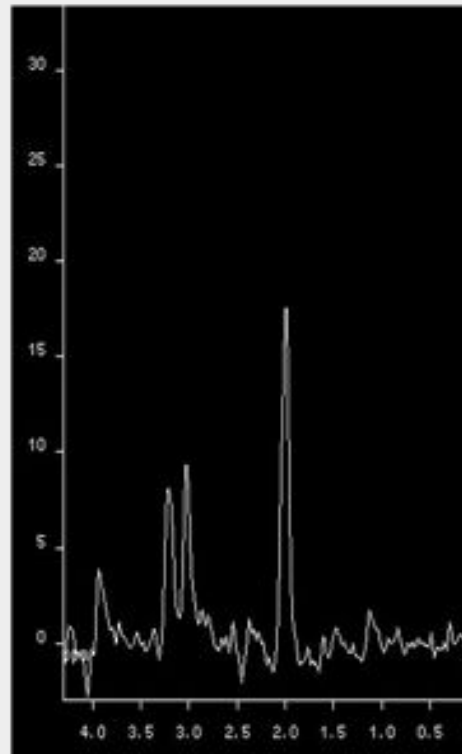
1 cc



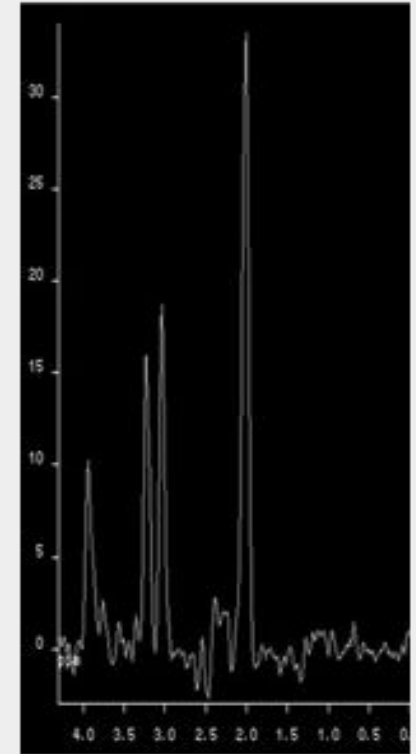
2 cc



4 cc

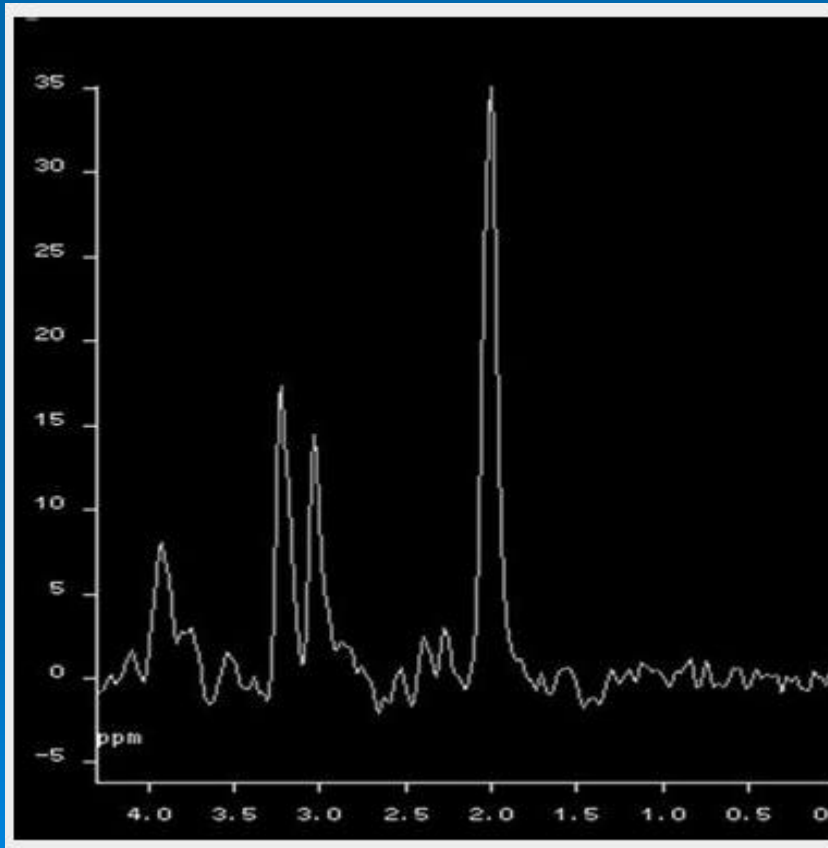


8 cc

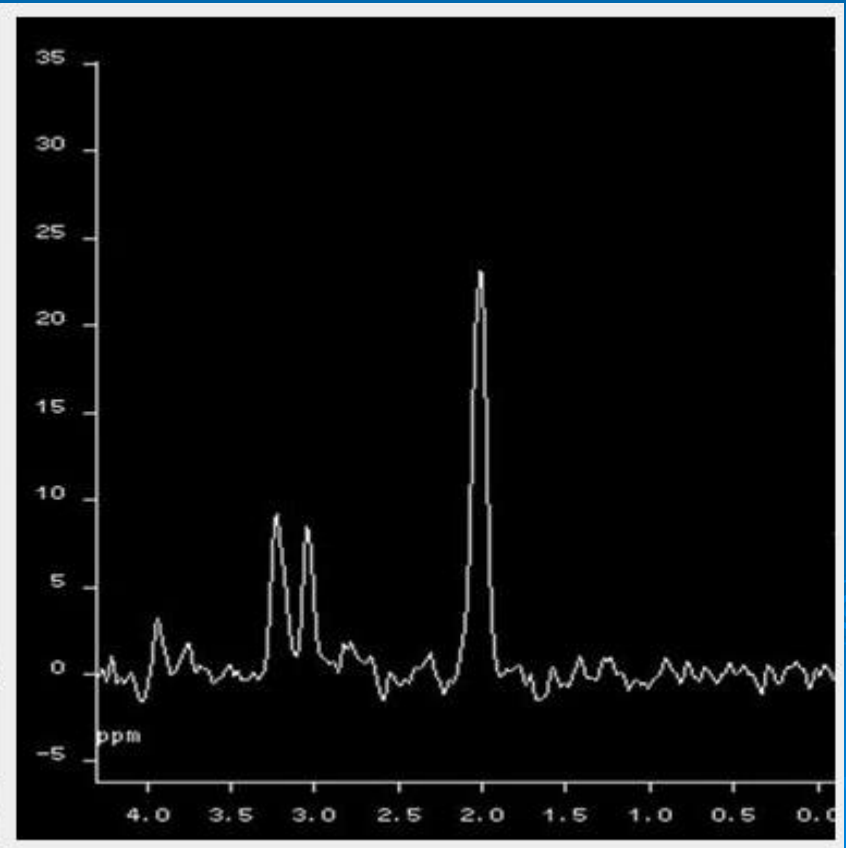


Effect of Echo Time, TE

TE = 144 ms

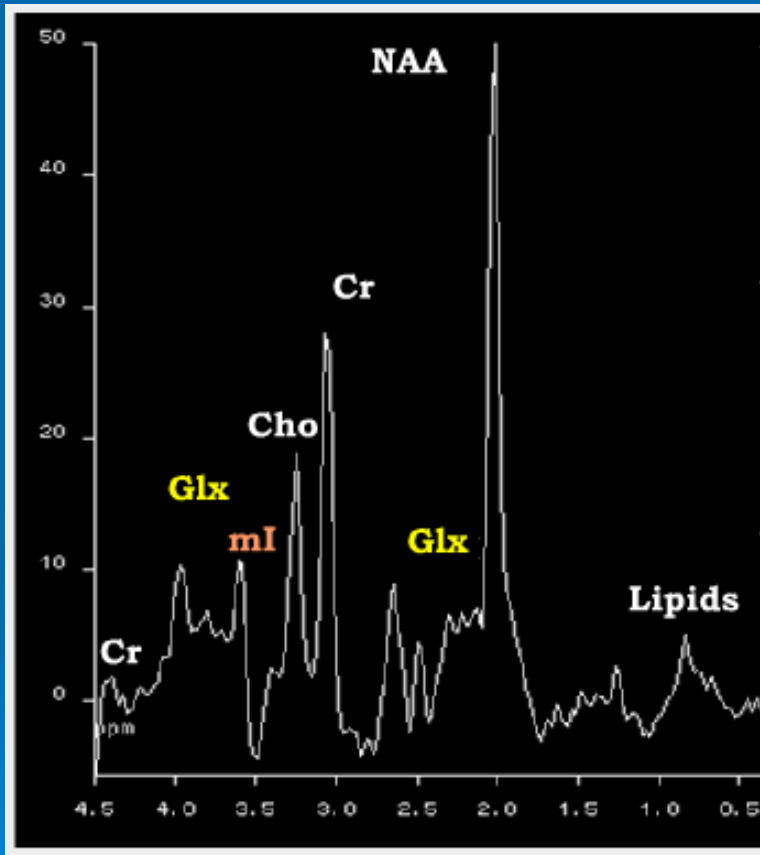


TE = 288 ms



Short TE ^1H Brain Spectrum

Healthy volunteer



Additional Peaks

Glx	2.05-2.45 ppm
	3.6 - 3.8 ppm
mI	3.56 ppm
Glucose	3.43 ppm
	3.8 ppm
And more	

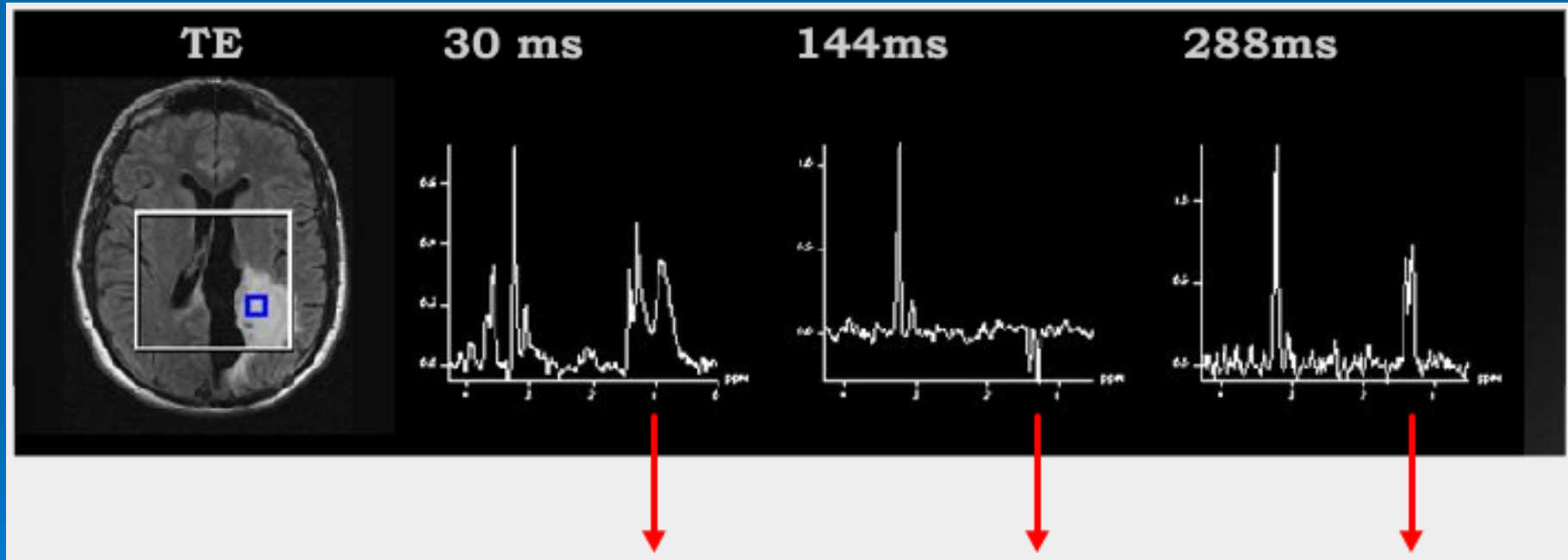
Table 2. Short-TE Neuro-MRS: Differential Diagnosis¹

Metabolite (normal cerebral concentration)	Increased concentration	Decreased concentration
Myoinositol (mI) (5 mM)	normal neonatal brain, Alzheimer disease, diabetes mellitus, recovered hypoxia, hyperosmolar states	chronic hepatic encephalopathy, hepatic encephalopathy, stroke, neoplasms
Creatine (Cr) and Phosphocreatine (PCr) (8 mM)	head trauma, hyperosmolar states, increases with age	hypoxia, stroke, neoplasms, infant brain
Glucose (G) (1 mM)	diabetes mellitus, ? parenteral feeding, ?hypoxic encephalopathy	not detectable
Choline (Cho) (1.5 mM)	head trauma, diabetes, neonatal brain, post liver transplant, neoplasms, chronic hypoxia, hyperosmolar states, ? Alzheimer disease	asymptomatic liver disease, hepatic encephalopathy, stroke, nonspecific dementia
Aceto-acetate, acetone, ethanol, aromatic amino acids, propane-diol	detectable in specific settings	not detectable

¹Behavior of lactate, N-acetylaspartate, glutamate and glutamine same as in Table 1

The Lactate Doublet

Tumor spectra: showing no NAA, \uparrow Cho, \uparrow ml, \uparrow lactate

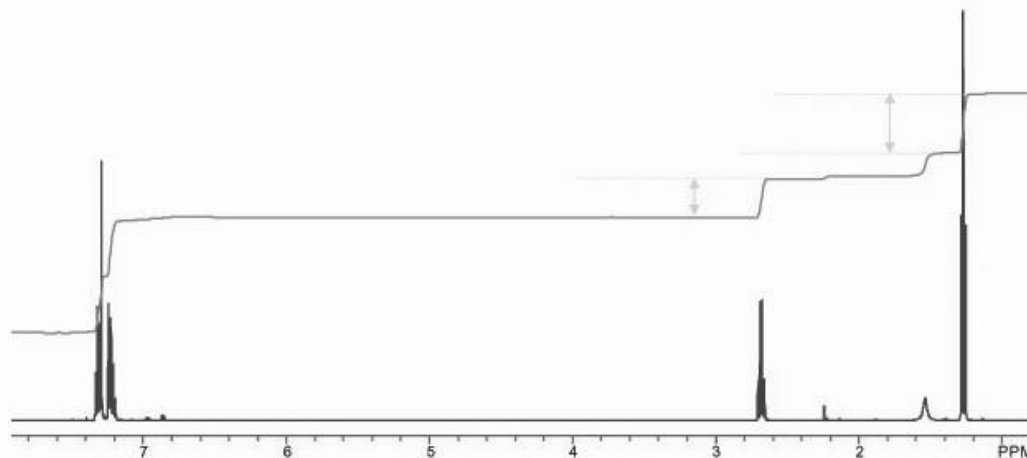


Lipids and
lactate

Inverted
lactate

Upright
lactate

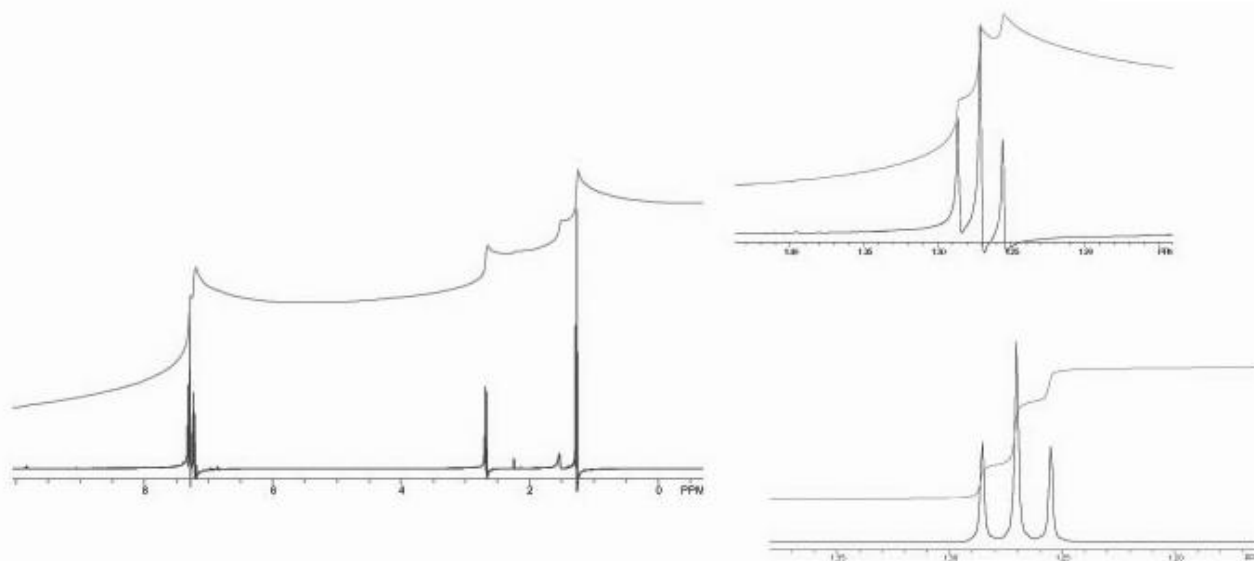
Integration/Quantitation



When you have resonances which are not overlapping with each other then the integral (area) of the spectral resonances (peaks) can be used to calculate the number of protons under each peak.

You need good baseline and correct phase

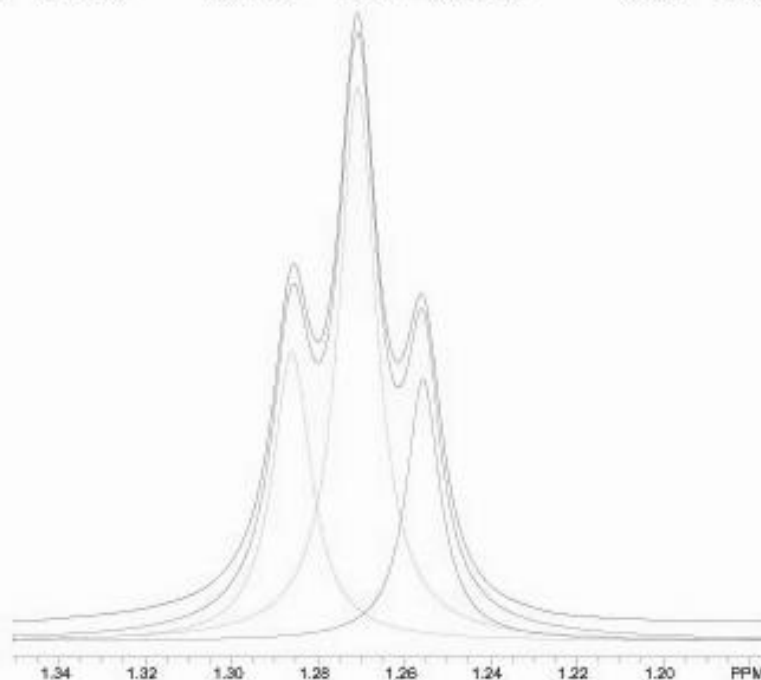
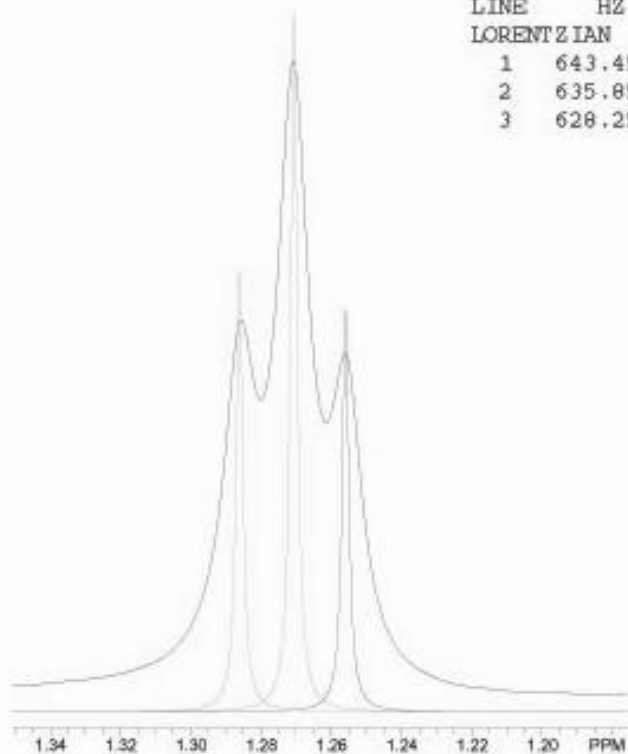
Good Baseline, Bad Phase



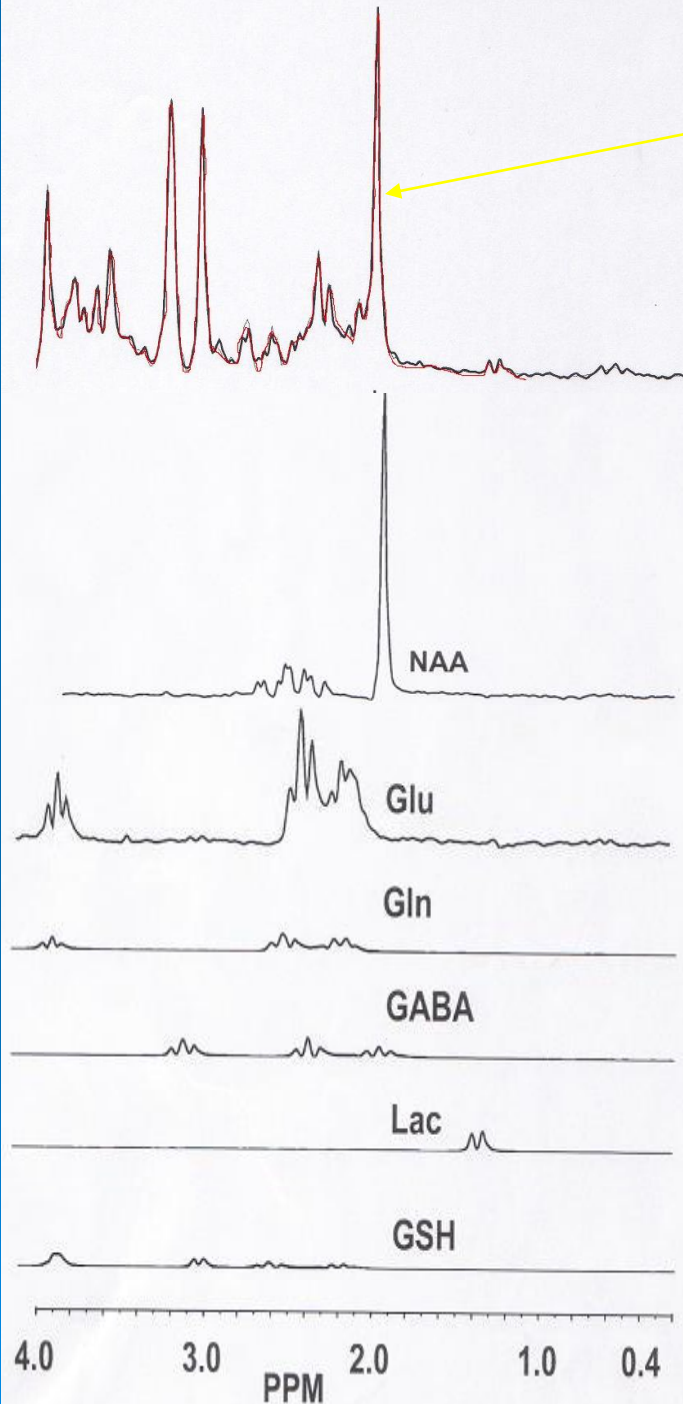
You need sophisticated spectral fitting algorithms for quantification

Deconvolution...line-fitting

LINE	HZ	PPM	HEIGHT	REL_HT	WIDTH	AREA	REL_AREA	FRACTION
LORENTZIAN								
1	643.45	1.286	720384	46.132	5.23	3766398	1.01	1.000
2	635.85	1.271	1395686	89.377	5.36	7481549	2.00	1.000
3	628.25	1.256	668149	42.787	4.97	3318865	0.89	1.000

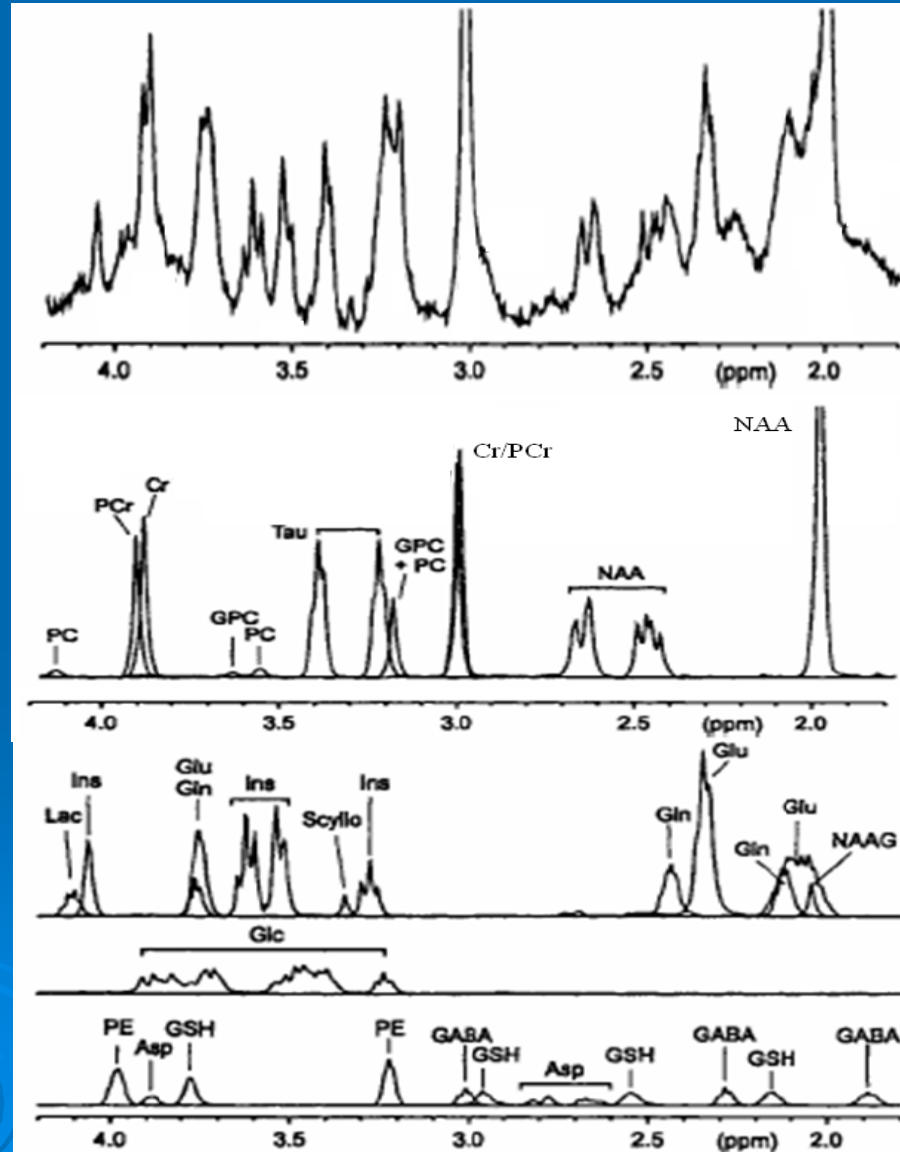


LCModel Fitting



1D MRS Quantitation

- LC-Model for 1D MRS quantitation.
- Works in frequency domain using prior knowledge

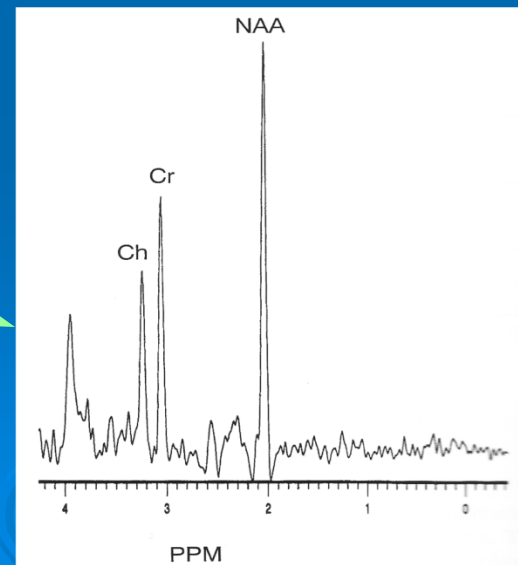
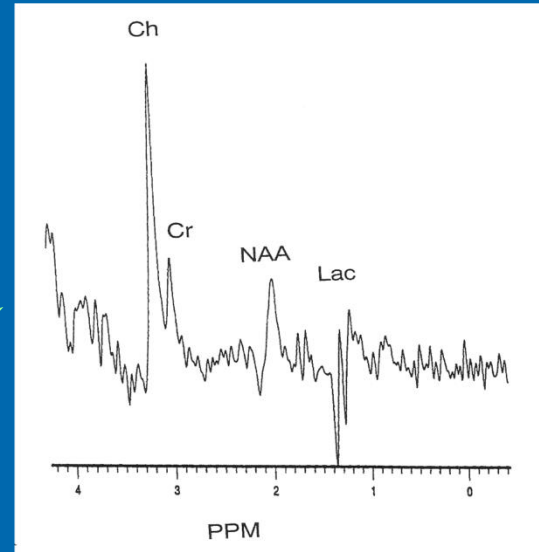
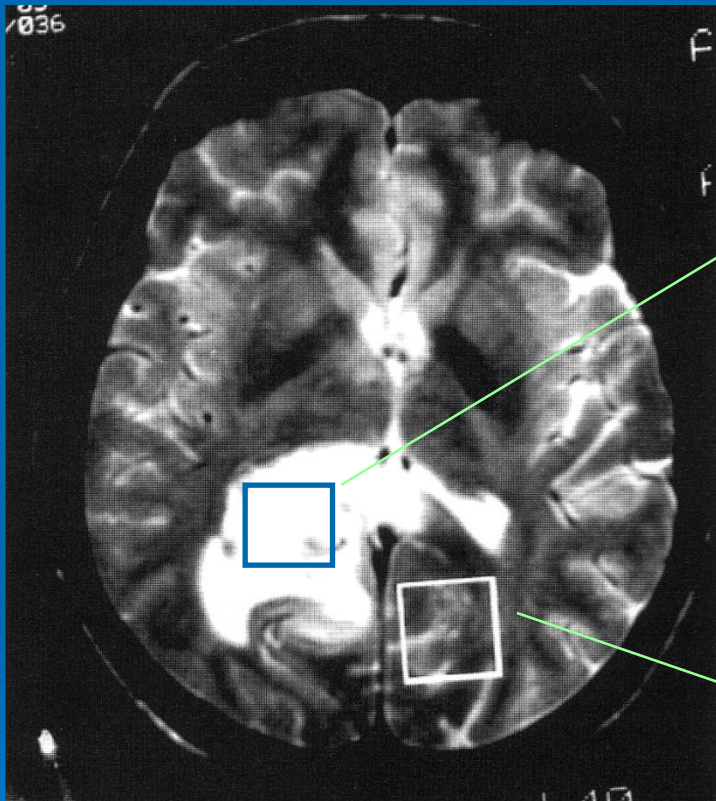


Provencher (2001)



3. Selected Applications of MR Spectroscopy





IDH1 R132H mutation and 2-HG

- Somatic mutations of the isocitrate dehydrogenase 1 and 2 genes (IDH1 and IDH2) have recently been implicated in gliomagenesis and are found in approximately 80% of World Health Organization (WHO) grade II-III gliomas and secondary glioblastomas (WHO grade IV) in humans.

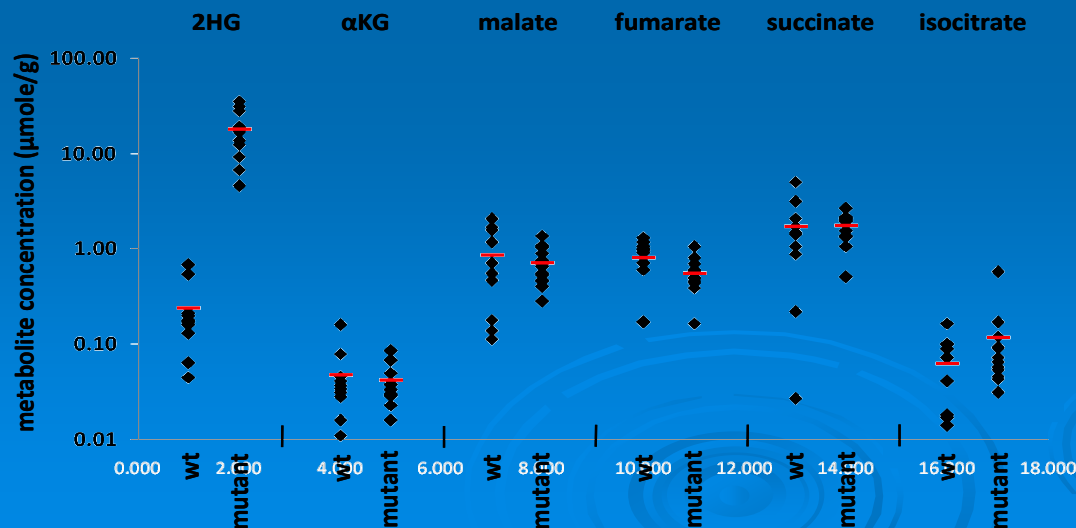
- Vast majority of IDH1 mutant, high-grade gliomas have evolved from lower grade lesions.





IDH1 R132H mutation and 2-HG

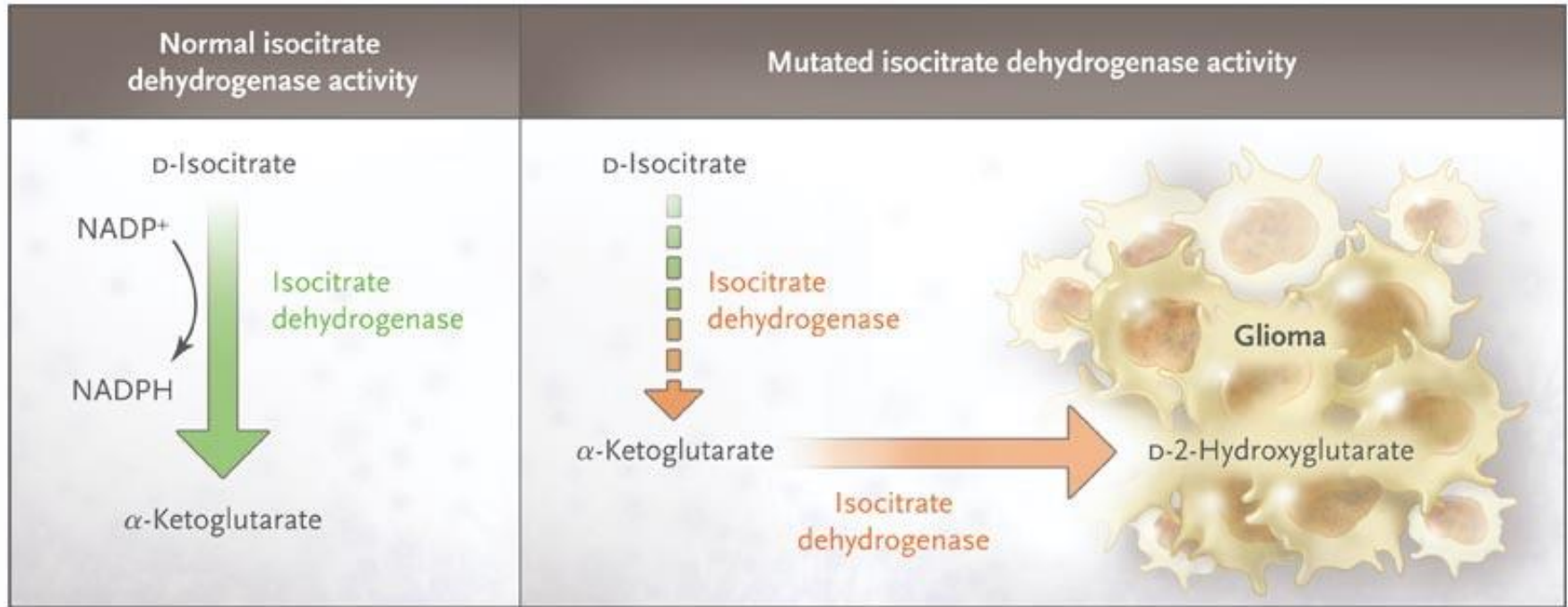
A recent work by Dang and co-workers reported a mutation observed in the isocitrate dehydrogenase1 (IDH1) gene, which occurs in the majority of grade II and grade III gliomas and secondary glioblastomas, resulting in significant elevation of 2HG in these tumors.



Dang et al. 2010, Nature



IDH1 R132H mutation produces 2-HG

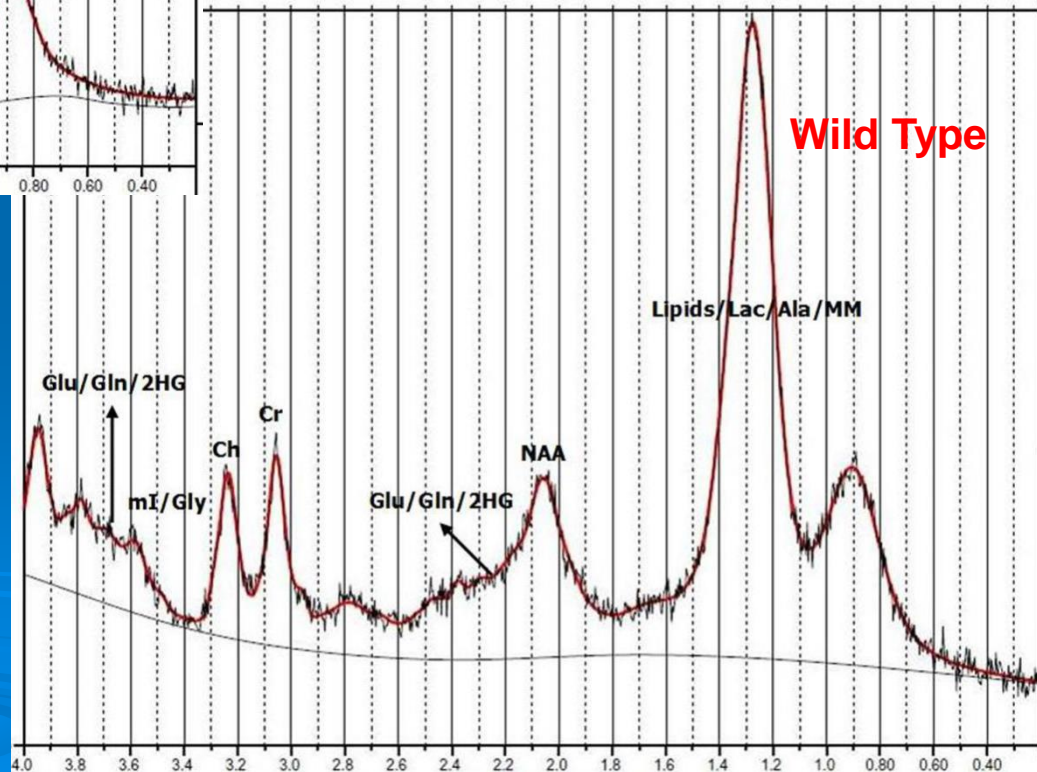
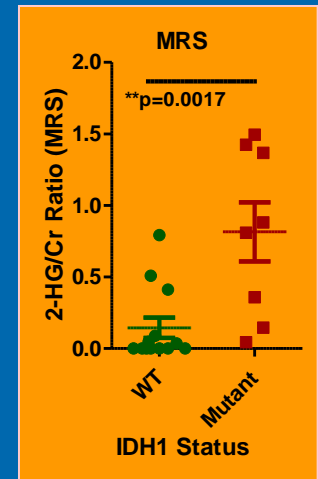
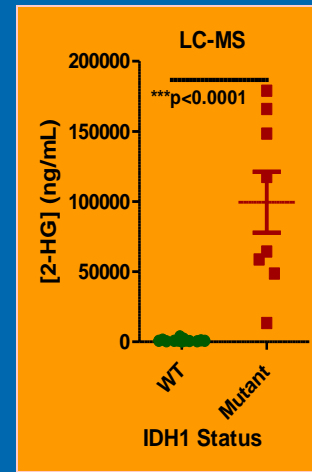
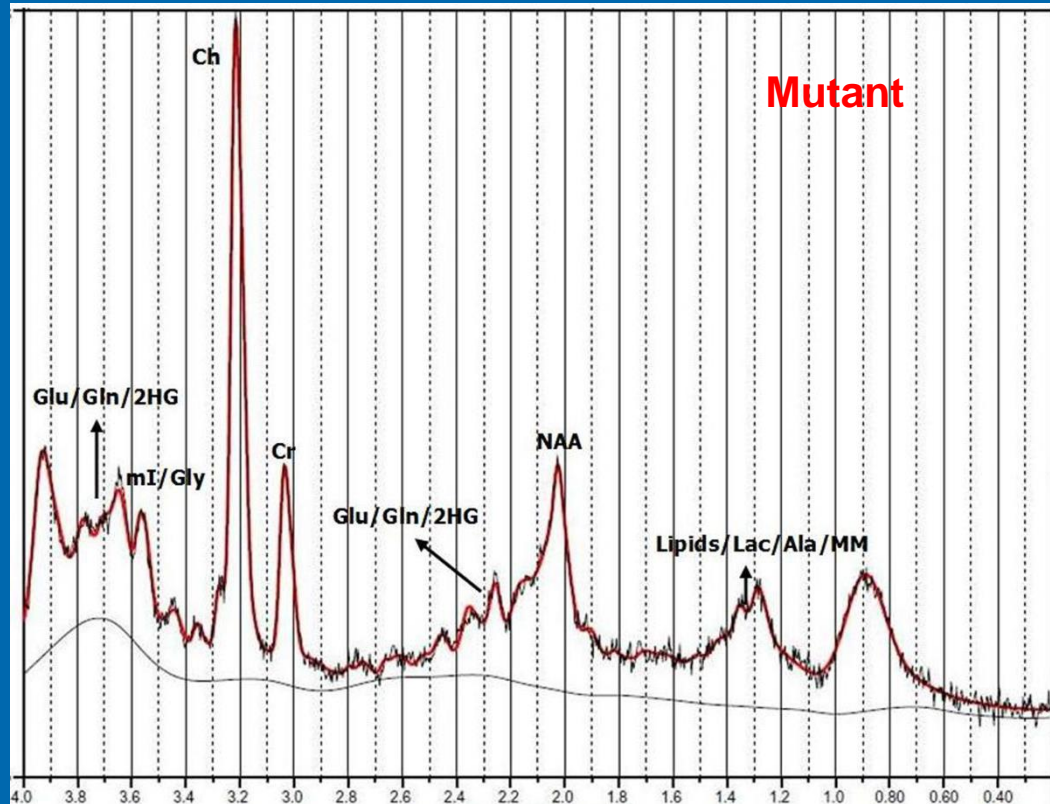


Smeitnik, J. "Metabolism, Gliomas, and IDH1," *N Eng J Med* 362: 1144-45, 2010

Pope et al. 2012
Andrenosi et al. 2012
Elkhaked et al. 2012
Choi et al. 2012



Scanner	:	Siemens 3T Trio-Tim
Coil	:	12 Channel receive
Subjects	:	24 brain tumor
Mutant Tumor	:	9 (Mean age 43 years)
Wild Tumor	:	15 (Mean age 59 years)
Tumor Grade	:	14 primary GBM (grade IV), 6 oligodendroglioma (grade III), and 4 low grade (grade II)



NIH Public Access
Author Manuscript

J. Neurosci. Author manuscript; available in PMC 2013 May 10.

Published in final edited form as:
J. Neurosci. 2012 March ; 107(1): 197–205. doi:10.1007/s11060-011-0737-8.

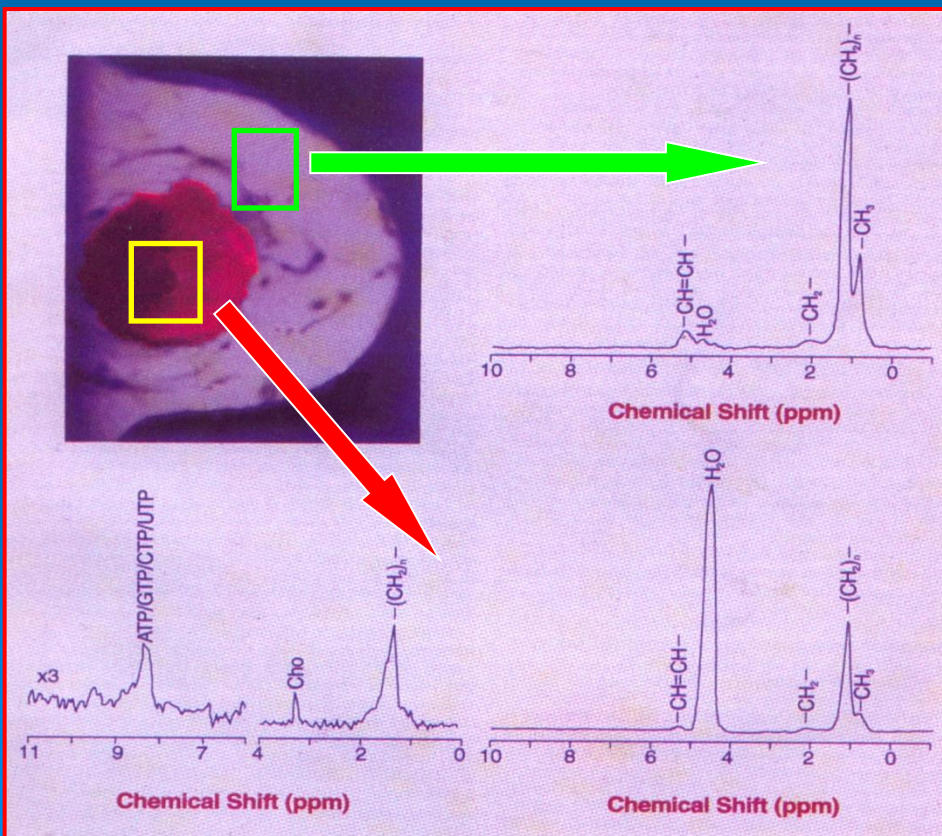
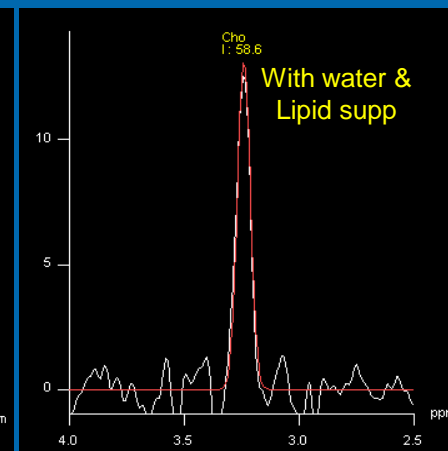
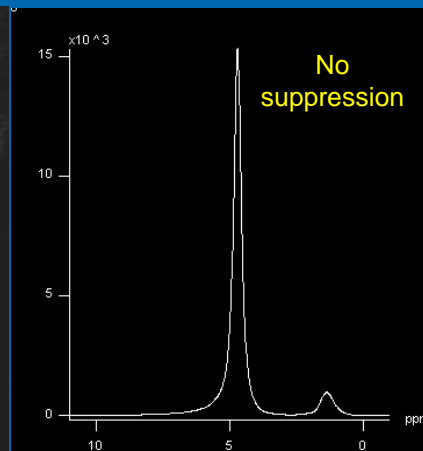
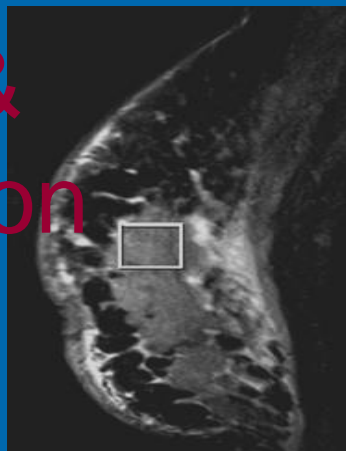
Non-invasive detection of 2-hydroxyglutarate and other metabolites in *IDH1* mutant glioma patients using magnetic resonance spectroscopy

Whitney B. Pope, Department of Radiological Sciences, David Geffen School of Medicine at UCLA, University of California at Los Angeles, Los Angeles, CA 90095, USA
Robert M. Prins, Department of Neurosurgery, David Geffen School of Medicine at UCLA, University of California at Los Angeles, Gonda Building, Room 3357, 695 Charles Young Drive, Los Angeles, CA 90095-1761, USA LLIU@mednet.ucla.edu
M. Albert Thomas, Department of Radiological Sciences, David Geffen School of Medicine at UCLA, University of California at Los Angeles, Los Angeles, CA 90095, USA
Rajakumar Nagarajan, Department of Radiological Sciences, David Geffen School of Medicine at UCLA, University of California at Los Angeles, Los Angeles, CA 90095, USA
Katharine E. Yen, Mark A. Bittinger, Noriko Salamon, Department of Radiological Sciences, David Geffen School of Medicine at UCLA, University of California at Los Angeles, Los Angeles, CA 90095, USA
Arthur P. Chou, Department of Neurosurgery, David Geffen School of Medicine at UCLA, University of California at Los Angeles, Gonda Building, Room 3357, 695 Charles Young Drive, Los Angeles, CA 90095-1761, USA LLIU@mednet.ucla.edu
William H. Yong, Department of Pathology & Laboratory Medicine, David Geffen School of Medicine at UCLA, University of California at Los Angeles, Los Angeles, CA 90095, USA
Horacio Soto, Department of Neurosurgery, David Geffen School of Medicine at UCLA, University of California at Los Angeles, Gonda Building, Room 3357, 695 Charles Young Drive, Los Angeles, CA 90095-1761, USA LLIU@mednet.ucla.edu
Neil Wilson, Department of Radiological Sciences, David Geffen School of Medicine at UCLA, University of California at Los Angeles, Los Angeles, CA 90095, USA
Edward Driggers, Hyun G. Jang,

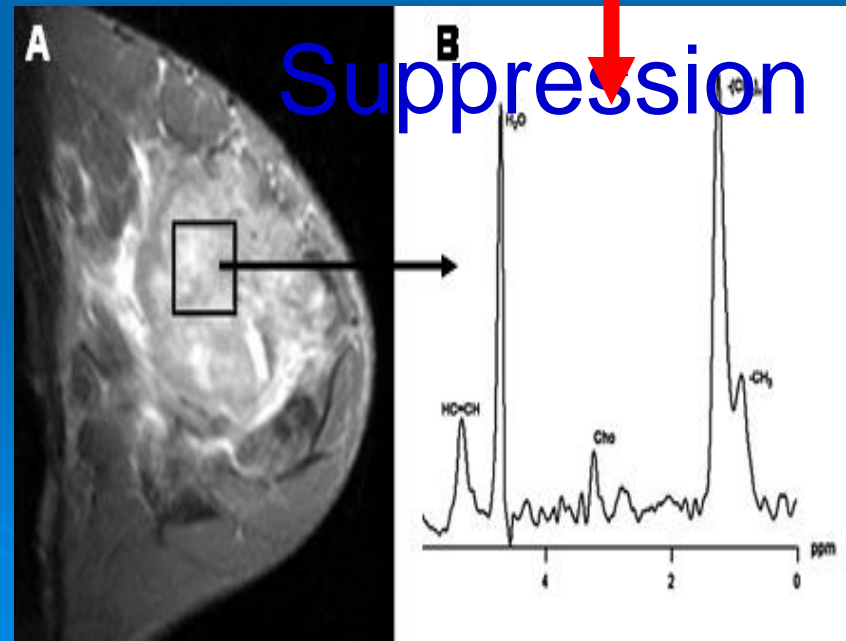
Single voxel MRS – Detection of tCho

With water & fat suppression

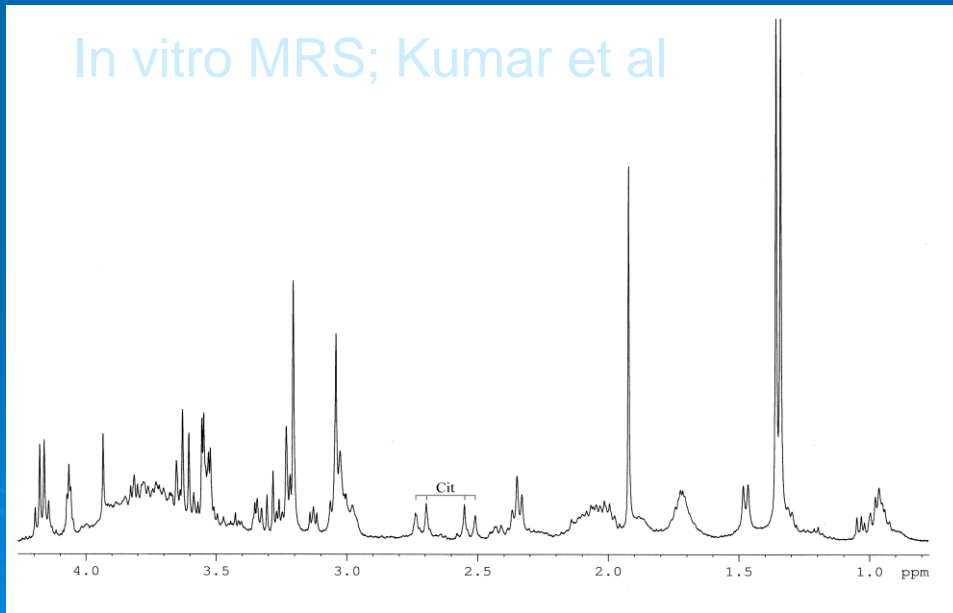
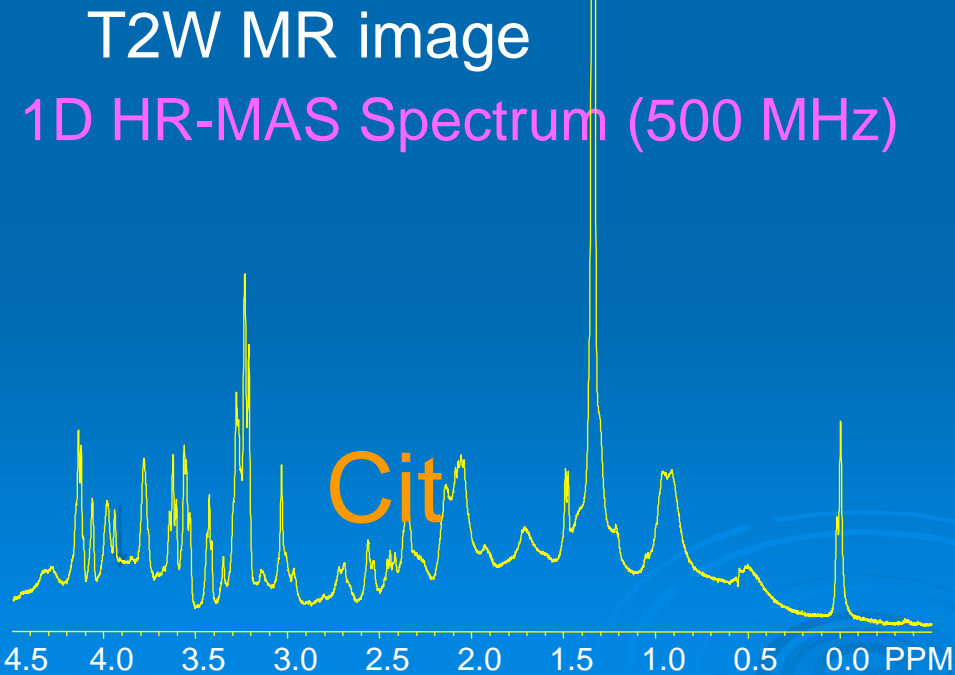
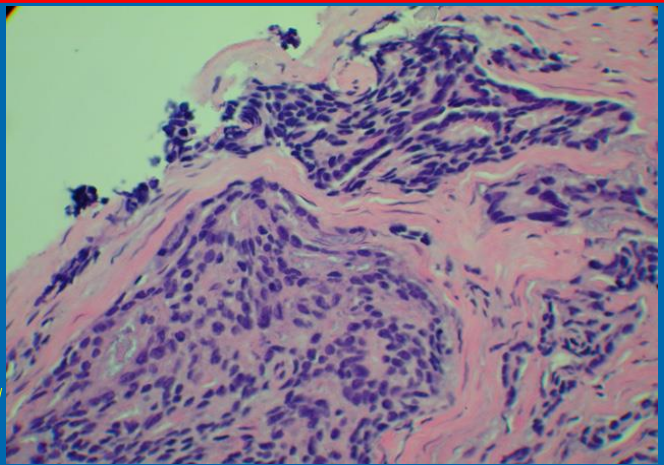
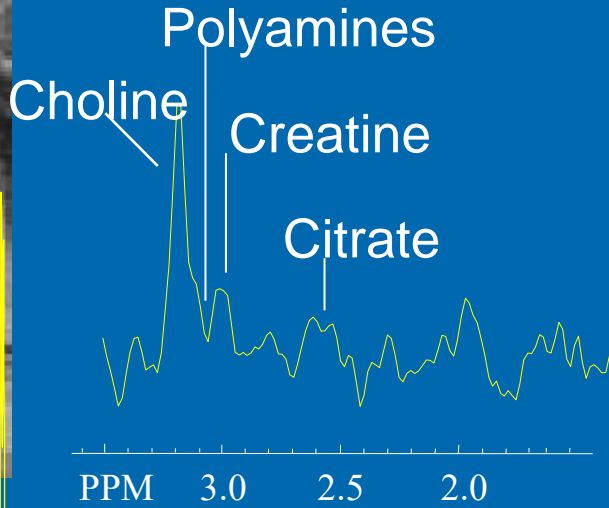
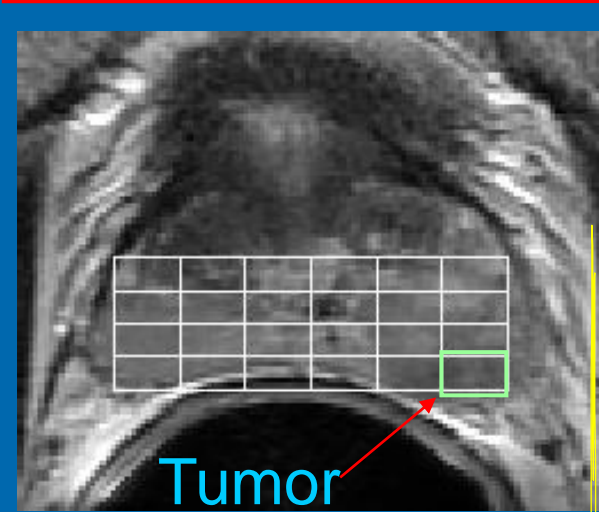
Spectra from tumor & Normal portion with only Water suppression



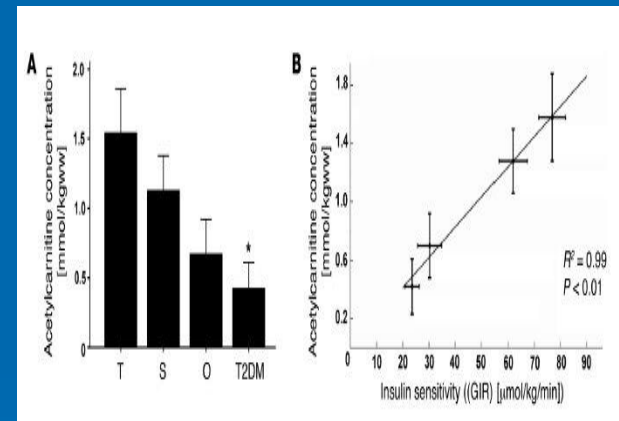
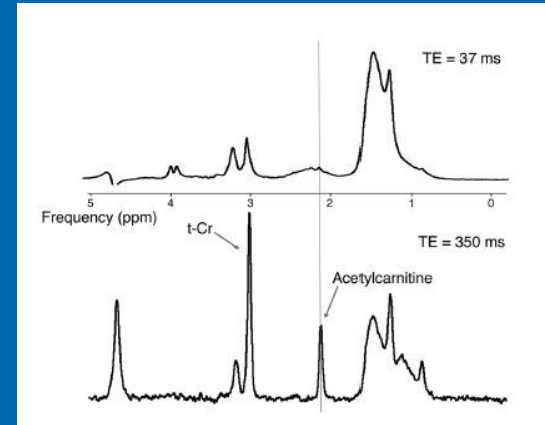
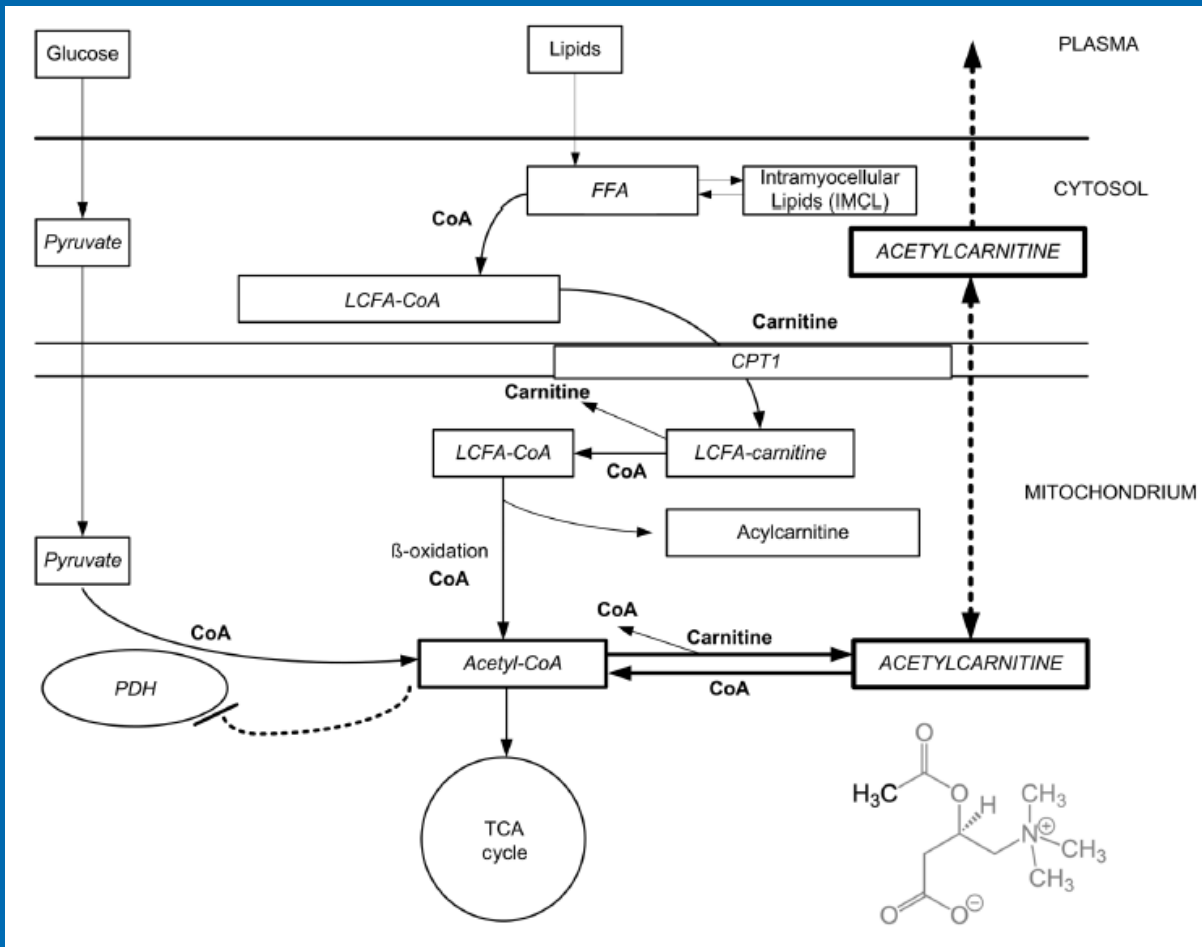
With water suppression



Malignant Prostate Metabolism



Courtesy: Prof. John Kurhanewicz



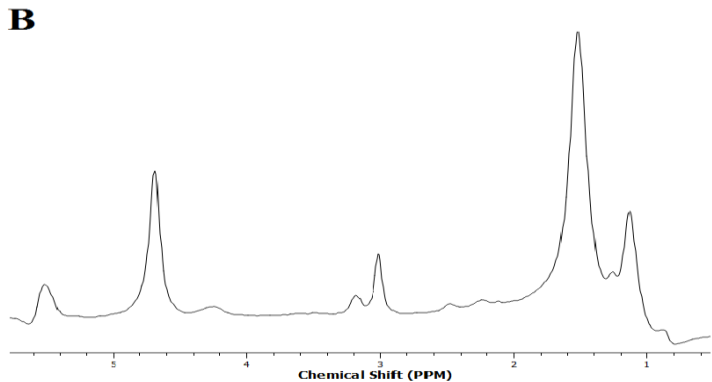
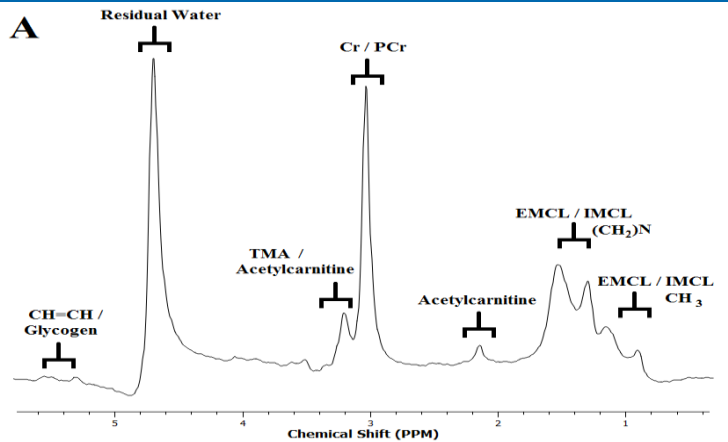
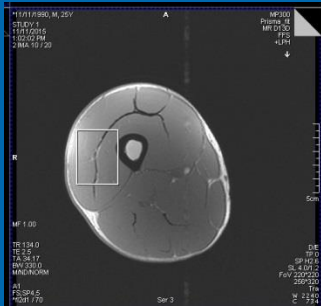
Acetylcarnitine is formed in conditions in which acetyl-CoA formation, either as end product of glycolysis or β -oxidation, exceeds its entry into the tricarboxylic (TCA) cycle. Free carnitine can act as a sink for excess acetyl groups in a reversible reaction catalyzed by the enzyme carnitine acetyltransferase (CRAT).

Acetylcarnitine, like other acylcarnitine esters, can readily be exported out of the mitochondria

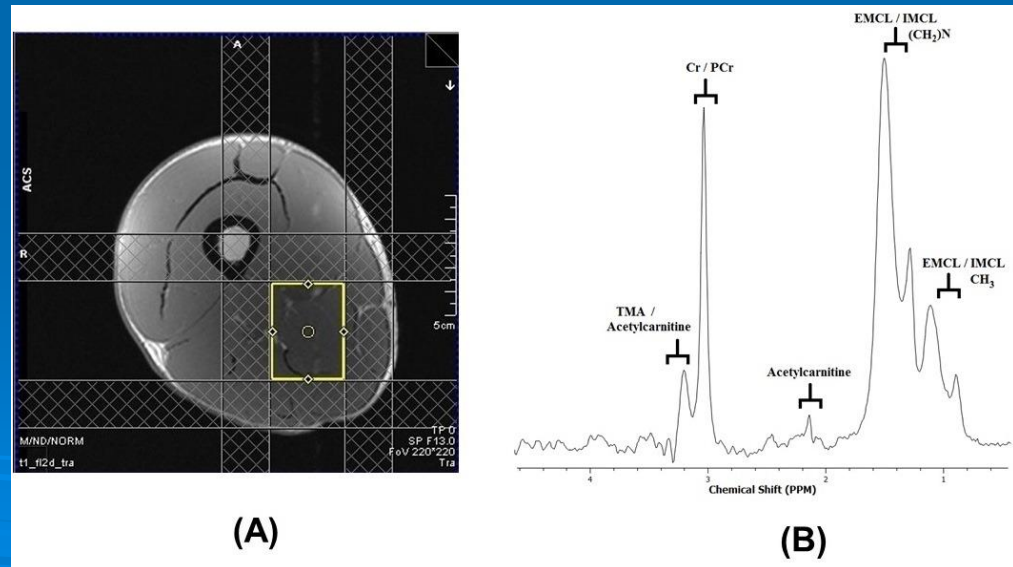
1D MR Spectroscopy to detect AcetylCarnitine

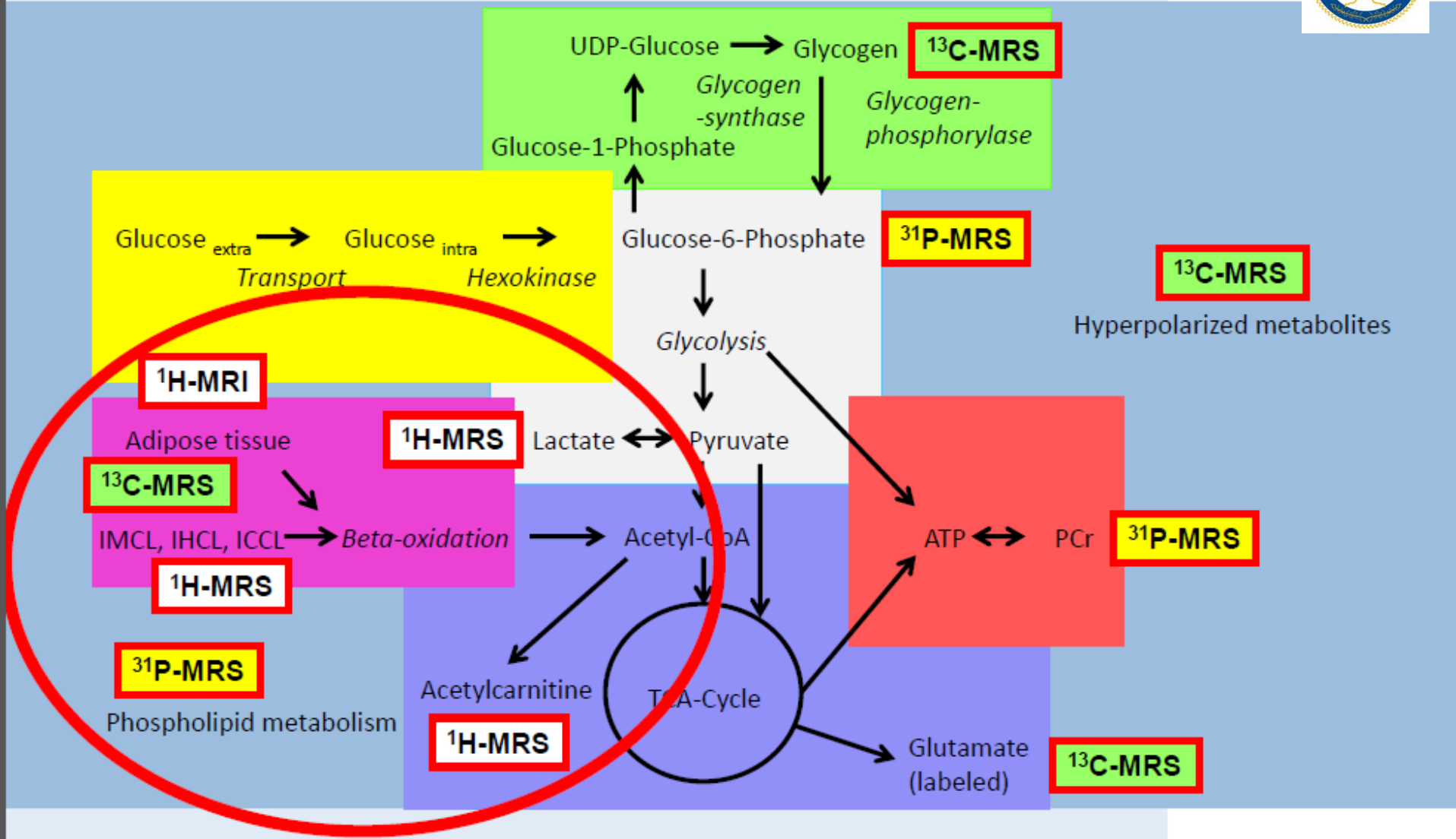


PRESS-localized long TE spectra recorded in the vastus muscles of (A) a 25 year-old healthy subject and (B) a 61 year-old T2D patient



PRESS localization (white box) shown on an axial thigh MRI of a 25 year-old healthy male subject recorded in the mixed medial hip adductor and posterior knee flexor muscle region.







Important Nuclei for Biomedical MR

- ^1H** – Neurotransmitters, amino acids, membrane constituents
- ^2H** – Perfusion, drug metabolism, tissue and cartilage structure.
- ^{13}C** – Glycogen, metabolic rates, substrate preference, drug metabolism, etc.
- ^{19}F** – Drug metabolism, pH, Ca^{2+} and other metal ion concentration, pO_2 , temperature, etc
- ^{23}Na** – Transmembrane Na^+ gradient, tissue and cartilage structure.
- ^{31}P** – Cellular energetics, membrane constituents, pH_i, $[\text{Mg}^{2+}]$, kinetics of creatine kinase and ATP hydrolysis.

Important Nuclei for Biomedical MR

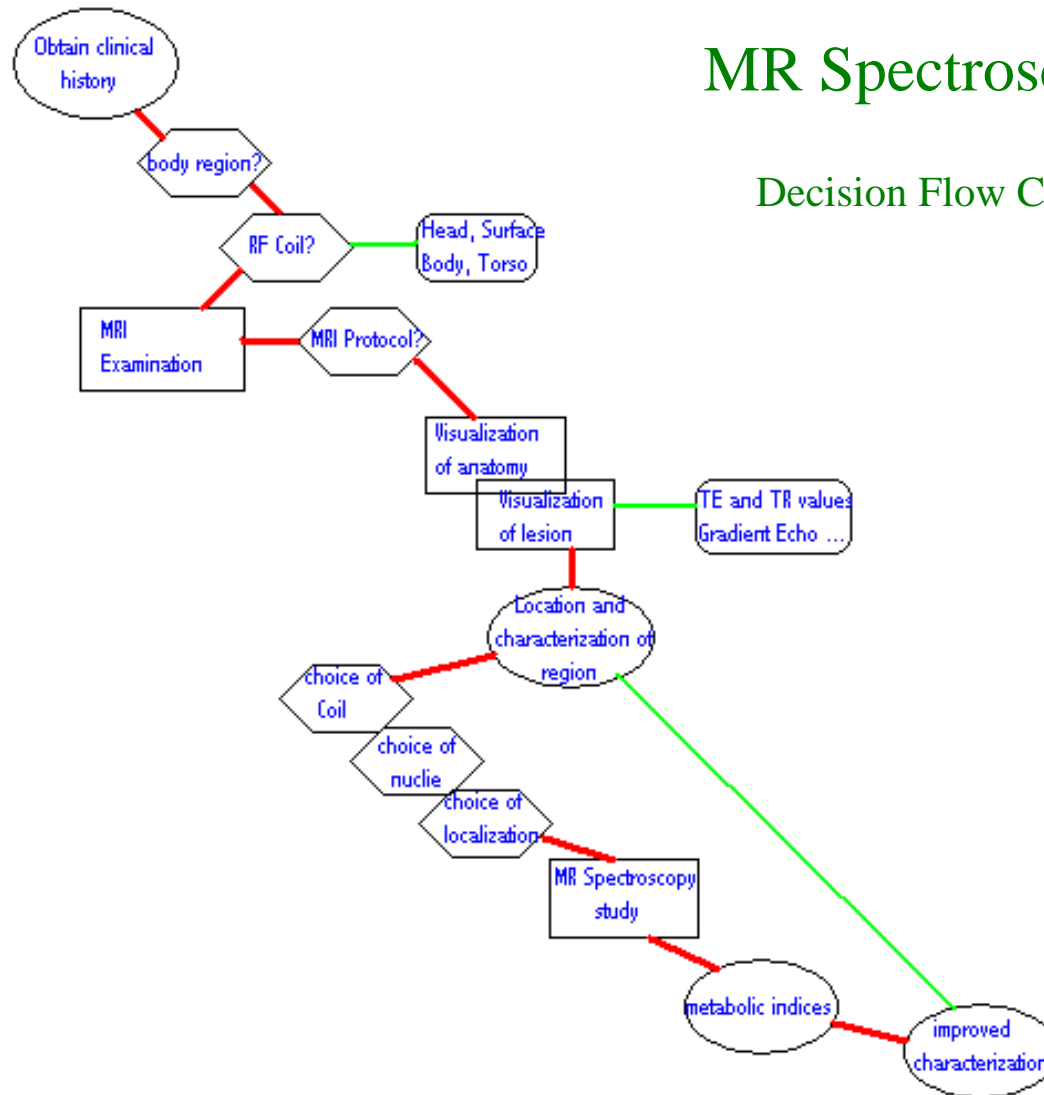
Nucleus	Spin	γ , MHz/T	Natural Abundance	Relative Sensitivity
^1H	1/2	42.576	99.985	100
^2H	1	6.536	0.015	0.96
^3He	1/2	32.433	.00013	44
^{13}C	1/2	10.705	1.108	1.6
^{17}O	3/2	5.772	0.037	2.9
^{19}F	1/2	40.055	100	83.4
^{23}Na	3/2	11.262	100	9.3
^{31}P	1/2	17.236	100	6.6
^{39}K	3/2	1.987	93.08	.05

How long it takes to perform a single voxel MR Spectroscopy?

Steps	Long ago	Now-a-days
Prescription	2-5 min.	1 min
Adjustment	2 min 5-15 min 5-10 min	2 min
Acquisition	4-16 min	2-8 min
Data reconstruction	10 min	1 min

MR Spectroscopy

Decision Flow Chart





2. Fast MR Spectroscopic Imaging

M. Albert Thomas Ph.D.
Professor

Department of Radiological Sciences
University of California, Los Angeles

M219: Introduction to Magnetic Resonance Imaging/03/06/24



THANK YOU

